

A NUCLEAR MAGNETIC RESONANCE STUDY OF  
THE METHYLTHIO GROUP CONFORMATION AND  
BARRIER TO INTERNAL ROTATION  
IN SOME THIOANISLES

by

James D. Baleja

A Thesis Submitted to  
The Faculty of Graduate Studies  
of the University of Manitoba  
In partial fulfillment of the Degree  
Master of Science

Winnipeg, Manitoba

July, 1984

A NUCLEAR MAGNETIC RESONANCE STUDY OF  
THE METHYLTHIO GROUP CONFORMATION AND  
BARRIER TO INTERNAL ROTATION IN SOME THIOANISOLE

BY

JAMES D. BALEJA

A thesis submitted to the Faculty of Graduate Studies of  
the University of Manitoba in partial fulfillment of the requirements  
of the degree of

MASTER OF SCIENCE

© 1984

Permission has been granted to the LIBRARY OF THE UNIVERSITY OF MANITOBA to lend or sell copies of this thesis, to the NATIONAL LIBRARY OF CANADA to microfilm this thesis and to lend or sell copies of the film, and UNIVERSITY MICROFILMS to publish an abstract of this thesis.

The author reserves other publication rights, and neither the thesis nor extensive extracts from it may be printed or otherwise reproduced without the author's written permission.

## Abstract

The carbon, fluorine, and proton nuclear magnetic resonance spectra of thioanisole and some nineteen thioanisole derivatives have been analysed in order to investigate the conformational preference of the methylthio group. Ab initio molecular orbital calculations with geometry optimization at the STO-3G level and some INDO MO FPT calculations have been performed for thioanisole, 2,6-difluorothioanisole, 3,5-difluorothioanisole, 2-chlorothioanisole, 2,6-dichlorothioanisole, 3,5-dichlorothioanisole, 3,5-dimethylthioanisole, 4-methylthioanisole, and 4-fluorothioanisole.

On the basis of spin-spin coupling constants and molecular orbital calculations, compounds with one or no substituent ortho to the methylthio group favour coplanarity of all heavy atoms. Long-range spin-spin coupling constants over six or seven formal bonds between  $^{13}\text{C}$  nuclei in the methyl group and para protons or fluorines, or ring methyl protons at the para position are reported for twelve thioanisole derivatives. The couplings are  $\sigma$ - $\pi$  mediated, as indicated by INDO MO FPT computations and by measurements on thioanisole, 2,6-dichlorothioanisole, 2,6-dibromothioanisole, 2,6-dibromo-4-methylthioanisole, 4-methylthioanisole, and

2,6-dibromo-4-fluorothioanisole. Two-fold barriers for the reorientation of the methylthio group have been estimated on the basis of the measured magnitudes of the coupling constants and a hindered rotor model (the J method†) for 4-fluorothioanisole, 4-methylthioanisole, thioanisole, 3,5-dimethylthioanisole, and 3,5-dichlorothioanisole ( $3.7 \pm 0.6$ ,  $3.9 \pm 0.1$ ,  $5.1 \pm 0.2$ ,  $6.1 \pm 0.4$ , and  $9.6 \pm 0.7$  kJ mol<sup>-1</sup>, respectively).

For thioanisole derivatives with both ortho positions occupied by groups other than protons, an out-of-plane conformer is most stable. Barriers, presumed two-fold, for internal rotation in 2,6-difluorothioanisole, 2,4,6-trifluorothioanisole, 2,3,5,6-tetrafluorothioanisole, and 2,3,4,5,6-pentafluorothioanisole, have also been determined ( $6.9 \pm 0.8$ ,  $8.1 \pm 1.0$ ,  $4.1 \pm 0.6$ , and  $7.9 \pm 1.1$  kJ mol<sup>-1</sup>, respectively).

Measurements of  $^5J(\text{CH}_3, \text{H})$  in thioanisole, 3,5-dichlorothioanisole, 4-nitrothioanisole, and in ortho substituted thioanisoles reflect the angle by which the methylthio group twists out of the aromatic plane. The increasing magnitude of the coupling in the series thioanisole, 3,5-dichlorothioanisole, 4-nitro-

---

† W. J. E. Parr and T. Schaefer, Acc. Chem. Res. 13,400 (1980).



thioanisole, 2-methyl-3-fluorothioanisole, 2-bromo-4-fluorothioanisole, 2-bromothioanisole, 2-iodothioanisole, and 2,4,5-trichlorothioanisole indicates increasing coplanarity of the heavy atoms.

The five bond spin-spin coupling between the  $\alpha$  carbon of the methyl group and the meta proton or meta fluorine are shown to result from a combination of the  $\sigma$ - $\pi$  electron and  $\sigma$  electron coupling mechanisms. INDO MO FPT calculations on 3,5-difluorothioanisole, as well as measurements on 2,4,6-tribromo-3-fluoro-, 2-methyl-3-fluoro-, pentafluoro-, and 2,3,5,6-tetrafluorothioanisoles, indicate that the two mechanisms give contributions of opposite sign.

Sign determinations have been made for spin-spin couplings between the  $\alpha$  carbon of the methyl group and ortho, meta, and para protons, between the  $\alpha$  carbon and ortho and meta fluorines, and between the methyl protons and the meta proton.

to my grandmother,

Ludmila Baleja

## Acknowledgements

I must first thank Professor Ted Schaefer for his criticism and encouragement, during the course of this work. He has, on occasion, tamed some of my wilder speculations, in an attempt to allow me to reach wide conclusions. The time spent in this laboratory has been beneficial.

I thank Professor Frank Hruska for access to the Bruker WH-90 spectrometer. I also appreciate the marvelous technical abilities of Kirk Marat, and the computing skills of Rudy Sebastian.

I am grateful for useful and engaging conversations with Glenn Penner, Rudy Sebastian, Kirk Marat, Dr. James Peeling, and Mike Sowa. The financial support of the Natural Sciences and Engineering Council of Canada and of the University of Manitoba is much appreciated.

The love of my grandmother, and the numerous pastries she has provided, have been a great boost to my moral, and my weight, respectively. But I appreciate most the questions relating to science which have shown me a purpose to scientific research. I thank her affectionately.

## List of Publications

1. J. D. Baleja, "The facile conversion of aromatic amines to arylmethylsulfides". Synth. Commun. 14,215 (1984).
2. T. Schaefer, R. Laatikainen, T. A. Wildman, J. Peeling, G. H. Penner, J. Baleja, and K. Marat, "Long-range  $^{13}\text{C}$ ,  $^1\text{H}$  and  $^{13}\text{C}$ ,  $^{19}\text{F}$  coupling constants as indicators of the conformational properties of 2,3,5,6-tetrafluoroanisole and pentafluoroanisole." Can. J. Chem. 62, July, 1984.
3. T. Schaefer and J. D. Baleja, "The highly resolved  $^1\text{H}$  nmr spectrum of thioanisole. Precise long range couplings to the Methyl Protons." J. Mag. Res., Nov., 1984 (in press).

## Table of Contents

List of Figures	xii
List of Tables	xv
INTRODUCTION	1
A. Experimental Investigations	2
(i) Ultraviolet and Infrared spectroscopy	4
(ii) Dipole moments and Kerr constants	5
(iii) Microwave spectroscopy	7
(iv) Photoelectron spectroscopy	8
(v) X-ray fluorescence spectra	11
(vi) Electron Spin Resonance	12
(vii) Nuclear Magnetic Resonance(NMR)	
(a) $^1\text{H}$ shifts	13
(b) $^{13}\text{C}$ shifts	14
(c) liquid crystal NMR	16
(d) long-range couplings	17
(viii) Molecular orbital calculations	19
B. Introduction to the problem	22
EXPERIMENTAL METHODS	25
A. Materials and Syntheses	26
(i) Methylation of thiophenols	27
(ii) Syntheses of thioanisoles from anilines	29
(iii) Syntheses of 2-iodo- and 3,5-dimethyl- thiophenols	30

	ix
(iv) Bromination of 4-fluoroaniline	31
B. Sample Preparation	32
C. Spectroscopic method	33
D. Computations	36
 EXPERIMENTAL RESULTS	 37
A. High resolution spectra	38
(i) thioanisole	40
(ii) 2-iodothioanisole	57
(iii) 2,4,5-trichlorothioanisole	64
(iv) 2,6-dichlorothioanisole	66
(v) 2,6-dibromothioanisole and 2,6-dibromo- 4-methylthioanisole	72
(vi) 2-bromothioanisole	76
(vii) 2-bromo-4-fluorothioanisole	83
(viii) 4-nitrothioanisole	88
(ix) 4-fluorothioanisole and 2,6-dibromo- 4-fluorothioanisole	91
(x) 2,3,4,5,6-pentafluorothioanisole and 2,3,5,6-tetrafluorothioanisole	92
(xi) 2,4,6-trifluorothioanisole	103
(xii) 2,6-difluorothioanisole	106
(xiii) 2,4,6-tribromo-3-fluorothioanisole	111
(xiv) 2-methyl-3-fluorothioanisole	113
(xv) Thiophenols	114
(xvi) 3,5-dichlorothioanisole	116
(xvii) 3,5-dimethylthioanisole	120

	x
(xviii) 4-methylthioanisole	121
B. Molecular Orbital Calculations	124
DISCUSSION	138
A. The Hindered Rotor Model and the J Method	139
B. MO calculations of the internal barrier in thioanisole	143
C. Stereospecific Coupling Constants	
(i) ${}^6J(C\alpha, H4)$	145
(ii) ${}^6J(C\alpha, F4)$	148
(iii) ${}^5J(C\alpha, H)$	150
(iv) ${}^5J(C\alpha, F)$	152
(v) ${}^4J(C\alpha, H)$ and ${}^4J(C\alpha, F)$	154
D. Barriers to internal rotation	
(i) Thioanisole, 4-fluorothioanisole, 4-methylthioanisole, 3,5-dimethylthioani- sole, and 3,5-dichlorothioanisole	155
(ii) Fluorothioanisoles	159
(a) 2,6-difluorothioanisole	162
(b) 2,4,6-trifluorothioanisole	162
(c) 2,3,5,6-tetrafluorothioanisole	163
(d) pentafluorothioanisole	163
(e) 2-bromo-4-fluorothioanisole	165

	xi
E. Conformational implications of $^3J(\text{CH}_3, \text{H})$ in thioanisole derivatives.	166
SUMMARY AND CONCLUSIONS	172
FUTURE CONSIDERATIONS	178
REFERENCES	182



## List of Figures

1.	Thioanisole in benzene	6
2.	Correlation diagram for benzene, planar thioanisole, and non-planar thioanisole	9
3.	A conformation for phenol or benzaldehyde	23
4.	Spectrum of the ring protons of thioanisole	41
5.	The methyl proton spectrum of thioanisole	43
6.	The <u>ortho</u> proton resonance of thioanisole	45
7.	Part of the <u>para</u> proton resonance of thioanisole	47
8.	Part of the <u>meta</u> proton resonance of ( $\alpha$ - $^{13}\text{C}$ )thioanisole	52
9.	Part of the <u>para</u> proton resonance of ( $\alpha$ - $^{13}\text{C}$ )thioanisole	54
10.	The H6 resonance of 2-iodo( $\alpha$ - $^{13}\text{C}$ )thioanisole	60
11.	A first order representation of the H6 resonance of 2-iodo( $\alpha$ - $^{13}\text{C}$ )thioanisole	61
12.	Spectrum of the ring protons of 2,6-dichlorothioanisole	68
13.	Sign determination of $^5\text{J}(\text{C}\alpha, \text{H})$ in 2,6-dichlorothioanisole	70
14.	Parts of the $\alpha$ methyl carbon spectra for 2,6-dibromothioanisole and 2,6-dibromo-4-methylthioanisole	73
16.	The H3, H5, and H6 proton resonances of 2-bromothioanisole	77
16.	The H4 proton resonance of 2-bromothioanisole	79

17. Spectrum of the ring protons of 2-bromo-4-fluoro-thioanisole 86
18. The proton decoupled carbon spectrum of penta-fluorothioanisole 94
19. Sign determination of  $^4J(C\alpha,F)$  in 2,3,5,6-tetrafluorothioanisole 97
20. Sign determination of  $^5J(C\alpha,F)$  in 2,3,5,6-tetrafluorothioanisole 99
21. The methyl protons spectra of pentafluorothioanisole and 2,3,5,6-tetrafluorothioanisole 101
22. The temperature dependence of  $^5J(CH_3,F)$  in some fluorothioanisoles 107
23. Part of the methyl carbon spectrum of 2,6-difluorothioanisole 109
24. The methyl decoupled ring proton spectrum of 3,5-dichloro( $\alpha$ - $^{13}C$ )thioanisole 118
25. The methylthio carbon of 4-methylthioanisole 122
26. STO-3G calculated geometry for planar thioanisole 125
27. STO-3G calculated potential curve for internal rotation in thioanisole 127
28. STO-3G calculated potential curve for internal rotation in 2,6-difluorothioanisole 129
29. STO-3G calculated potential curve for internal rotation in 2,6-dichlorothioanisole 131
30. STO-3G calculated potential curve for internal

	xiv
rotation in 3,5-difluorothioanisole	133
31. INDO calculated ${}^6J(C\alpha,H)$ for conformations of thioanisole	136
32. Barriers to internal rotation in some thioanisoles	175

## List of Tables

1.	Spectral parameters for thioanisole	49
2.	Spectral parameters for ( $\alpha$ - $^{13}\text{C}$ )thioanisole	51
3.	Spectral parameters for 2-iodothioanisole	58
4.	Spectral parameters for 2,4,5-trichlorothioanisole	65
5.	Spectral parameters for 2,6-dichlorothioanisole	67
6.	Coupling constants for 2,6-dibromothioanisole and 2,6-dibromo-4-methylthioanisole	75
7.	Spectral parameters for 2-bromothioanisole	81
8.	Spectral parameters for 2-bromo-4-fluorothioanisole	84
9.	Spectral parameters for 4-nitrothioanisole	89
10.	Coupling constants for 2,3,5,6-tetrafluorothioanisole and pentafluorothioanisole	96
10a.	Spectral parameters for 2,4,6-trifluorothioanisole	104
11.	Spectral parameters for 2,4,6-tribromo-3-fluorothioanisole	112
12.	Spectral parameters for 3,5-dichlorothiophenol, 3,5-dimethylthiophenol, and 4-methylthiophenol	114
13.	Spectral parameters for 3,5-dichlorothioanisole	117
14.	STO-3G barriers to internal rotation	126
15.	INDO calculated coupling constants	137
16.	Barriers to internal rotation	155

17. Barriers to internal rotation for some thioaniso-  
les and corresponding thiophenol derivatives 157
18. Coupling constants for some 2,6-difluorothio-  
anisoles 161
19. Comparisons of observed and calculated five-bond  
methyl proton-ortho proton coupling constants 171

INTRODUCTION

## A. Experimental Investigations

The conformational behaviour of the methylthio group in thioanisoles cannot yet be considered as resolved. The data reported in the literature concerning the departure of the methylthio moiety from the plane of the aromatic ring generally agree that the conformation in which all heavy atoms are co-planar is favoured and suggest that non-planar conformers are possible. Therefore, the barrier to internal rotation must be of the same order of magnitude as  $kT$  at ambient temperatures. The data, however, differ significantly as to the shape and size of the barrier.

Nuclear magnetic resonance spectroscopy (NMR) has been applied to the study of thioanisole, but most studies have been concerned with the interpretation of chemical shifts. Spin-spin coupling constants have not been widely used, since the numbers are usually small and their mechanism and conformational dependence are not well understood. Coupling constants have been shown to be useful conformational indicators in other molecules such as thiophenol<sup>1-4</sup> and toluene derivatives<sup>5-9</sup>.

This thesis extends the use of coupling constants to thioanisole and its derivatives. The conformational dependence of NMR parameters is adduced such that the

barrier to internal rotation and conformational preferences of the methylthio group in aryl methyl sulfides (thioanisoles) are indicated.

The reader is referred to the standard monographs for a description of the theory of the NMR experiment and of spectral analysis<sup>10-17</sup>.

The balance of this chapter reviews experimental investigations of the conformation of the methylthio group in thioanisole and several derivatives. The conformational behaviour is described and factors which regulate conformation are illustrated.



(i) UV and IR spectroscopy

Vibrational analysis<sup>18</sup> of the first singlet-singlet transition in thioanisole vapour gave the torsional frequency of the methylthio group in the ground state as 67.4 cm.<sup>-1</sup>. This was in rough agreement with the tentative assignment by Green<sup>19</sup> to the IR absorption at 79 cm.<sup>-1</sup> in the liquid.

From the separation of torsional levels, an estimate of the barrier to internal rotation can be obtained, once  $\theta$ , the value of the torsional angle at equilibrium is known. In the high-barrier approximation, and for  $\theta$  nearly zero, the barrier height is estimated<sup>18</sup> to be 26.3 kJ mol<sup>-1</sup>. In the small-barrier limit, this approximation is said to underestimate the barrier<sup>20</sup>. Assuming that the excited state is planar, the torsional levels derived from the vibrational analysis suggest that the ground electronic state must have out-of-plane conformers.

(ii) Dipole moments and Kerr Constants

Dipole moment comparisons for 2-chlorothioanisole and 2,4-dichlorothioanisole convinced Lumbroso and co-workers<sup>21</sup> that they exist predominantly as the trans conformation, to the exclusion of the hindered cis form. Therefore, there exist possible steric influences on the conformation of the methylthio group.

In an earlier paper<sup>22</sup>, dipole moments and molar Kerr constants were reported for thioanisoles substituted at the para position as solutes in CCl<sub>4</sub> and in benzene. The experimental data were analysed to provide information on preferred solute conformations and on the incidence and stereospecificity of benzene-solute complex formation. Using bond and group polarizability data, the molecular polarisability tensor was calculated<sup>23</sup> for differing conformations of the methylthio group. The experimental Kerr constants were consistent with dihedral angles of 23° for thioanisole, ca. 20° for p-chloro- and p-bromothioanisole, and nearly 0° for p-nitrothioanisole. This was attributed to possibly a greater degree of conjugative interaction of the methylthio and para substituents in the series H<Cl,Br<NO<sub>2</sub>. The pronounced solvent effect in changing from carbon tetrachloride to benzene was interpreted as an indication that stereospecific solute-benzene interactions

occur which result in transient collision complexes having the associated solvent molecule preferentially disposed perpendicular to  $\mu$ , the methylthio group moment vector (see Figure 1).

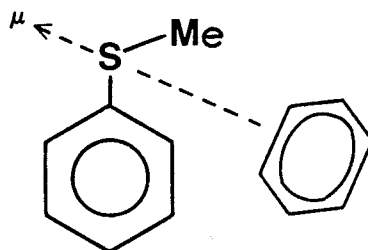


Figure 1

Edge-on associations in which benzene protons approach sulfur lone pairs were not excluded. Benzene solvent molecules were inferred to solvate electron-deficient sites. No discussion of effects on the barrier to internal rotation or conformational consequences was offered for the disposition of the SMe group relative to the aromatic ring plane. Different solvent molecules may well alter the rate at which the methylthio group re-orientates, but need not alter the intrinsic barrier<sup>24</sup>.

(iii) Microwave spectroscopy

The relative intensities of two band series in the low-resolution microwave spectrum of para-fluorothioanisole suggested an energy difference of  $3.0 \pm 1.0$  kJ mol<sup>-1</sup> between conformers described as nearly planar and nearly perpendicular<sup>2,5</sup>. The two bands were assigned to rotamers having a planar and perpendicular configuration, respectively, based on model calculations from presumed geometries, to give a calculated frequency difference between the two sets of rotational constants. A release of what was termed 'steric tension' between the two forms could affect the assignment and thus the measured barrier to rotation.

(iv) Photoelectron and Electron Transmission Spectroscopy

Qualitative  $\pi$  MO schemes suggest that the splitting of the lowest ionization energy band of the photoelectron spectrum of a monosubstituted benzene is an indication of the removal of the degeneracy of the  ${}^2E_{1g}$  ground state<sup>26</sup> (Figure 2). The spectrum of thioanisole can be explained without resort to unoccupied d-orbitals on sulfur. Conformational equilibrium between the planar and the less stable perpendicular conformers is reported for the methyl, ethyl, isopropyl, and t-butyl phenyl sulfides<sup>27</sup>. The two conformers are described as one having maximum p- $\pi$  orbital overlap (all heavy atoms co-planar) and another, of increasing importance through the series methyl, ethyl, isopropyl, and t-butyl, having reduced p- $\pi$  overlap. The first ionization energies of para-substituted thioanisoles are sensitive to the degree of conjugation between the methyl side chain and the ring and decrease in the order  $\text{NO}_2$ , H,  $\text{CH}_3$ ,  $\text{SCH}_3$ ,  $\text{OCH}_3$ ,  $\text{NH}_2$ ,  $\text{N}(\text{CH}_3)_2$ . Since the HOMO is almost entirely sulfur lone-pair, changes are not as great as in the corresponding anisoles<sup>28</sup>.

Schweig and Thon estimated the conformational equilibrium constant between 293 and 773K<sup>29</sup>. A two-state model implied an energy difference of  $3.5 \pm 0.3 \text{ kJ mol}^{-1}$

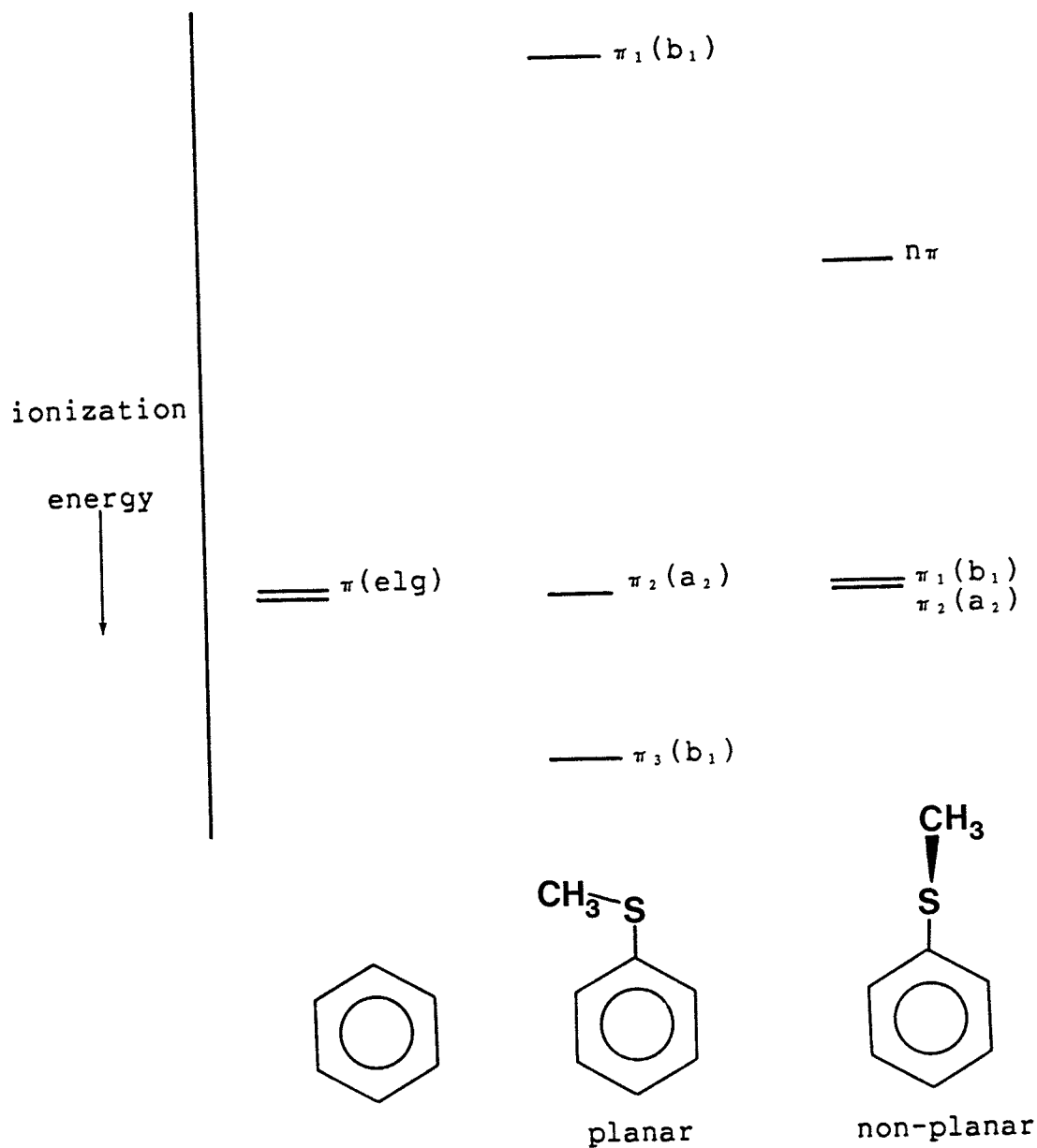


Figure 2

Correlation diagram for the lowest ion states of benzene, planar thioanisole, and non-planar thioanisole. The states are classified according to the designation of orbitals from which they arise<sup>29</sup>.

but Honegger and Heilbronner demonstrated that a more careful analysis, which accounts for all conformations, is required<sup>30</sup>. Although the correct potential curve for internal rotation was considered necessary for an accurate determination of the conformer distribution, it was indicated that the true energy difference between the 0 and 90° conformers was somewhat higher than that deduced from the two-site model.

Electron transmission (ET) spectroscopy of thiophenol, thioanisole, and t-butyl phenyl sulfide demonstrated the existence of interacting empty orbitals localized at sulphur containing substituents<sup>31</sup>. Mixing of sulfur 3d orbitals with the  $\pi^*b_1$  ring orbitals could explain the observed electron affinity trend, i.e., the significant stabilization of the  $\pi^*b_1$  molecular orbitals and the small (if any) stabilization of the  $\pi^*2a_1$  molecular orbitals. Assuming that thiophenol and thioanisole were more stable in the planar conformation, and that t-butyl phenyl sulfide was more stable in the conformation with the S-C(sp<sub>3</sub>) bond normal to the benzene ring plane<sup>27, 32, 35</sup>, comparison of d/ $\pi^*$  interactions, as reflected in electron affinity values, indicated that the stabilizing effect of the S 3d orbitals did not change significantly within the  $\sigma$  framework of the alkylthio substituent nor with its torsional angle about the phenyl-sulfur bond.

(v) X-ray fluorescence spectra

Dolenko, Voityuk, Dolenko, and Mazalov have studied the X-ray fluorescence K-spectra ( $SK\beta$  spectra) of solid thiophenol, thioanisole, and pentafluorothioanisole<sup>33</sup>. The  $\pi_1-\pi_3$  energy differences (Figure 2) were measured, and reflected the effectiveness of  $\pi$ -conjugation of the lone sulfur pair into the aromatic ring. INDO calculations showed that this energy difference was always larger for thiophenol than that for thioanisole for the same dihedral angle. However, the measured values were the converse of the trend calculated with INDO, indicating that the dihedral angle of thioanisole was smaller than that of thiophenol. Since the planar conformations are likely most stable for both molecules, and assuming that both have similar features for the potential function to internal rotation, it follows that the rotational barrier in thioanisole must be larger than that in thiophenol. The absence of the  $\pi_1-\pi_3$  energy difference for pentafluorothioanisole indicated a nearly orthogonal conformation. The data were considered consistent with dipole moment and Kerr constants<sup>23,34</sup>, which suggested a dihedral angle of  $23\pm 5^\circ$  for thioanisole and  $64\pm 5^\circ$  for pentafluorothioanisole.



(vi) Electron spin resonance

Pedulli and co-workers investigated the angular dependence of the electron-acceptor character of alkylthio groups in organic radicals<sup>35</sup>. Progressive deviation from planarity with increasing size of the alkyl group was demonstrated by the temperature dependence of the coupling constant at the  $^{13}\text{C}$  nucleus of the alkyl group bonded directly to the sulfur. Electron transfer from the  $\pi$ -orbital of the nitrobenzene moiety containing the unpaired electron to the vacant  $\sigma$  orbital of the alkylthio bond illustrated the electron-acceptor character of the alkylthio group. The barrier to internal rotation in the p-nitroxide thioanisole radical was estimated at  $3.22 \text{ kJ mol}^{-1}$ . As well, INDO calculations indicated that the radical was more stable in the planar conformation, with the energy differences with respect to the non-planar (orthogonal) conformation being  $4.56$  and  $9.41 \text{ kJ mol}^{-1}$ , respectively, in the unprotonated and protonated anion.

(vii) Nuclear magnetic resonance

(a)  $^1\text{H}$  shifts

The proton resonances are shifted to low field in the order  $\text{H}_2 > \text{H}_3 > \text{H}_4$  for thioanisole and selenoanisole, but  $\text{H}_2 > \text{H}_4 > \text{H}_3$  for telluroanisole<sup>41</sup>. The methyl proton resonance is shielded as Group VIA is descended. In 2-hydroxythioanisole, the methylthio group lies nearly orthogonal to the ring plane and although the additivity of substituent-induced shifts is only approximate<sup>43,44</sup>, the ring and methyl proton shifts are consistent with this preference. A so-called 'heavy atom' effect, resulting in a marked downfield shift of  $\text{H}_6$ , is attributed to the proximity of the mainly 3p lone-pair on sulfur.

In a series of alkyl phenyl sulfides, the protons in the para position are more shielded than in non-substituted benzene<sup>42</sup>. Since changes in chemical shift of the para proton and the para carbon are mainly determined by the effect of conjugation, the  $\pi$  donor properties of alkylthio groups decrease in the sequence  $\text{SCH}_3 > \text{SCH}_2\text{CH}_3 > \text{SCH}_2\text{CH}_2\text{CH}_3 > \text{SCH}(\text{CH}_3)_2$ . The t-butylthio group may be ranked as a weak  $\sigma$  and  $\pi$  acceptor, with the chemical shift of the para proton more deshielded than in benzene. The differences may perhaps be attributed to the

dimensions of the alkyl group attached to sulfur, which lead to changes in the spatial orientation of the lone-pairs on sulfur with respect to the benzene ring  $\pi$ -system.

(b)  $^{13}\text{C}$  chemical shifts

Carbon-13 chemical shifts are useful indicators of steric and electronic influences of substituent groups<sup>36</sup>. As with anisole, when substituents are placed at one or both ortho positions, the methyl carbon shift depends on the size of the ortho substituent. The order of the aromatic carbon chemical shifts in thioanisole is  $\text{C1} > \text{C3} > \text{C2} > \text{C4}$ ; i.e., C4 is most shielded.

The methylthio carbon is shielded by about 39 ppm relative to the methoxy carbon of anisole. In addition, the methylthio carbon in 4-methoxythioanisole is deshielded by about 2 ppm relative to thioanisole, and in 4-nitrothioanisole is shielded by about 1 ppm. This trend opposes that observed for the corresponding anisoles<sup>37</sup>, for which the electron-withdrawing nitro group at the para position deshields the methoxy carbon. The lack of sensitivity of the methylthio carbon shift to electron donation or withdrawal by the para substituent, relative to that for the corresponding anisoles, suggests that there is little conjugation between the sulfur lone-pair and the  $\pi$ -orbitals of the ring.

Kalabin and collaborators found that the trends begun in the spectra of substituted thioanisoles continue in the selenoanisoles<sup>38</sup>. The decrease in electronegativity upon descending Group VIA was seen to increase the shielding of the methyl carbon and the Cl-carbon. No evidence for d-orbital participation was found.

The shielding of the methylthio carbon in 4-nitrothioanisole demonstrates that an electron-withdrawing para-substituent can increase the degree of conjugation, indicating that thioanisole itself may not be effectively planar. The trend in hybridization of the heteroatom upon descending Group VIA involves an increase in the s-character of one lone pair and an increase in the p-character of the other<sup>31,39</sup>. The increase may be accompanied by a decrease in the bond angle at the heteroatom and therefore an increase in steric crowding in the planar conformation. The expected shielding at the heteromethyl and ortho carbons may be masked by the inductive effect of the heteroatom or by the proximate, mainly p-character, lone pair<sup>40</sup> which may be responsible for the deshielding of the ortho carbons of selenoanisole and telluroanisole<sup>41</sup>.

As the size of the alkylthio group increases, the shielding of the ortho carbon decreases, consistent with the idea that orthogonal conformations are populated

more with increasing alkyl size and therefore cause a closer approach of the sulfur lone pair to the ortho carbon<sup>42</sup>.

In summary, carbon chemical shifts can indicate heteromethyl group conformation in both liquid and solid phases. However, errors in the interpretation of deviant behaviour may be made since the additivity of substituent-induced shifts is only approximate.

(c) Liquid crystal NMR

The NMR spectra of ( $\alpha$ -<sup>13</sup>C)thioanisole, 4-chloro( $\alpha$ -<sup>13</sup>C)thioanisole, and 4-nitro( $\alpha$ -<sup>13</sup>C)thioanisole in liquid crystalline solvents were analysed by Emsley and co-workers<sup>49</sup>. It was concluded that the molecules cannot be entirely in the conformations with all heavy atoms co-planar. The data were shown to be consistent with a two-state model for the orientation of the SCH<sub>3</sub> group about the phenyl-sulfur bond, where there is one minimum at 0 and a local minimum at 90°, as well as with another model, considered less probable, having one minimum between 0 and 90°. The percentage of the planar form was estimated as between 84 and 50% for thioanisole and between 87 and 78% for 4-nitrothioanisole.

(d) Long range coupling constants to methyl protons.

Lunazzi and Macciantelli proposed that the observed long range coupling constants between methylthio and ortho protons,  ${}^5J(\text{SCH}_3, \text{H}_6)$ , in ortho substituted thioanisoles were dependent on the size of the substituent<sup>45</sup>. However, a careful analysis of the proton spectrum of 2,5-dichlorothioanisole<sup>46</sup> yielded a  ${}^5J(\text{CH}_3, \text{H}_6)$  of  $-0.35 \pm 0.02$  Hz, about twice the reported value for 2-chlorothioanisole. When the methylthio group preferred the plane perpendicular to the ring plane, as for 2-hydroxythioanisole<sup>40</sup>, the magnitude of  ${}^5J(\text{CH}_3, \text{H}_6)$  was less than 0.02 Hz. Therefore, the proximity of the protons involved seemed to dictate the magnitude of this type of coupling constant. The mechanism of other long range couplings in 2,5-dichlorothioanisole was not examined, but  ${}^6J(\text{CH}_3, \text{H}_3)$  and  ${}^7J(\text{CH}_3, \text{H}_4)$  were  $0.05 \pm 0.02$  Hz and  $-0.03 \pm 0.02$  Hz respectively.

The analogous couplings in pentafluorothioanisole and derivatives are generally larger and thus have been studied more extensively<sup>47,48</sup>. In a series of para-substituted tetrafluorothioanisoles, it is observed that the size of the coupling is dependent on the electron withdrawing ability of the substituent. The measured magnitudes are 1.6, 1.0, 0.95, 0.7, 0.6, and 0.5 Hz for the para substituents  $\text{NO}_2$ , Cl, H, F,  $\text{OCH}_3$ , and OH,

respectively. In 2,3,5-tri(methylthio)-4,6-difluorophenol, no coupling is reported between the methylthio group ortho to the hydroxyl and the adjacent fluorine--presumably an indication that this methylthio group prefers the plane orthogonal to the ring plane. In the corresponding compound where the hydroxyl group is replaced by a nitro group, the observed splittings in the SCH<sub>3</sub> peaks are 1.0, 2.65, and 2.65 Hz for the 2,3, and 5 positions respectively. Thus, the behaviour of  $^5J(\text{CH}_3, \text{F})$  is qualitatively similar to that of  $^5J(\text{CH}_3, \text{H})$ .

(viii) Molecular Orbital Calculations

Several molecular orbital calculations are available for thioanisole, generating a variety of potential curves and barrier heights for rotation about the C(sp<sub>2</sub>)-S bond. Most have employed partial geometry optimization and agree that the most stable conformation is planar.

Matsushita and co-workers studied the contribution of 3d orbitals of sulfur to the electronic structure<sup>50</sup>. Ab initio MO calculations utilized a minimal STO-3G basis set with the POLYATOM version 2<sup>51</sup> and GAUSSIAN 70<sup>52</sup> program packages. The calculated barrier in thioanisole was 1.0 kJ mol<sup>-1</sup> without the inclusion of d orbitals, and 1.3 kJ mol<sup>-1</sup> including d orbitals, suggesting a very small effect of 3d orbitals on the stable conformation and rotational barrier. The potential curve was said to be very flat because of cancellation between conjugation and steric hindrance in the interaction of the phenyl and SCH<sub>3</sub> groups. Two shallow minima were seen, one at which the dihedral angle was 0° and another at approximately 30°, with the methylthio group described as rotating almost freely. Similar conclusions were reached by Palmieri<sup>18</sup>.

An INDO SCF investigation gave the potential curve for para-nitrothioanisole<sup>55</sup>. The calculated energy was



directly proportional to  $\sin^2\theta$ , where  $\theta$  is the angle that the methyl carbon-sulfur bond makes with the phenyl ring plane. As noted in part (vi), the calculated barrier was  $13.2 \text{ kJ mol}^{-1}$ .

Schweig and Thon used a CNDO/2 method<sup>53</sup> in an spd basis with standard bond lengths<sup>54</sup> to calculate the total energy of thioanisole<sup>29</sup>. The planar form was seen to be most stable and the perpendicular conformer was described as a second stable form,  $8.6 \text{ kJ mol}^{-1}$  above the first. It was noted that the  $\text{C}(sp_2)\text{-S-C}(\text{methyl})$  angle decreased on going from the planar to the orthogonal form, indicating  $\text{CS}/\pi$  hyperconjugative and  $\text{d}/\pi$  conjugative interactions.

The calculated barrier in para-fluorothioanisole is  $4.0 \text{ kJ mol}^{-1}$ , as given by SCF ab initio calculations<sup>25</sup>. The minimum in the potential curve for the internal rotation about the phenyl-sulfur bond is at a dihedral angle of  $0^\circ$ . Very shallow local minima are seen at ca.  $60$  and  $120^\circ$ , perhaps indicating a small four-fold component in addition to a predominant two-fold component for the potential curve.

In summary, rotational isomerism in thioanisole appears to be the result of a delicate balance between steric interactions, which favour a non-planar heavy

atom skeleton, and  $\pi$ -conjugation, which favours a planar heavy atom skeleton.

## B. Introduction to the problem

Experimental studies of thioanisole suggest that, although the methylthio group prefers to lie in the plane of the aromatic ring, out-of-plane conformers are certainly not excluded. The shape, and notably the height, of the potential function describing the disposition of the exocyclic chain with respect to the benzene ring plane is uncertain. The conformation of the heteromethyl group may be dictated by steric interactions, which favour an orthogonal conformation, and by conjugation with the ring, which favours a planar heavy atom skeleton.

According to the J method<sup>55</sup> for the determination of small twofold rotational barriers in benzene derivatives, the barrier to internal rotation in thiophenol is 3.4 kJ mol<sup>-1</sup>. This method is based on the sin<sup>2</sup>ϕ dependence of the spin-spin coupling constant over six bonds between alpha and para nuclei and its analogy to the angular dependence of β-proton hyperfine interactions in radicals. One may write

$${}^6J = {}^6J_{,0} \langle \sin^2\phi \rangle + {}^6J_0 \quad (1)$$

where  ${}^6J_{,0}$  is the value of  ${}^6J$  when the bond of the side-chain lies orthogonal to the benzene ring plane,  $\phi$  is the dihedral angle between the bond of the sidechain and the benzene ring plane, the brackets indicate the expect-

tation value of  $\sin^2\theta$ , and  ${}^6J_0$  is the value of  ${}^6J$  when the sidechain is in the benzene plane.  ${}^6J_0$  is most often effectively zero<sup>5</sup>.

A possible extension of the  $J$  method to both onefold and twofold barriers is suggested by the five-bond spin-spin coupling constant between  $\alpha$  nuclei and nuclei at the meta position of the benzene ring<sup>4,7,56</sup>. This coupling is a composite of  $\sigma$ - $\pi$  and  $\sigma$  electron interactions. The former, discussed above, varies as  $\sin^2\theta$  and the latter as  $\sin^2(\theta/2)$ . Therefore, one may write

$${}^5J = {}^5J_{90} \langle \sin\theta \rangle + {}^5J_{180} \langle \sin^2(\theta/2) \rangle \quad (2)$$

where  ${}^5J_{90}$  is the size of the  $\sigma$ - $\pi$  component for  $\theta = 90^\circ$ , and  ${}^5J_{180}$  is the magnitude of the  $\sigma$  component for  $\theta = 0^\circ$ , or planar zigzag bond arrangement. The  $\sigma$ - $\pi$  contribution vanishes for conformations in which the sidechain lies in the molecular plane and the  $\sigma$  contribution vanishes only at  $\theta=0^\circ$ . When the sidechains are hydroxylic or aldehydic groups which have the conformation of Figure 3,

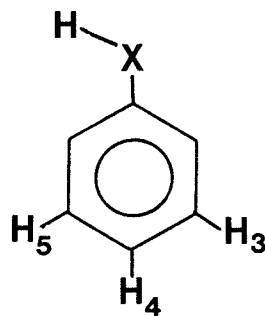


Figure 3

studies show the coupling to H-3 to be large ( $\theta=180^\circ$ )

and that to H-5 and H-4 ( $\phi=0^\circ$ ) to be very small or, more often, undetectable<sup>57-63</sup>.

The intent of this study is the description of the conformational preferences, and potential functions for internal rotation, in thioanisole and derivatives using stereospecific long-range NMR coupling constants and suggestions from MO calculations. The barriers may be larger in thioanisoles than in the corresponding thio-phenols because the methyl group is a stronger electron donor and may increase conjugation with the ring. Alternatively, the barrier may be smaller since steric interactions with ortho substituents destabilize the preferred planar conformation.

The J method utilizes the observed coupling between  $\alpha$  and ring protons. However, no  $\alpha$  proton exists in thioanisole. Therefore, one must resort to spin-spin couplings between the  $\alpha$  carbon (methyl carbon) and ring nuclei (proton and fluorine). The conformational and substitutional dependences of the NMR parameters are analysed in order that the principal mechanisms of spin-spin coupling, barriers to internal rotation, and conformational preferences may be estimated.

EXPERIMENTAL METHODS

## A. Materials and Syntheses

Thioanisole (Aldrich Chemical Company), 4-fluorothioanisole (PCR, Inc.), 3,5-dichlorothiophenol (Fairfield Chemical Company), 2-iodothioanisole (Maybridge Chemical Company), and 4-methylthiophenol (Aldrich) were commercially available. The syntheses of other compounds are described below.

Acetone- $d_6$ , benzene- $d_6$ , and cyclohexane- $d_{12}$  were all from Aldrich and of 99.5 atom% purity. These were used as an internal deuterium lock signal and as solvents, except that cyclohexane- $d_{12}$  was used with 80% (w/w) carbon tetrachloride (Fisher Scientific Company). Either tetramethylsilane or acetone- $d_6$  was used as an internal proton reference.

## (i) methylation of thiophenols

The methylation of the thiol group of thiophenol(Aldrich), 2-iodothiophenol, 2,6-chlorothiophenol (Fairfield), tetrafluorothiophenol(Aldrich), 3,5-dichlorothiophenol(Fairfield), and 3,5-dimethylthiophenol to obtain the corresponding thioanisoles isotopically enriched with  $^{13}\text{C}$  in the methyl group was accomplished by the standard method<sup>6,4</sup> of adding ( $^{13}\text{C}$ )methyl iodide (99 atom%, MSD Isotopes, Inc.) to a mixture of the thiophenol and anhydrous potassium carbonate in dry acetone. Products were identified by  $^1\text{H}$  NMR and mass spectrometry.

The methylation of 2-iodothiophenol, 2,4,5-trichlorochlorothiophenol(Aldrich), 2,6-dichlorothiophenol (Fairfield), 2-bromothiophenol(Aldrich), 4-nitrothiophenol (Aldrich), pentafluorothiophenol(Aldrich), 2,3,5,6-tetrafluorothiophenol(Aldrich), and 4-methylthiophenol (Aldrich) was accomplished via a somewhat faster method of adding dimethyl sulfate (Eastman-Kodak Company) to the aqueous sodium thiolate. A typical procedure involved dissolving ca. 1.5 g of the thiophenol in 10 ml of 20% NaOH and adding dropwise a 10% stoichiometric excess of dimethyl sulfate over a fifteen minute period to the magnetically stirred solution. This was stirred



for an additional forty-five minutes and then extracted twice with 50 ml ether. The ethereal layer was washed twice with water (2X50 ml), dried over magnesium sulfate and then the solvent was removed on a rotary evaporator. Yields of the corresponding thioanisoles were typically greater than 85%. Product identity was established by the absence of the characteristic smell of the thiophenol, the NMR spectra of the appropriate nuclei, and often by mass spectrometry.

(ii) Syntheses of thioanisoles from anilines

The remaining thioanisoles were prepared from the diazonium salts of the corresponding anilines, by a procedure developed in this laboratory<sup>65</sup>. 2,6-dibromoaniline, 2,6-difluoroaniline, and 2-methyl-3-fluoroaniline were available from Aldrich. 2,6-dibromo-4-methylaniline (Alfa Division), 2-bromo-4-fluoroaniline (Maybridge), 2,6-dibromo-4-fluoroaniline, 2,4,6-trifluoroaniline (Fairfield), and 2,4,6-tribromo-3-fluoroaniline (gift from Dr. L. J. Kruczynski) were also used. The procedure involved the treatment of the aqueous diazonium hydrosulfate salt with cuprous methylmercaptide (methylthiocopper)<sup>65</sup>. The method is similar to the widely applicable introduction of a thiocyanato group into an aromatic ring<sup>66</sup>. Product identity was confirmed by <sup>13</sup>C, <sup>19</sup>F, and <sup>1</sup>H NMR spectroscopies and by mass spectrometry.

(iii) Synthesis of 2-iodo- and 3,5-dimethylthiophenol

2-iodothiophenol and 3,5-dimethylthiophenol were prepared from the corresponding anilines (available from Aldrich) via diazotization, treatment with potassium ethyl xanthate, and xanthate decomposition by hydroxide ion<sup>67,68</sup>. Products were identified by their characteristic odour and by <sup>1</sup>H NMR spectroscopy. Identity of the methylated products was established by <sup>1</sup>H NMR spectroscopy and mass spectrometry.

## (iv) Bromination of 4-fluoroaniline

The bromination of 4-fluoroaniline (Aldrich) was accomplished by the addition of bromine to a cooled solution of the compound in dry tetrahydrofuran. The hydrobromic acid produced was neutralized by a stoichiometric amount of 20% sodium hydroxide. The tetrahydrofuran layer was pipetted out, reduced in volume almost to dryness, and the residue was taken up in carbon tetrachloride. This solution was washed once with an aqueous bisulfite solution and with water, and then dried over magnesium sulfate. The solvent was removed on a rotary evaporator to yield crude product, which was recrystallized from ethanol to yield long pale yellow needles. The  $^1\text{H}$  NMR spectrum was confirmatory for 2,6-dibromo-4-fluoroaniline.

## B. Sample Preparation

Solutions of thioanisoles were prepared by weight to consist generally of 2 mol per cent of the compound of interest in acetone- $d_6$  or benzene- $d_6$  for  $^1H$  and  $^{19}F$  NMR. Thiophenols were prepared in carbon tetrachloride/cyclohexane- $d_{12}$ , or benzene- $d_6$ , and solutions were dried according to the procedure of Rowbotham and Schaefer<sup>69</sup>.

Each solution was filtered through a pipette, containing a wad of cotton wool cleaned with carbon tetrachloride, into a precision bore 5 mm o.d. NMR tube fitted with a ground glass joint. Tubes with thiophenol solutions also held one or two pieces of molecular sieve (pore mesh size of 3 Å) to hinder intermolecular exchange. Sample depth lay between approximately 3.5 and 5 cm. Samples were degassed by at least five freeze-pump-thaw cycles before the tube was sealed with a torch.

Samples for  $^{13}C$  NMR spectroscopy were prepared by volume or by weight as solutions in acetone- $d_6$ . Filtered solutions in 10 mm o.d. NMR tubes were degassed if the required resolution was better than 0.2 Hz. Otherwise, the samples were filtered into 10 mm tubes which were then fitted with pressure caps. Sample depth lay between four and six centimetres.

### C. Spectroscopic method

Proton, fluorine, and carbon magnetic resonance free induction decays were recorded on a Bruker WH90-DS spectrometer at a probe temperature of 305K and at transmitter frequencies of 90.02, 84.70, and 22.63 MHz respectively. The spectrometer uses a Bruker magnet and console, except that it employs a 293 A' programmer and an 1180 data system and the associated software from Nicolet Technology Corporation. The B<sub>1</sub> fields for multiple resonance experiments were previously calibrated with off-resonance techniques and could be regulated in 1-db steps<sup>70,71</sup>. In order to obtain proton spectra at temperatures between 250 and 305K, a standard Bruker B-VT-100 variable temperature accessory was used. This temperature controller had been previously calibrated<sup>72</sup> and was found to be within  $\pm 1$ K of the temperature indicated by the controller. Cooling of the probe below ambient room temperature was accomplished by the passage of a stream of nitrogen gas, which was passed through a heat-exchange coil immersed in liquid nitrogen, before passing through the probe assembly.

Proton and carbon spectra were also recorded on a Bruker AM300 spectrometer, which employs an ASPECT 3000 data system. Spectra from this spectrometer were generally preferred over those from the WH90 because of the

greater signal-to-noise ratio and relative simplicity of the spectra due to the higher field and because of the better resolution due to the higher stability of the superconducting magnet.

Pulse lengths produced approximately  $70^\circ$  flip angles, with equilibrium delays of approximately 5 seconds. In order to measure C,H spin-spin coupling constants the INEPT sequence<sup>7,3</sup> was used. Digital resolution was typically 0.05 Hz/real point or better. Typically,  $^1\text{H}$  spectra from the WH90 were recorded with 1 scan summed into 16K, and zero-filling with an additional 16K was performed before Fourier transformation. At times, the digital resolution was not as high as desired, due to limitations of computer capability of the 1180 data system, resulting in some slight discrepancies between observed and calculated spectra.  $^1\text{H}$  spectra from the AM300 were usually recorded with 8 scans summed into sufficient memory to give acquisition times of at least thirty seconds.

32 transients were summed into 16K, with an additional 16K of zero filling for  $^{19}\text{F}$  spectra.  $^{13}\text{C}$  spectra were recorded with enough scans to yield a sufficient signal-to-noise ratio. The acquisition parameters are noted specifically in the next chapter.

Resolution enhancement was performed in most cases by manipulation of the free induction decay (FID) with either sine multiplication or with a combination of an increasing exponential function and a negative line broadening parameter. Both of these methods emphasize the FID data at long times, resulting in increased resolution with a decreased signal-to-noise ratio, and more or less retain the non-enhanced line shape of the NMR signal.



#### D. Computations

Spectral simulations were performed with the LAME<sup>74,75</sup> program or with NUMARIT<sup>76,77</sup> in non-iterative and iterative modes. These were coupled to a plotting routine on a Versatec plotter. Unfortunately, the scaling of plots of the plotter was often two or three per cent incorrect. Therefore, comparisons between some observed and calculated spectra should take this into consideration.

Ab initio molecular orbital calculations were performed at the STO-3G<sup>78</sup> level with the MONSTERGAUSS<sup>79</sup> program. Semi-empirical calculations<sup>53</sup> and calculations of coupling constants were performed with INDO MO FPT<sup>80</sup> on the optimized geometry from the ab initio calculations.

The computations were performed on an Amdahl 470/V7 or on an Amdahl 5850.

EXPERIMENTAL RESULTS

### A. High Resolution Spectra

The observations and numerical results in this chapter represent analyses of proton, fluorine, and carbon spectra of some of the thiophenol and thioanisole derivatives investigated. Spectral parameter values from proton and/or fluorine spectra are calculated by LAME unless otherwise stated. Useful confidence intervals<sup>1,2</sup> on parameter values are probably given by thrice the standard deviation calculated by LAME, or NUMARIT, which follow after the value in parentheses. The given linewidths are the narrowest observed in the spectrum of the compound of interest. Frequencies and coupling constants are given in Hz. All proton chemical shifts are referenced relative to TMS, unless otherwise stated. Only transitions with intensities greater than 0.05 are considered in most cases. Rms deviation refers to the root-mean-square difference between calculated and observed line positions (frequencies).

In some proton spectra, and in most carbon spectra, coupling constants are set equal to the observed spectral line splittings under the assumption of first order behaviour<sup>3-5</sup>. The 95% confidence limits of the parameters are calculated from the number of measurements and the root-mean-square deviation of the magnitude of the observed splittings<sup>6</sup>. The confidence limits of the

parameter are denoted by a plus or minus sign, and follow the parameter value. Tabulations of parameter values and errors deduced by other means specifically state the method used. Parameters that appear without an estimation of the associated error were held constant for the iterative part of the calculation of parameters. The quoted values reflect the magnitudes of linewidth and digital resolution. Unless specifically mentioned, spectral parameters correlate poorly with each other (a correlation coefficient, as calculated by LAME, of less than 0.30).

The signs of proton-proton<sup>4,6</sup>, proton-fluorine<sup>8,7</sup>, and carbon-fluorine<sup>8,7-8,9</sup> spin-spin coupling constants were assumed from the literature, unless otherwise indicated.

(i) thioanisole

The aromatic region of the  $^1\text{H}$  NMR spectrum of a 2 mol % solution of thioanisole in benzene- $d_6$  appears as Figure 4. The methyl protons are shown in Figure 5. Figures 6 and 7 show the ortho proton and part of the para proton resonances in order to illustrate the spectral quality. The spectral simulations in figures 5-7 are based upon the spectral parameters given in Table 1.

Spectral parameters for a 1.7 mol % solution of thioanisole isotopically enriched with  $^{13}\text{C}$  at the methyl carbon in benzene- $d_6$  at 300K are given in Table 2. The parameters are for the coupled spectrum obtained by the Fourier transformation of 32 free induction decays with a negative line broadening of 0.12 Hz and a Gaussian factor of 0.5. The acquisition time for the data was 35 seconds, which was accumulated into 16K of memory with an additional 48K for zero-filling added before Fourier transformation. Figures 8 and 9 show parts of the meta and para proton resonances. The additional splitting for the para proton spectrum is due to the  $\alpha$ - $^{13}\text{C}$  nucleus and is  $-0.147(1)$  Hz (cf. Figure 7).

## Figure 4

Spectrum of the ring protons of a 2 mol % solution of thioanisole in benzene-d<sub>6</sub> at 300.135 MHz at 293K.

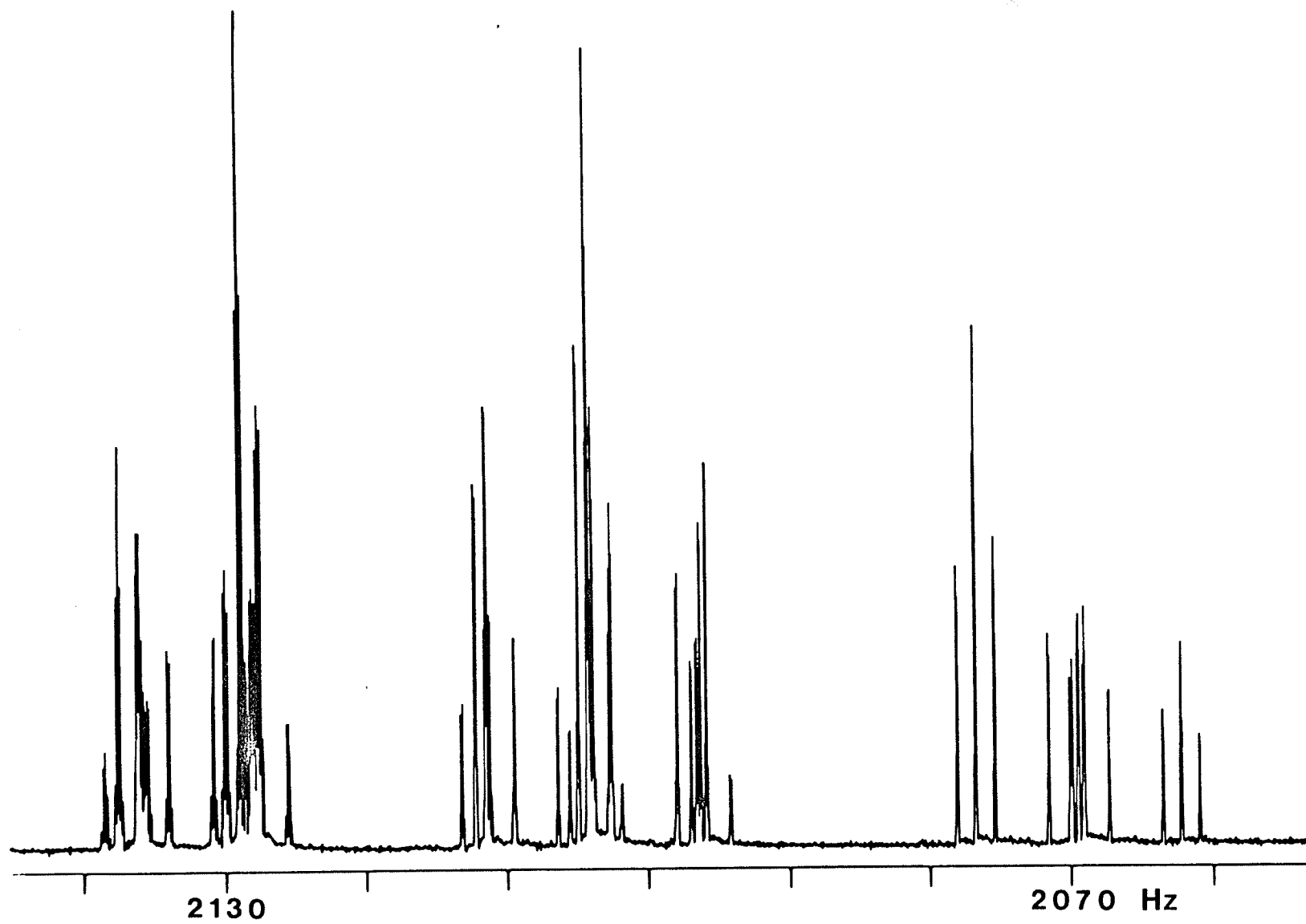


## Figure 5

The experimental and calculated spectra of the methylthio protons of thioanisole in benzene- $d_6$ .



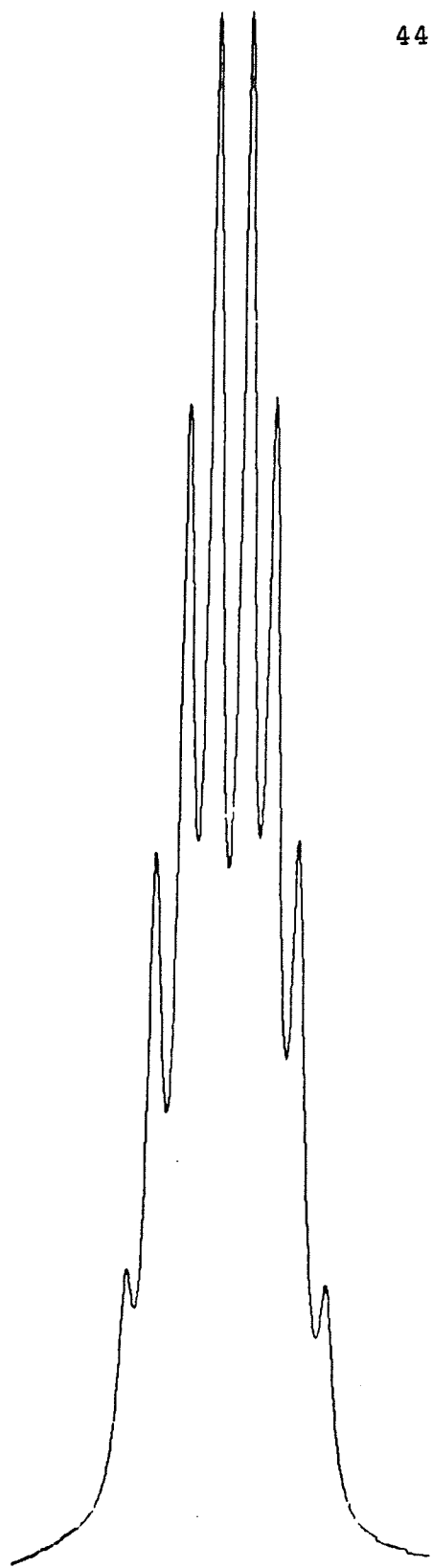
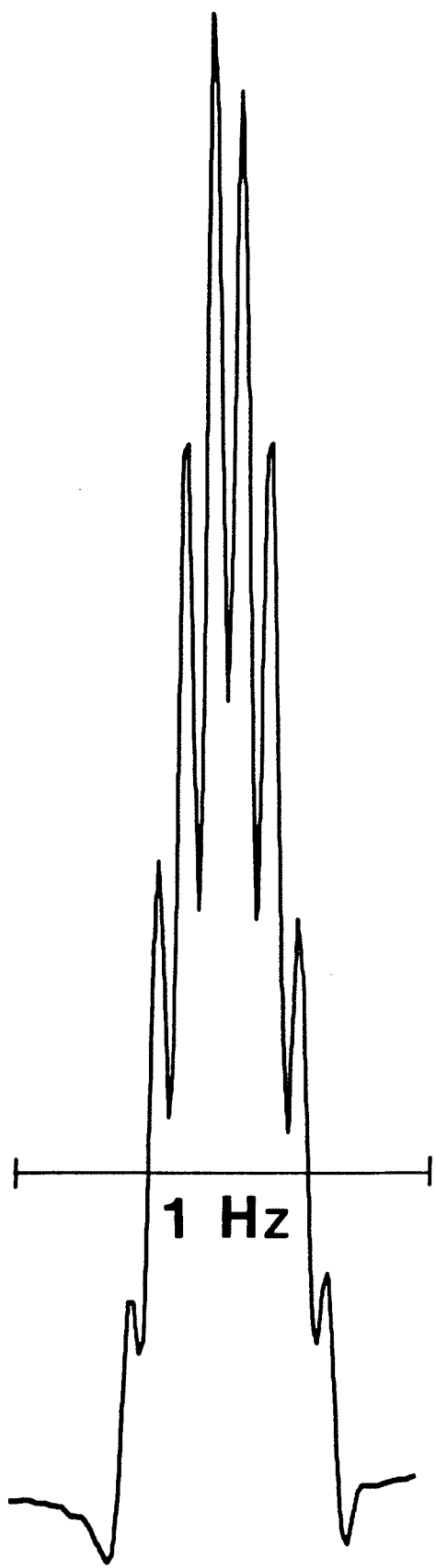


## Figure 6

The ortho proton resonance of thioanisole in benzene-d<sub>6</sub>.

(a) calculated spectrum

(b) observed spectrum

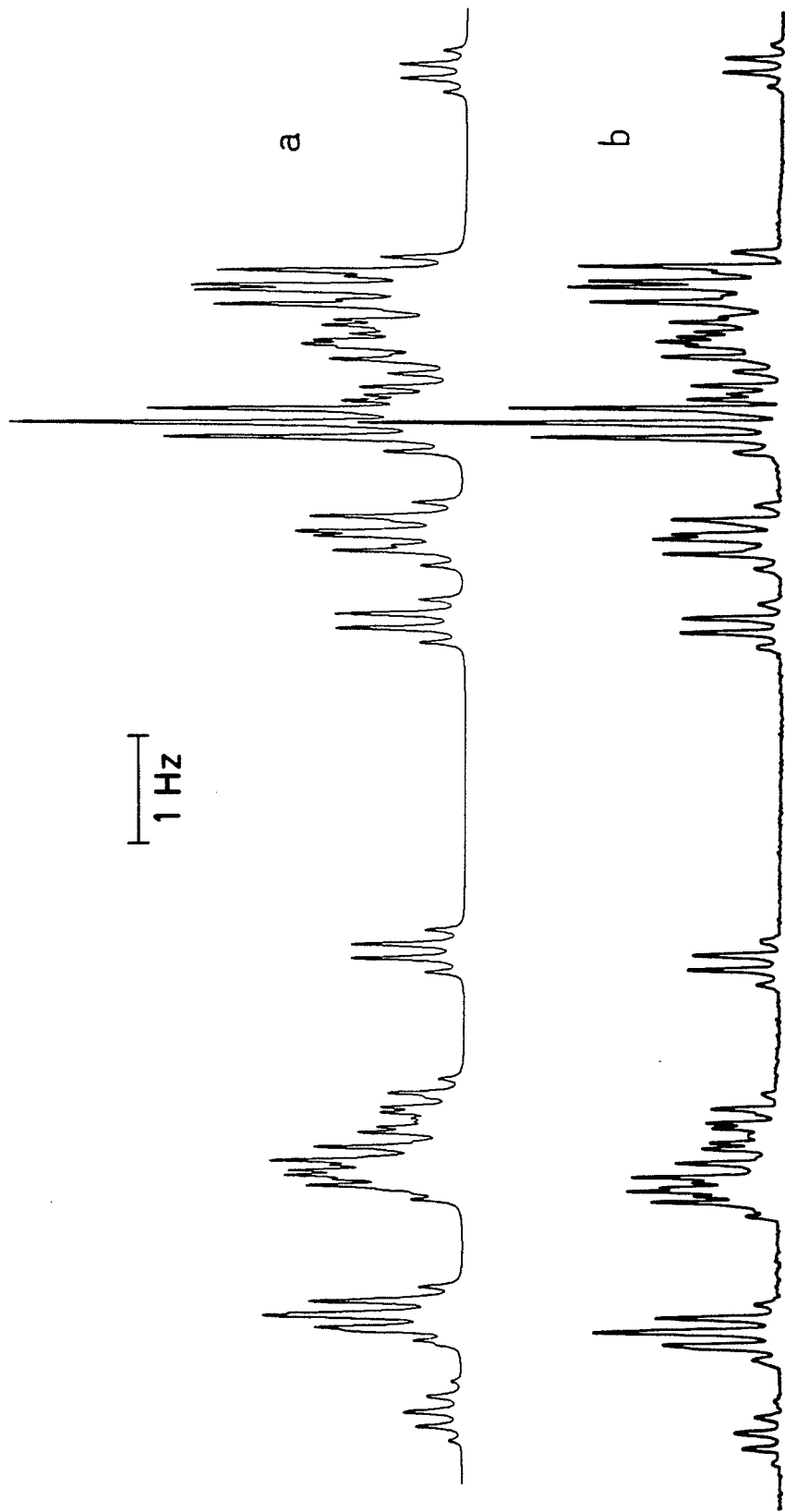


## Figure 7

Part of the para proton resonance of thioanisole in benzene-d<sub>6</sub>.

- (a) observed spectrum
- (b) calculated spectrum

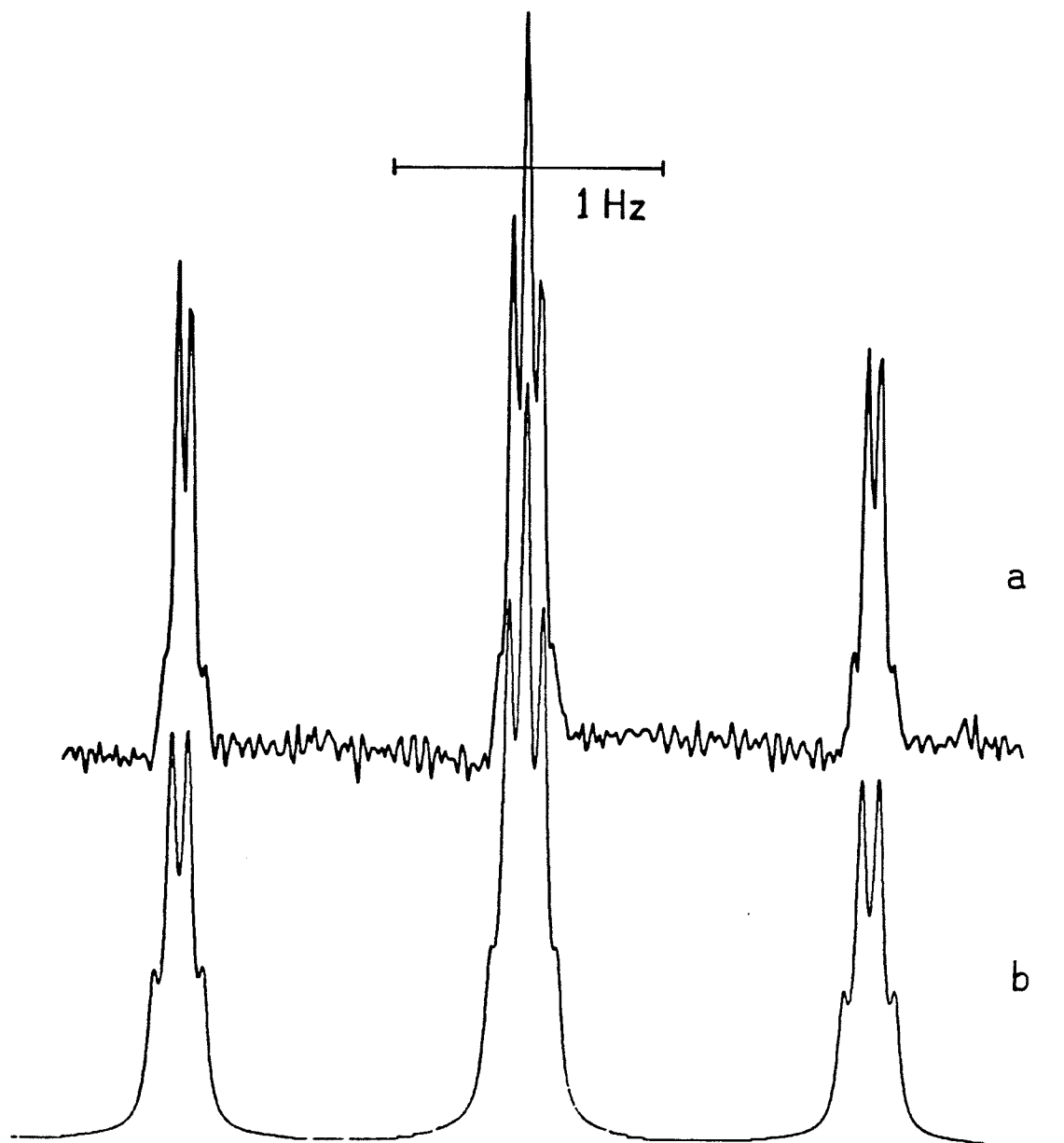
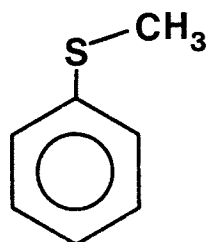


Table 1

Spectral parameters for thioanisole in benzene-d<sub>6</sub>.

	300.135MHz
$\nu(\text{CH}_3)$	590.665(0)
$\nu_2 = \nu_6$	2131.905(1)
$\nu_3 = \nu_5$	2104.034(1)
$\nu_4$	2070.157(1)
$J(\text{CH}_3, \text{H}_2)$	-0.141(0)
$J(\text{CH}_3, \text{H}_3)$	0.075(0)
$J(\text{CH}_3, \text{H}_4)$	-0.053(1)†
$J(\text{H}_2, \text{H}_3)$	7.938(1)
$J(\text{H}_2, \text{H}_4)$	1.155(1)
$J(\text{H}_2, \text{H}_5)$	0.547(0)
$J(\text{H}_2, \text{H}_6)$	2.109(1)
$J(\text{H}_3, \text{H}_4)$	7.435(1)
$J(\text{H}_3, \text{H}_5)$	1.551(1)
observed peaks	178
assigned peaks	167

...Table 1 continued...

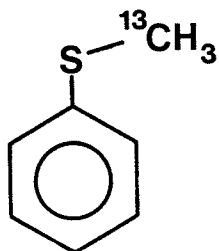
Table 1...

transitions calcd.	512
assigned transitions	426
largest deviation	0.014
rms deviation	0.0054
line width	0.045

† This result is from an analysis that does not include the methyl protons. Since the couplings to the methyl protons are of the magnitude and sign that they are, the methyl peaks consist of several overlapping lines, and therefore analysis including these spectral lines may be inaccurate for certain spectral parameters. Such is the case for  ${}^1J(\text{CH}_3, \text{H}_4)$ , which was given as 0.065(1) in an analysis including the methyl protons. Other parameters were not sensitive to overlapping lines in the methyl region<sup>90</sup>.

Table 2

Spectral parameters for a 1.7 mol % solution of ( $\alpha$ - $^{13}\text{C}$ )thioanisole in benzene- $d_6$ .



$\nu(\text{CH}_3)$	590.665†
$\nu_2 = \nu_6$	2133.389(0)
$\nu_3 = \nu_5$	2104.120(0)
$\nu_4$	2070.173(1)
$J(\text{CH}_3, \text{H}_2)$	-0.137(0)
$J(\text{CH}_3, \text{H}_3)$	0.079(0)
$J(\text{CH}_3, \text{H}_4)$	-0.055(1)
$J(\text{H}_2, \text{H}_3)$	7.936(0)
$J(\text{H}_2, \text{H}_4)$	1.154(1)
$J(\text{H}_2, \text{H}_5)$	0.550(0)
$J(\text{H}_2, \text{H}_6)$	2.104(1)
$J(\text{H}_3, \text{H}_4)$	7.436(1)
$J(\text{H}_3, \text{H}_5)$	1.551(1)
$J(\text{C}_\alpha, \text{H}_2)$	0.00
$J(\text{C}_\alpha, \text{H}_3)$	0.078(1)
$J(\text{C}_\alpha, \text{H}_4)$	-0.147(1)
$J(\text{C}_\alpha, \text{CH}_3)$	139.76

...Table 2 continued...



## Table 2...

observed peaks	202†
calculated peaks	194
transitions calcd.	800
transitions assigned	612
largest deviation	.017
rms deviation	0.0058
line width	0.045

† Only peaks in the aromatic region are assigned. The CH<sub>3</sub> resonance frequency is that of the non-enriched compound. The one-bond coupling constant is not accurately determined.

## Figure 8

Part of the meta proton resonance of ( $\alpha$ - $^{13}\text{C}$ )thioanisole  
in benzene- $\text{d}_6$ .

(a) calculated

(b) observed

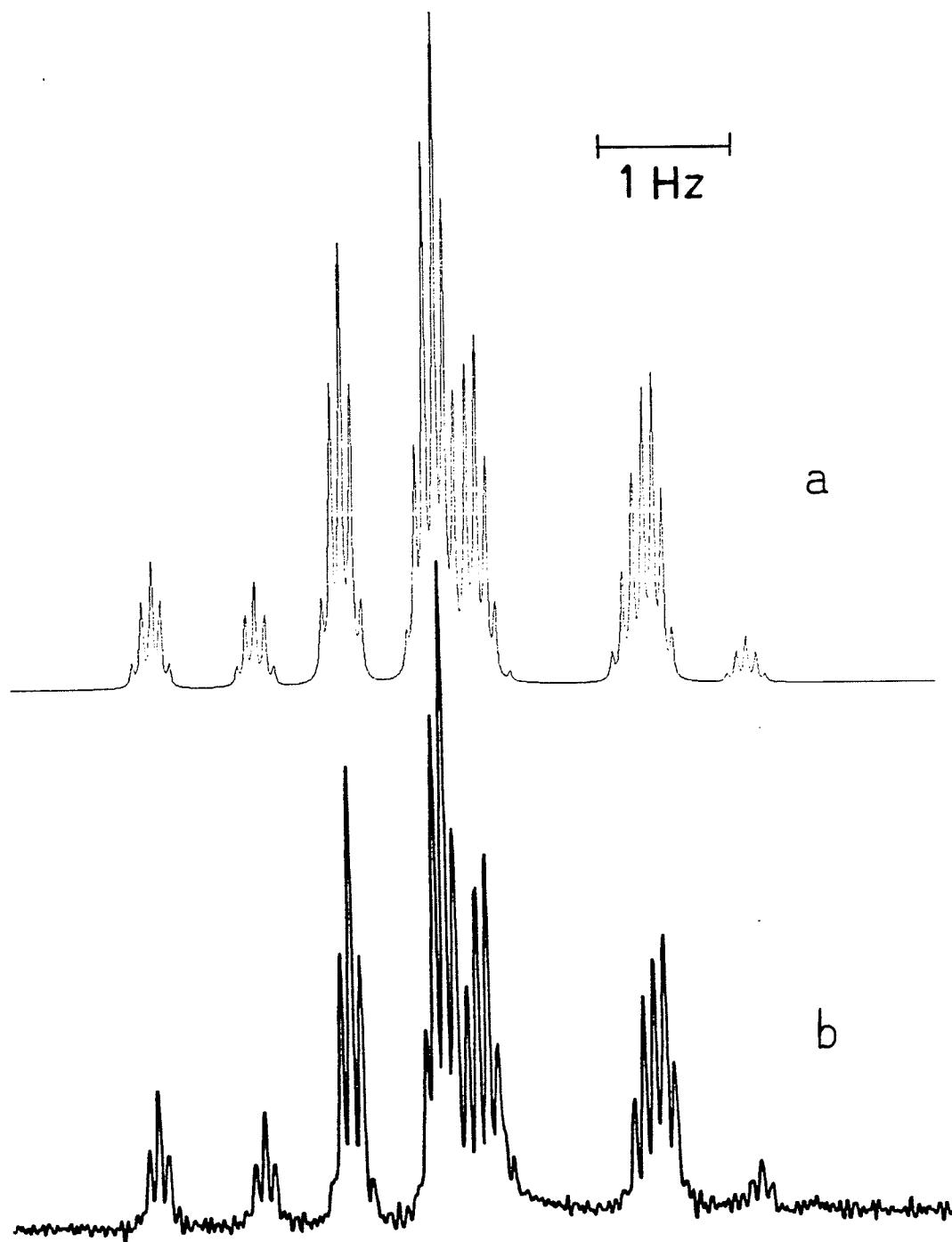
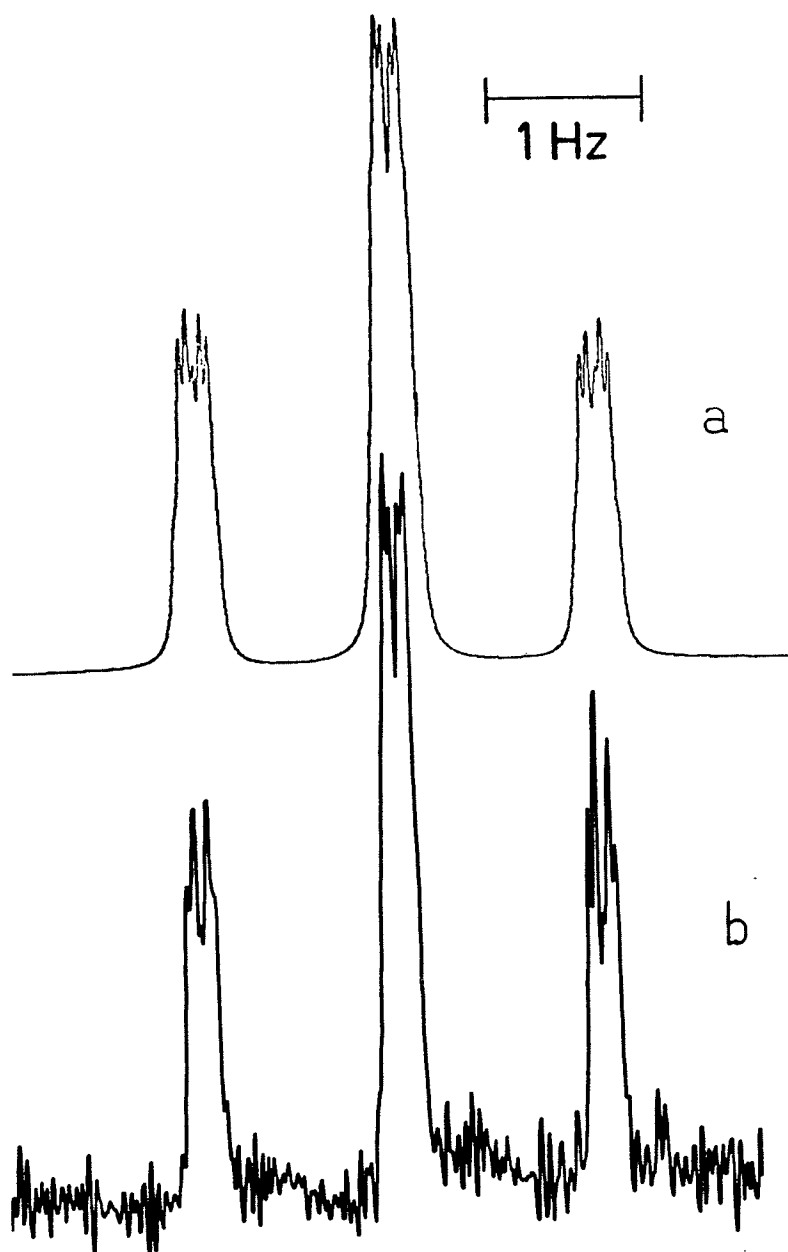


## Figure 9

Part of the para proton resonance of ( $\alpha$ - $^{13}\text{C}$ )thioanisole  
in benzene- $\text{d}_6$ .

(a) calculated

(b) observed

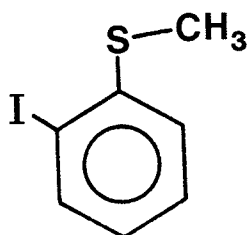


(ii) 2-iodothioanisole

Analysis of the  $^1\text{H}$  NMR spectrum of 2.0 mol % solutions of 2-iodothioanisole and 2-iodo( $\alpha$ - $^{13}\text{C}$ )thioanisole in acetone- $d_6$  yielded the results in Table 3. Six- and seven-bond proton-proton coupling constants were held at zero. From comparisons of line widths between H6 and the other proton spectral lines, the magnitude of these unresolved long range couplings to the methylthio protons are all about 0.05 Hz (data not shown). The sign of the four-bond carbon-proton coupling constant was determined by decoupling of the methyl resonances, first, with the carbon in what is designated as the - spin state (Figure 10a), and, second, with the carbon nucleus in the + spin state (Figure 10b), while observing the H6 proton spectral region. Since the ratio of the  $C\alpha$ - $H\alpha$  and  $C\alpha$ -H6 coupling constants is shown to be positive in Figure 10, and the former can be safely assumed to be positive, the latter is also positive. A first order representation of the line spectrum of the decoupling experiment appears in Figure 11.

Table 3

Parameters from the  $^1\text{H}$  NMR spectrum of 2-iodothioanisole in acetone- $d_6$ .



	90.024MHz
$\nu(\text{CH}_3)$	222.130
$\nu_3$	702.027(1)
$\nu_4$	619.823(1)
$\nu_5$	665.081(2)
$\nu_6$	647.888(1)
$J(\text{CH}_3, \text{H6})$	-0.394(1)
$J(\text{CH}_3, \text{H5})$	0.000
$J(\text{CH}_3, \text{H4})$	0.000
$J(\text{CH}_3, \text{H3})$	0.000
$J(\text{H5}, \text{H6})$	7.980(2)
$J(\text{H4}, \text{H6})$	1.492(2)
$J(\text{H3}, \text{H6})$	0.314(2)
$J(\text{H4}, \text{H5})$	7.376(2)
$J(\text{H3}, \text{H5})$	1.388(6)
$J(\text{H3}, \text{H4})$	7.844(6)

...Table 3 continued...

Table 3...

$^4J(C\alpha, H6)$	+0.172±0.012
$^5J(C\alpha, H3)$	+0.133±0.013
largest deviation	0.021
rms deviation	0.0082
observed peaks	45
assigned peaks	42
transitions calcd.	191
assigned transitions	172
line width	0.1 Hz

The parameter values listed above that do not refer to  $C\alpha$  are from a LAME analysis of a 2.0 mol % solution of 2-iodothioanisole in acetone- $d_6$ . The  $C\alpha$ -H coupling constants are set equal to the observed splittings of the spectral lines of a 2.0 mol % solution of 2-iodo( $\alpha$ - $^{13}C$ )thioanisole in acetone- $d_6$ .

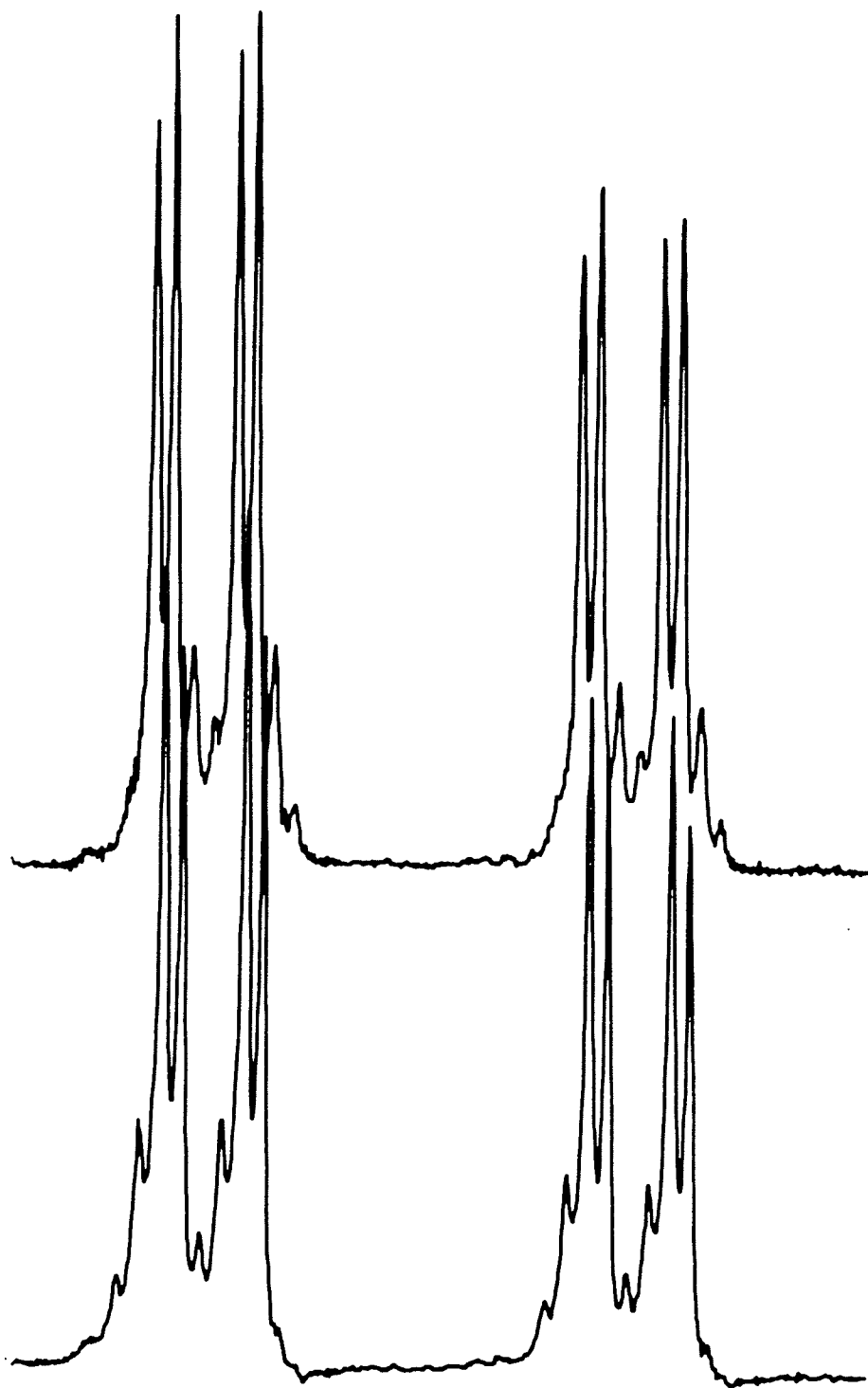


## Figure 10

The H6 region of 2-iodo( $\alpha$ - $^{13}\text{C}$ )thioanisole in acetone- $d_6$  at 300 MHz with:

- (a) decoupling the  $\text{CH}_3$  protons for the + spin state of  $\text{C}\alpha$ .
- (b) decoupling the  $\text{CH}_3$  protons for the - spin state of  $\text{C}\alpha$ .

—|—  
2 Hz



a

b

## Figure 11

A first order representation of part of the H6 region of 2-iodo( $\alpha$ - $^{13}\text{C}$ )thioanisole. The scale is 0.5 Hz/cm.

- (a) decoupling of the methylthio protons
- (b) decoupling the  $\text{CH}_3$  protons for the + spin state of  $\text{C}\alpha$ , or alternatively, allowing only  $\text{CH}_3$  protons for the - spin state of  $\text{C}\alpha$  to couple in.
- (c) decoupling the  $\text{CH}_3$  protons for the - spin state of  $\text{C}\alpha$ , or alternatively, allowing only  $\text{CH}_3$  protons for the + spin state of  $\text{C}\alpha$  to couple in.

Diagrams (b) and (c) are drawn assuming that  $^4J(\text{C}\alpha, \text{H})$  is positive. The effect of the methylthio protons coupling in Figure 11a would be to further split the lines by 0.394 Hz into 1:3:3:1 quartets. Decoupling the methyl peak that corresponds to a spin state of the carbon yielded spectra analogous to (b) and (c).

Note that the diagrams are drawn only for one half of the H6 region (Figure 10).

CH<sub>3</sub>C $\alpha$ 

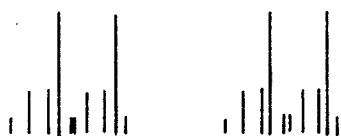
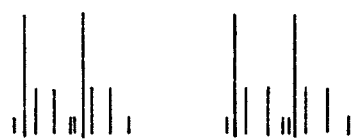
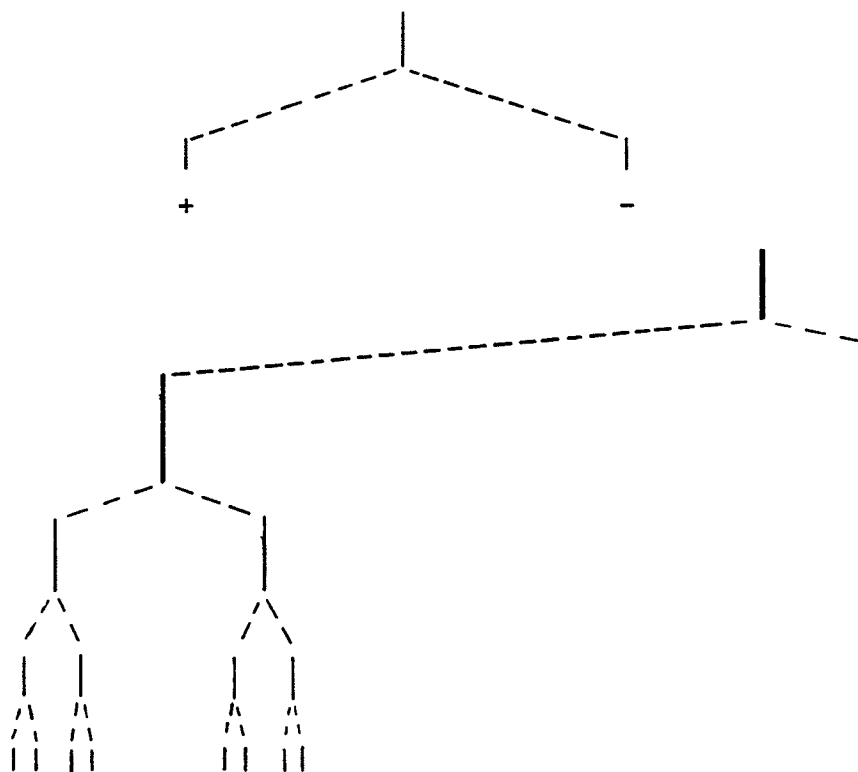
H6

(a)

H5	++	++	++	++
H4	++	++	--	--
H3	++	--	++	--
C $\alpha$	+-	+-	+-	+-

(b)

(c)



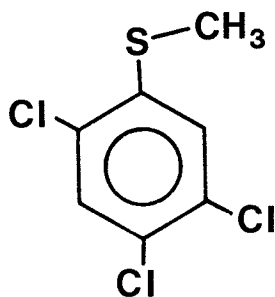
## (iii) 2,4,5-trichlorothioanisole

The spectral parameters for the  $^1\text{H}$  NMR spectrum (obtained at 300.135 MHz) of a 2.4 mol % solution of 2,4,5-trichlorothioanisole in acetone- $d_6$ , and for the  $^{13}\text{C}$  NMR spectrum (obtained at 75.486 MHz) of the methyl carbon of a 16.6 mol % solution in benzene- $d_6$ , appear in Table 4. The  $^1\text{H}$  NMR spectrum of the benzene solution established H3 as the higher field resonance, but for the benzene solution the chemical shift dispersion is ca. 106 Hz (data not shown). The origin of the coupling to the  $\alpha$  carbon is established by decoupling one of the aromatic protons and recording the coupled carbon spectrum. The spectrum obtained is the result of 128 transients summed into 32K memory with an acquisition time of about 27 seconds.

The proton spectrum was analysed by LAME for which all observed peaks were assigned. The rms deviation was 0.0041 Hz. The coupling constants involving  $\text{C}\alpha$  were set equal to the observed splittings of the spectral lines.

Table 4

Spectral parameters for 2,4,5-trichlorothioanisole



	300.135 MHz
$\nu(\text{CH}_3)$	777.816(0)
$\nu_3$	2284.727(1)
$\nu_6$	2219.060(1)
$J(\text{CH}_3, \text{H3})$	0.075(1)
$J(\text{CH}_3, \text{H6})$	-0.412(1)
$J(\text{H3}, \text{H6})$	0.284(1)
$J(\text{C}_\alpha, \text{CH}_3)$	140.229±0.013
$J(\text{C}_\alpha, \text{H3})$	0.194±0.011
$J(\text{C}_\alpha, \text{H6})$	-†

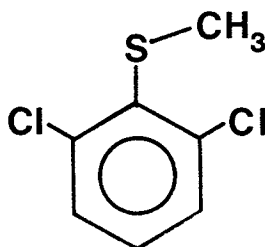
† not determined

## (iv) 2,6-dichlorothioanisole

The NMR spectrum of the methyl carbon of a 22 mol % solution of 2,6-dichlorothioanisole in benzene- $d_6$  yielded the spectral parameters appearing in Table 5, which also includes the spectral parameters for the  $^1\text{H}$  NMR spectrum of a 4 mol % solution of 2,6-dichloro( $\alpha$ - $^{13}\text{C}$ )thioanisole in acetone- $d_6$ . The proton spectrum of the ring protons of 2,6-dichloro( $\alpha$ - $^{13}\text{C}$ )thioanisole appears as Figure 12. Figure 13 shows the sign determination of the five-bond spin-spin coupling constant between the  $\alpha$  carbon and the meta proton. The method used is the same as for 2-iodo( $\alpha$ - $^{13}\text{C}$ )thioanisole. The spectral simulations in the figure show that  $^5J(\text{C}\alpha, \text{H})$  and  $^6J(\text{C}\alpha, \text{H})$  cannot be of the same sign, assuming that the three-bond proton-proton coupling constant is positive. The five-bond carbon-proton coupling constant is positive, and, therefore, the six-bond carbon-proton coupling constant is negative.

Table 5

Spectral parameters for 2,6-dichlorothioanisole



	90.024MHz	22.63 MHz†
$\nu(\text{CH}_3)$	218.875	-
$\nu_3 = \nu_5$	675.198(3)	-
$\nu_4$	661.968(2)	-
$J(\text{CH}_3, \text{H}3)$	0.05‡	-
$J(\text{CH}_3, \text{H}4)$	0.002(2)	-
$J(\text{C}\alpha, \text{H}3)$	0.211(5)	0.219±0.004
$J(\text{C}\alpha, \text{H}4)$	-0.519(4)	-0.500±0.005
observed peaks	15	20
assigned peaks	14	-
transitions calcd	87	-
transitions assigned	63	-
rms deviation	0.0104	-
largest difference	0.023	-

† The proton spectrum was of a 4 mol % solution in acetone- $d_6$ , and the carbon spectrum was of a 22 mol % solution in benzene- $d_6$ . Note that  $^6J(\text{C}\alpha, \text{H}4)$  is nearly the same for both solutions.

‡ Estimated from line width narrowing upon decoupling.



## Figure 12

The aromatic  $^1\text{H}$  spectrum of 2,6-dichloro( $\alpha$ - $^{13}\text{C}$ )thioanisole

- (a) Spectral simulation with  $^5\text{J}/^6\text{J} > 0$
- (b) Observed
- (c) Spectral simulation with  $^5\text{J}/^6\text{J} < 0$

The peaks marked by an asterisk are shown with higher spectral quality in Figure 13.

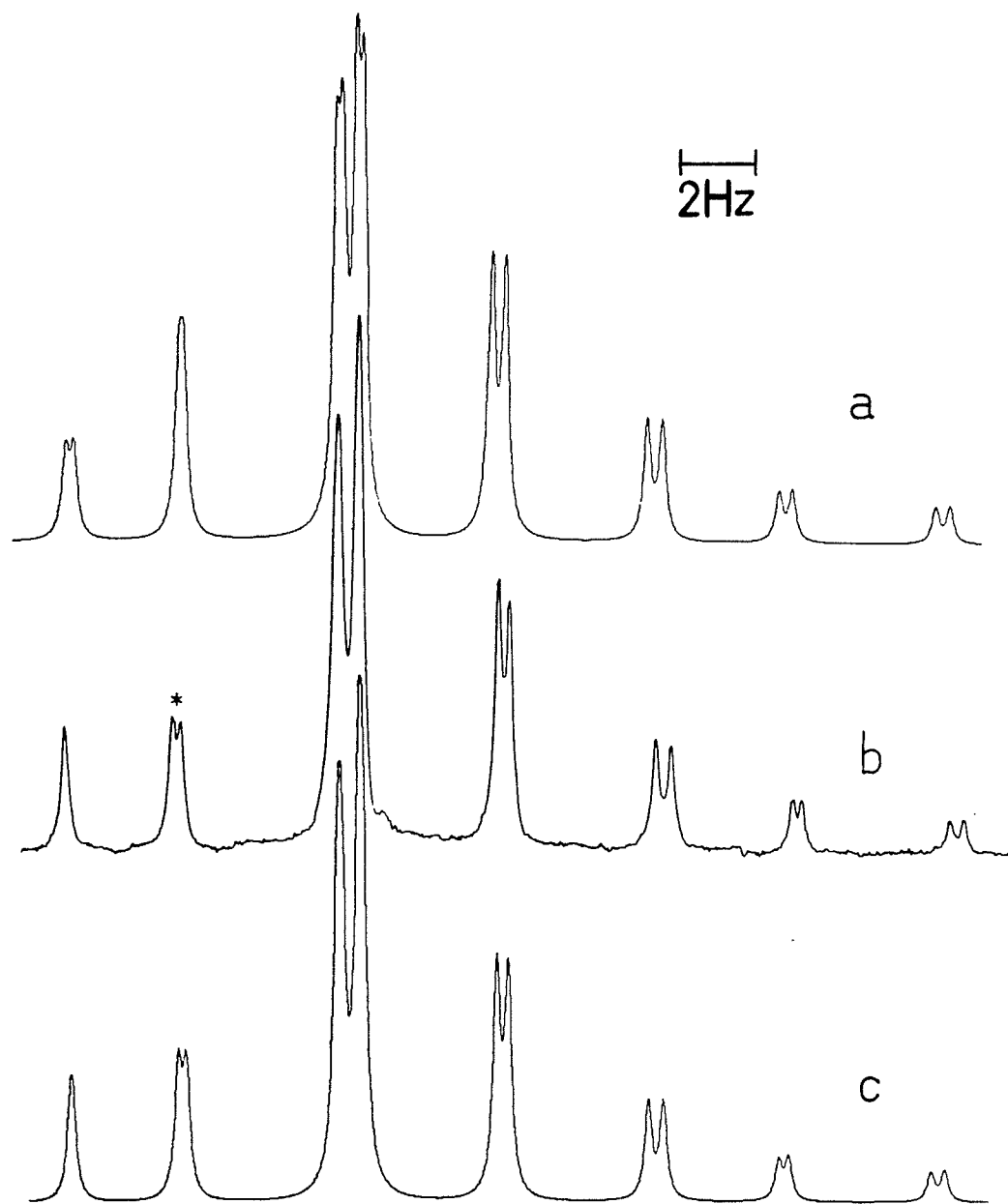
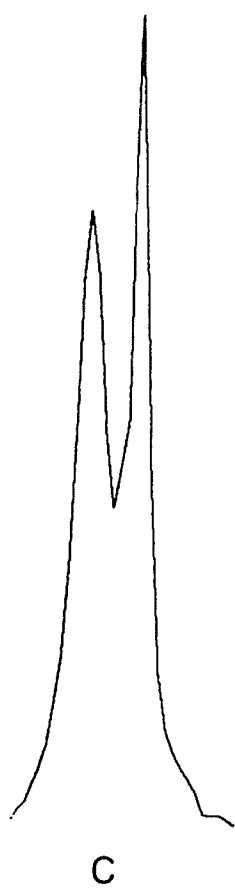
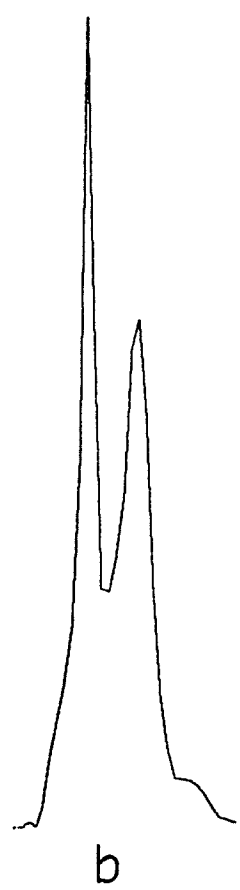
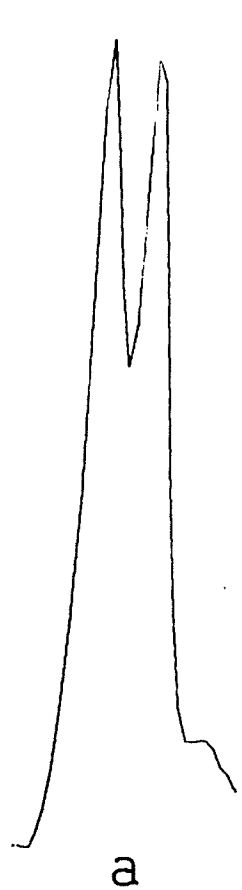


## Figure 13

Sign determination of  $^5J(C\alpha,H)$  in 2,6-dichloro( $\alpha$ - $^{13}C$ )-thioanisole. The illustrated spectrum is part of the meta proton resonance, and is designated by an asterisk in the preceding figure.

- (a) no decoupling of methyl protons
- (b) decoupling of higher frequency methyl protons
- (c) decoupling of lower frequency methyl protons

1 Hz



(v) 2,6-dibromo- and 2,6-dibromo-4-methylthioanisole

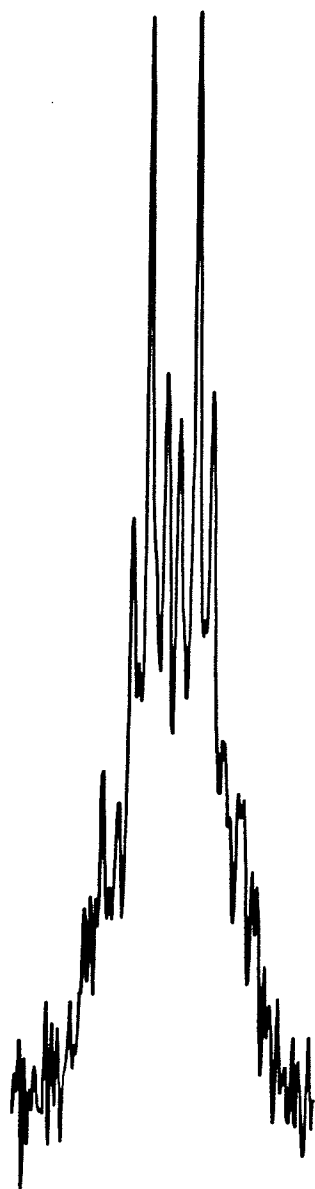
Parts of the methyl carbon spectra of 2,6-dibromothioanisole and 2,6-dibromo-4-methylthioanisole appear as Figure 14. The carbon spectrum for 2,6-dichlorothioanisole is similar to that for 2,6-dibromothioanisole.

For the 2,6-dibromo derivative, 259 scans with an acquisition time of ca. 16 seconds were accumulated into 16K of memory. Zero-filling to 64K, line broadening with -0.1 Hz and a Gaussian multiplication factor of 0.6 (ASPECT 3000 Data System) and Fourier transformation of the free induction decay yielded the typical INEPT spectrum for a CH<sub>3</sub> group. Acquisition parameters were the same for 2,6-dibromo-4-methylthioanisole, except that 297 scans were accumulated into 32K of memory, and that the acquisition time was approximately 25 seconds.

## Figure 14

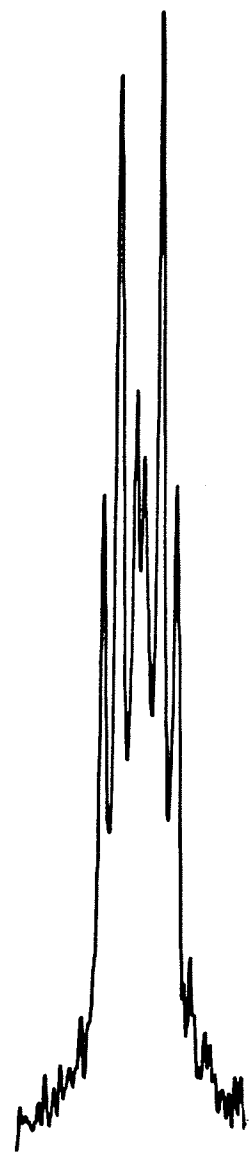
Part of the  $\alpha$  methyl carbon NMR spectra at 75.486 MHz of  
(a) 2,6-dibromo-4-methylthioanisole  
(b) 2,6-dibromothioanisole

The multiplets shown correspond to the  $1/2$  spin state of the methyl protons of the  $(-3/2, -1/2, 1/2, 3/2)$  quartet.



a

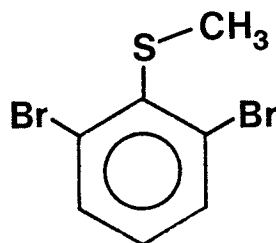
1 Hz



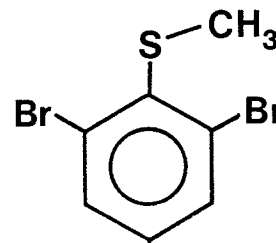
b

Table 6

Coupling constants for 2,6-dibromothioanisole(1) and 2,6-dibromo-4-methylthioanisole(2).



(1)



(2)

$^1J(C\alpha, CH_3)$	$140.925 \pm 0.006$	$140.778 \pm 0.005$
$^3J(C\alpha, H3)$	$0.217 \pm 0.005$	$0.209 \pm 0.004$
$^6J(C\alpha, H4)$	$-0.541 \pm 0.005$	-
$^7J(C\alpha, CH_3)$	-	$0.606 \pm 0.005$



## (vi) 2-bromothioanisole

The 90 MHz spectrum of the ring protons of a 2.0 mol % solution of 2-bromothioanisole in acetone- $d_6$  appears as Figures 15 and 16. The peak positions of partially resolved quartets were corrected by measuring the magnitude of the splitting of the inner lines of the quartet. The simulation of overlapping Lorentzian line shapes with a line width at half-height of 0.07 Hz gave correction factors for the observed degrees of splitting. The partially resolved splittings were multiplied by the appropriate correction factors and peak positions were adjusted accordingly. Analysis yielded the parameters in Table 7. Note that the experimental spectrum may only be simulated if  ${}^6J(\text{CH}_3, \text{H5})$  and  ${}^6J(\text{CH}_3, \text{H3})$  are of the same sign and nearly of the same magnitude. The signs of  ${}^5J(\text{CH}_3, \text{H6})$  and  ${}^7J(\text{CH}_3, \text{H4})$  are assumed<sup>46</sup>.

## Figure 15

The NMR spectrum of the H3, H5, and H6 protons of a 2.0 mol % solution of 2-bromothioanisole in acetone-d<sub>6</sub> at 90 MHz.

- (a) simulated
- (b) experimental

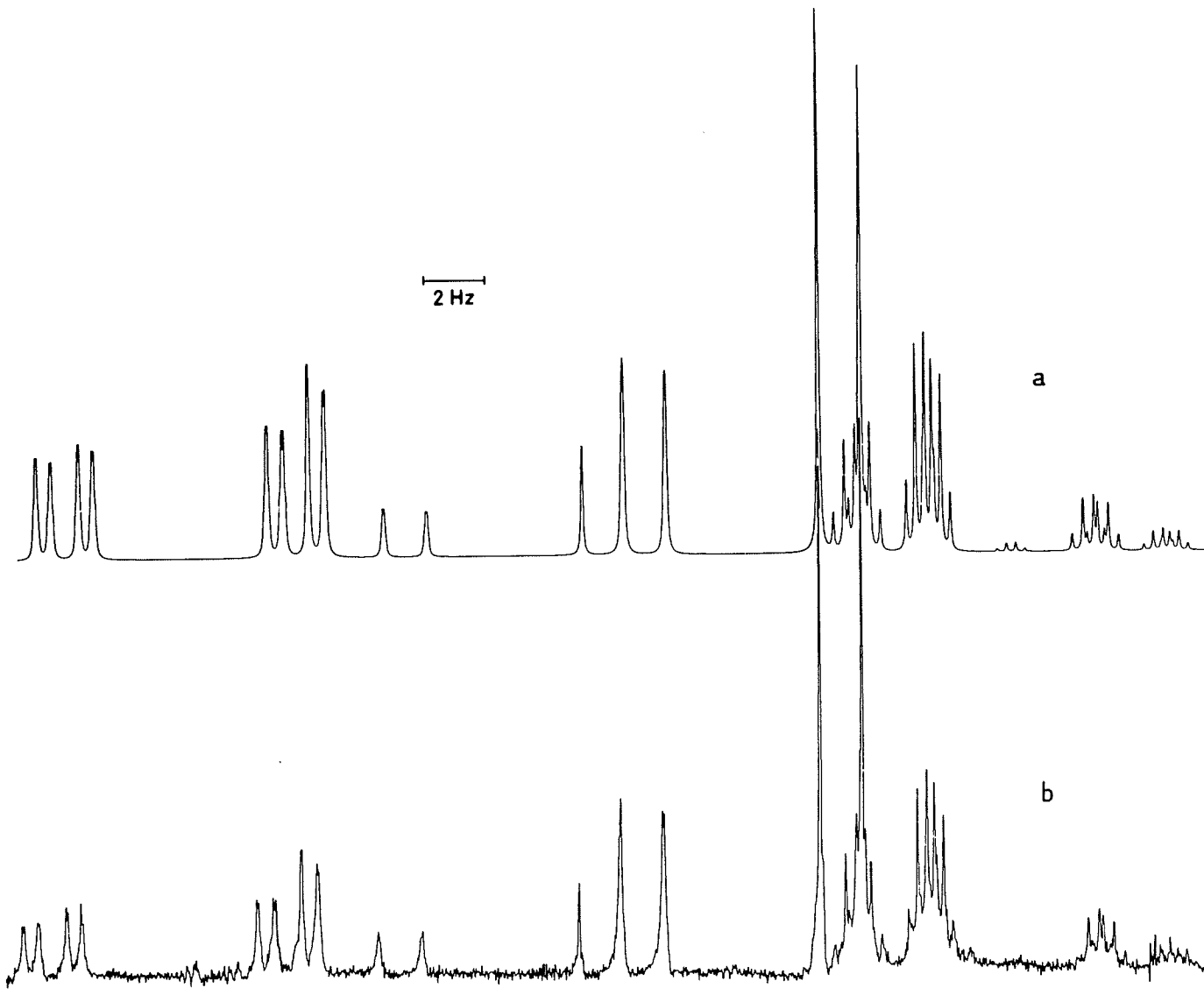
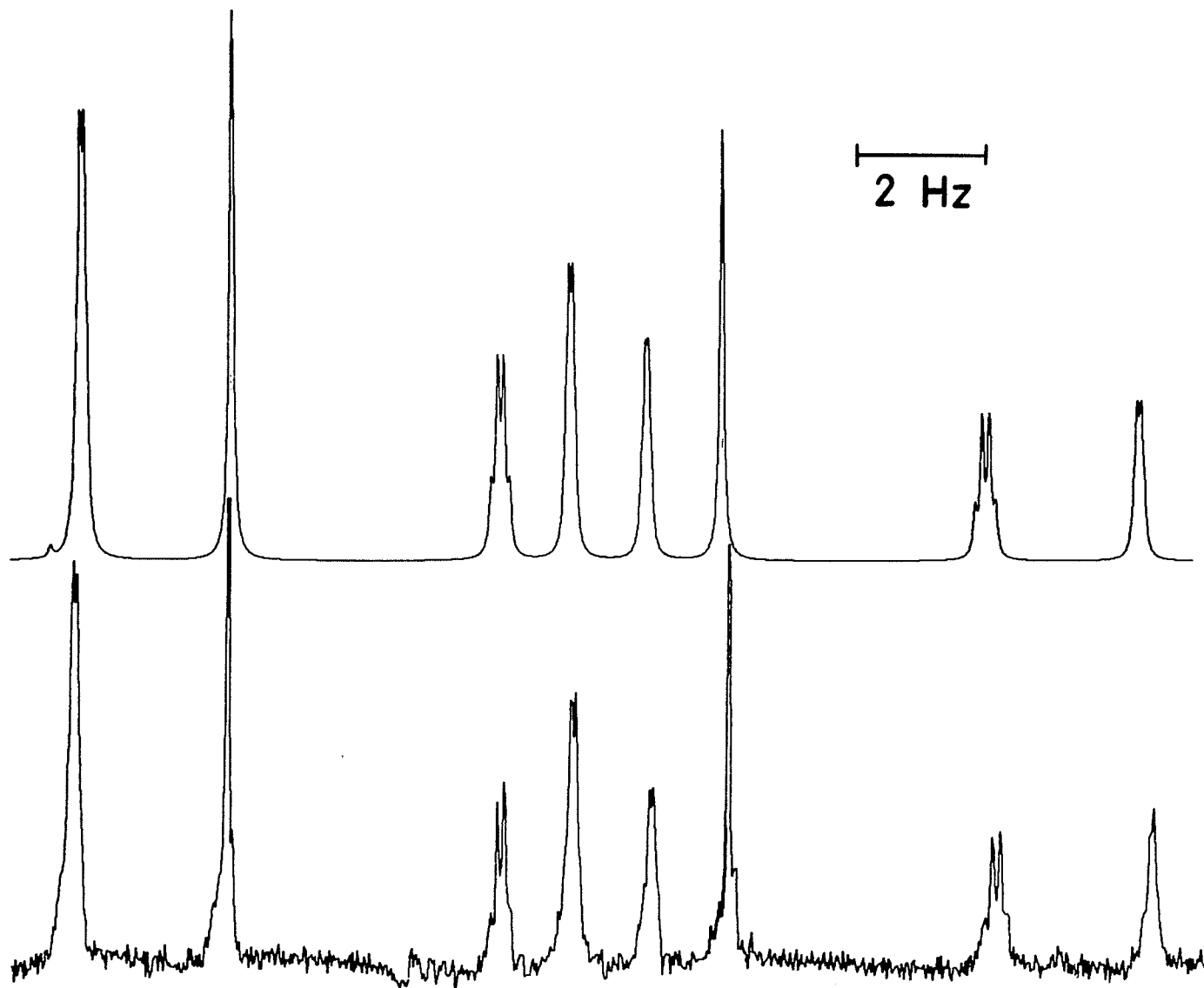


## Figure 16

The NMR spectrum of the H4 proton of a 2.0 mol % solution of 2-bromothioanisole in acetone-d<sub>6</sub> at 90 MHz.

(a) calculated

(b) experimental

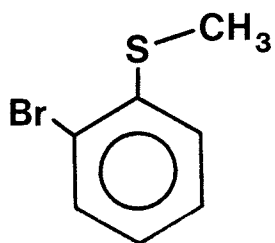


a

b

Table 7

Parameters from the proton spectrum of  
2-bromothioanisole



90.024MHz

	decoupled	coupled†
$\nu(\text{CH}_3)$	-	224.373
$\nu_6$	653.979(1)	4045.891(2)
$\nu_5$	663.647(1)	4055.554(2)
$\nu_4$	636.215(1)	4028.116(1)
$\nu_3$	679.956(1)	4071.870(1)
$J(\text{CH}_3, \text{H6})$	-	-0.387(2)
$J(\text{CH}_3, \text{H5})$	-	0.082(2)
$J(\text{CH}_3, \text{H4})$	-	-0.058(2)
$J(\text{CH}_3, \text{H3})$	-	0.057(2)
$J(\text{H5}, \text{H6})$	7.991(1)	7.991(2)
$J(\text{H4}, \text{H6})$	1.518(1)	1.515(2)
$J(\text{H3}, \text{H6})$	0.323(1)	0.326(2)
$J(\text{H4}, \text{H5})$	7.397(1)	7.394(2)
$J(\text{H3}, \text{H5})$	1.360(1)	1.357(2)
$J(\text{H3}, \text{H4})$	7.951(1)	7.949(2)

...Table 7 continued...

Table 7...

assigned peaks†	28	48
observed peaks	32	54
assigned transitions	28	121
transitions calcd.	34	203
rms deviation	0.0019	0.0064
largest difference	0.003	0.017

† Chemical shifts for the coupled spectra are arbitrary. The correlation matrix from the LAME analyses shows no significant correlations of  $J(\text{CH}_3, \text{H})$  with other parameters, but there are significant correlations for  $\nu_5/\nu_6$ ,  $\nu_6/J_{56}$ ,  $\nu_5/J_{56}$ , and  $\nu_5/J_{45}$ .

## (vii) 2-bromo-4-fluorothioanisole

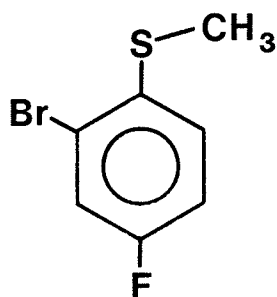
The spectral parameters for the proton NMR spectrum of a 2.0 mol % solution of 2-bromo-4-fluorothioanisole appears in Table 8. At 90 MHz, the  $^1\text{H}$  spectrum is nearly first order in appearance. As with most spectra discussed in this thesis, the proton resonances could be unequivocally assigned on the basis of the shifts calculated by an empirical additivity rule for substituents on the benzene ring<sup>13</sup> and on the basis of the expected coupling constants between methyl protons and aromatic protons, as well as between fluorine and the aromatic protons.

The 75.486 MHz proton decoupled methyl carbon spectrum was obtained by the Fourier transformation of 128 free induction decays. A power gated technique was used to minimize dielectric heating. The  $\alpha$  carbon-fluorine coupling constant was measured as 0.252 Hz.



Table 8

Parameters from the proton spectrum of  
2-bromo-4-fluorothioanisole in acetone-d<sub>6</sub>.



	90.024 MHz
$\nu(\text{CH}_3)$	225.080†
$\nu_3$	668.880(1)
$\nu_4$	1500.0
$\nu_5$	648.048(1)
$\nu_6$	658.792(2)
$J(\text{CH}_3, \text{H}_3)$	0.000‡
$J(\text{CH}_3, \text{F})$	0.000‡
$J(\text{CH}_3, \text{H}_5)$	0.000‡
$J(\text{CH}_3, \text{H}_6)$	-0.347(2)
$J(\text{H}_3, \text{F})$	8.291(2)
$J(\text{H}_3, \text{H}_5)$	2.764(2)
$J(\text{H}_3, \text{H}_6)$	0.251(2)
$J(\text{H}_5, \text{F})$	8.285(3)
$J(\text{H}_5, \text{H}_6)$	8.843(2)
$J(\text{H}_6, \text{F})$	5.579(3)

...Table 8 continued...

Table 8...

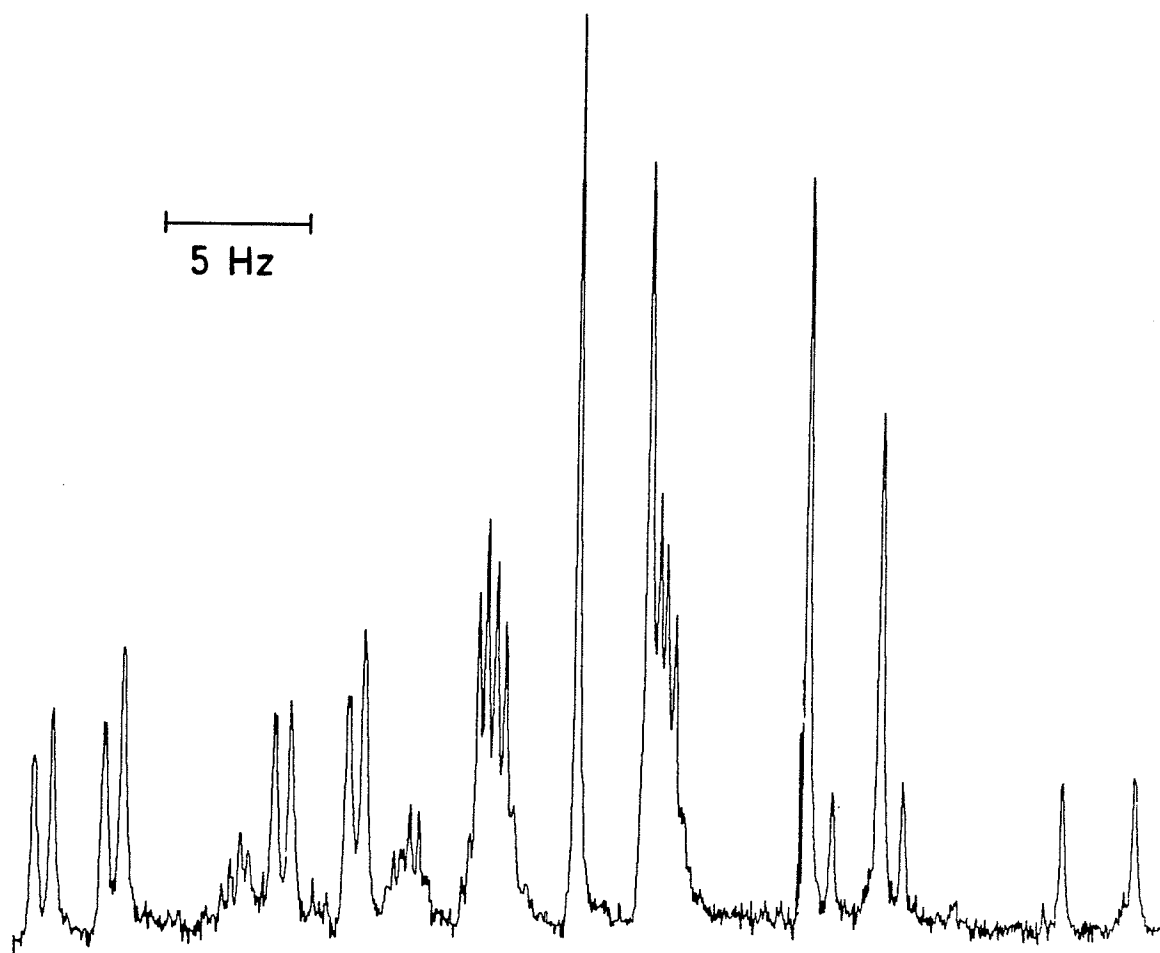
peaks observed	34
peaks assigned	33
transitions calcd.	149
assigned transitions	107
largest difference	0.015
rms deviation	0.0065
line width	0.08 Hz

† Shifts were measured relative to the middle peak of acetone-d<sub>6</sub>, which has been measured in dilute solution and occurs at  $2.054 \pm 0.001$  ppm relative to TMS. Therefore, although the shift frequencies are self-consistent, their absolute accuracy extends only to the first decimal place. The shifts, relative to acetone-d<sub>6</sub> at 2.054 ppm, are 7.430, 7.199, and 7.318 ppm for H3, H5, and H6 respectively. Fluorine and methyl chemical shifts were held in the X approximation, with no transitions assigned. The methyl protons shift is 2.500 ppm.

‡ Held constant during the analysis. Upon decoupling the methyl peak, only resonances attributable to H3 sharpen. The estimated coupling constant is  $0.02 \pm 0.01$  Hz.

Figure 17

The aromatic proton spectral region of  
2-bromo-4-fluorothioanisole.

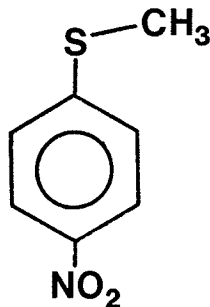


## (viii) 4-nitrothioanisole

The spectral parameters for the proton spectrum of 4-nitrothioanisole appear in Table 9.  $^3J(\text{CH},\text{H})$  is the corrected value for the partially resolved quartets in the aromatic region. The method used for deconvolution is the same as for 2-bromothioanisole. Quadrupolar coupling from the  $^{14}\text{N}$  of the nitro group broadens the spectral lines, especially those attributable to the protons ortho to the group.

Table 9

Parameters from the proton spectrum of  
4-nitrothioanisole



	90.024 MHz	
	decoupled	coupled†
$\nu(\text{CH}_3)$	-	235.931
$\nu_2 = \nu_6$	672.639(4)	672.596(2)
$\nu_3 = \nu_5$	733.843(4)	733.843
$J(\text{CH}_3, \text{H}_2)$	-	-0.178(4)
$J(\text{CH}_3, \text{H}_3)$	-	0.020
$J(\text{H}_2, \text{H}_3)$	8.797(6)	8.769(5)
$J(\text{H}_2, \text{H}_6)$	2.253(7)	2.250(5)
$J(\text{H}_2, \text{H}_5)$	0.405(6)	0.405
$J(\text{H}_3, \text{H}_5)$	2.619(7)	2.616(9)
peaks observed	20	19
peaks assigned	20	14
transitions calcd.	24	71
transitions assigned	22	26

...Table 9 continued...

Table 9...

rms deviation	0.013	0.0097
largest deviation	0.022	0.016

† The methyl coupled spectrum was analysed mainly for the the methyl splitting to the ortho protons. The shift of the meta proton was held constant and only ortho proton transitions were iterated upon. The methyl peaks were not iterated upon.

(ix) 4-fluorothioanisole and 2,6-dibromo-4-fluorothioanisole

The spectra of the proton-decoupled methyl carbons of 4-fluorothioanisole (50% v/v in acetone- $d_6$ ) and 2,6-dibromo-4-fluorothioanisole (ca. 3 mol % in acetone- $d_6$ ) appear as doublets with six-bond carbon-fluorine coupling constants of  $0.474 \pm 0.007$  and  $1.480 \pm 0.013$  Hz respectively. Both derivative spectra were recorded at 22.63 MHz under conditions of broadband decoupling of the protons.



(x) pentafluorothioanisole and 2,3,5,6-tetrafluorothioanisole

The  $^{13}\text{C}$  NMR spectrum of the methyl carbon of pentafluorothioanisole (27 mol % in acetone- $d_6$ ) appears as Figure 18. In addition, the proton spectrum of a 2.0 mol % solution in acetone- $d_6$  yielded the parameters given in Table 10. In the table, the parameters listed are only those most likely to be conformationally dependent. Data for tetrafluorothioanisole (2.0 mol % in acetone- $d_6$ ) and tetrafluoro( $\alpha$ - $^{13}\text{C}$ )thioanisole (2.0 mol % in acetone- $d_6$ ) are also included.

The carbon spectrum for pentafluorothioanisole was obtained by acquiring 256 free induction decays in 16K of memory under conditions of broadband decoupling. The acquisition time was 20.5 seconds. The transient decays were apodized by 0.10 Hz line broadening before Fourier transformation. The coupled  $^{13}\text{C}$  spectrum of the methyl carbon of tetrafluorothioanisole (23 mol % in acetone- $d_6$ ) shows quartets with a spacing of  $0.360 \pm 0.004\text{Hz}$ , arising from coupling to the meta fluorine nuclei and the para proton with equal magnitudes of the coupling constants. Therefore, the proton and fluorine spectra of the isotopically enriched compound (4.2 mol % in acetone- $d_6$ ) were examined. The couplings to the  $\alpha$ -carbon

were assumed to be first order and are given in Table 10.

Note that the magnitudes of  ${}^6J(C,F)$  and  ${}^6J(C,H)$  are quite similar, although perhaps somewhat larger than those observed in the carbon spectrum. The discrepancy in the magnitude of the coupling results either from overlapping lines in the carbon spectrum, or from a solvent effect. Figures 19 and 20 show the determinations of the signs of the four-bond carbon-fluorine (positive) and the five-bond carbon-fluorine (negative) coupling constants. The method is that utilized for 2-iodothioanisole.

Figure 21 shows the methylthio proton peaks for pentafluorothioanisole (300K) and 2,3,5,6-tetrafluorothioanisole (290K) as 2.0 mol % solutions in acetone- $d_6$ . In order to show  ${}^6J(CH_3,F)$ , spectra must be enhanced greatly, resulting in a much distorted line shape. Both spectra were measured with eight scans, instead of the typical one scan proton spectrum, at 90.024 MHz. The six-bond coupling between the methyl protons and the meta fluorine nuclei has not been previously reported.

## Figure 18

The proton decoupled methyl carbon spectrum of a 27 mol % solution of pentafluorothioanisole in acetone-d<sub>6</sub> at 22.63 MHz and 305K.

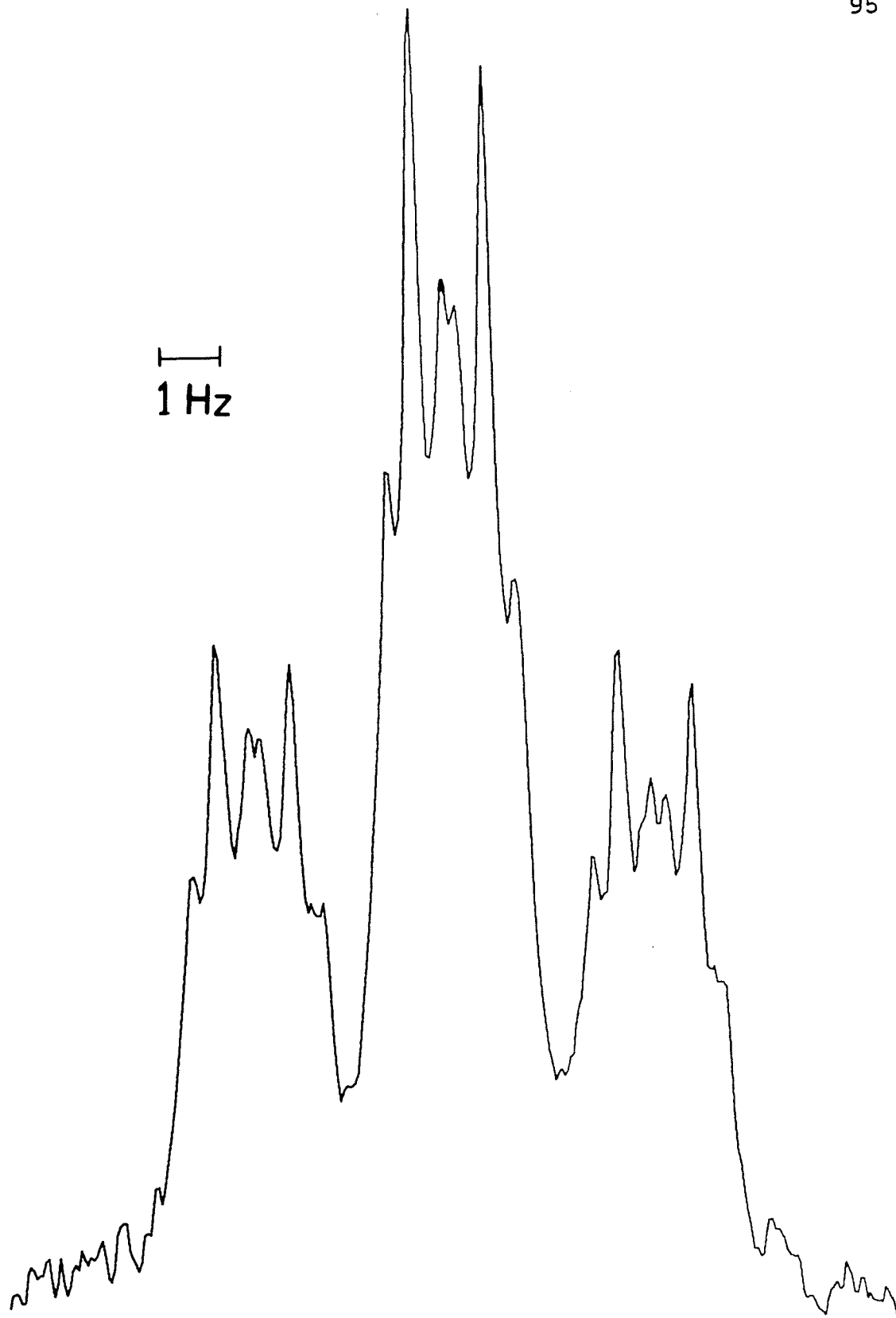
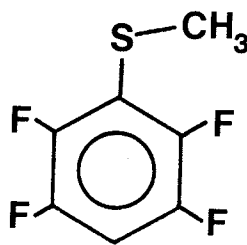
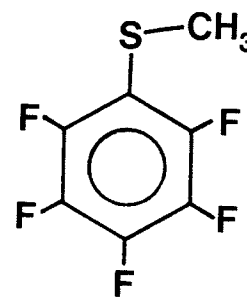


Table 10

Coupling constants for 2,3,5,6-tetrafluorothioanisole (1) and pentafluorothioanisole (2) in acetone-d<sub>6</sub>.



(1)



(2)

$^4J(C\alpha, F)$	$3.984 \pm 0.006$	$3.275 \pm 0.015$
$^5J(C\alpha, F)$	$0.376 \pm 0.008$	$0.463 \pm 0.006$
$^6J(C\alpha, F)$	-	$1.192 \pm 0.016$
$^6J(C\alpha, H)$	$0.370 \pm 0.005$	-
$^5J(H, F)$	$0.907 \pm 0.002$	$0.722 \pm 0.003$
$^6J(H, F)$	$0.141 \pm 0.002$	$0.141 \pm 0.002$

The coupling constants were measured directly from the carbon or proton spectra of the methyl group.

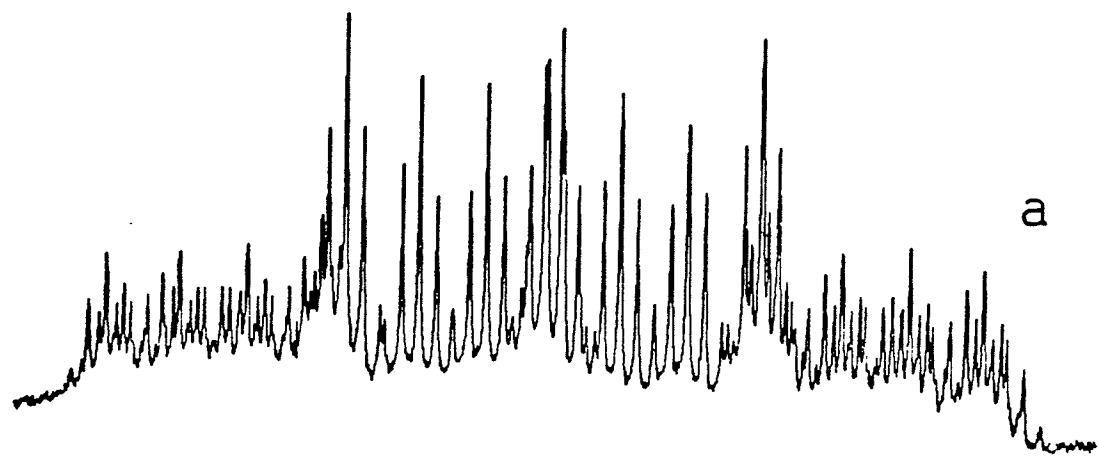
## Figure 19

Determination of the sign of the four-bond carbon-fluorine coupling constant ( $C_{\alpha-o-F}$ ) in tetrafluoro( $\alpha$ - $^{13}C$ )thioanisole. The ortho fluorine resonance is shown at 84.700 MHz.

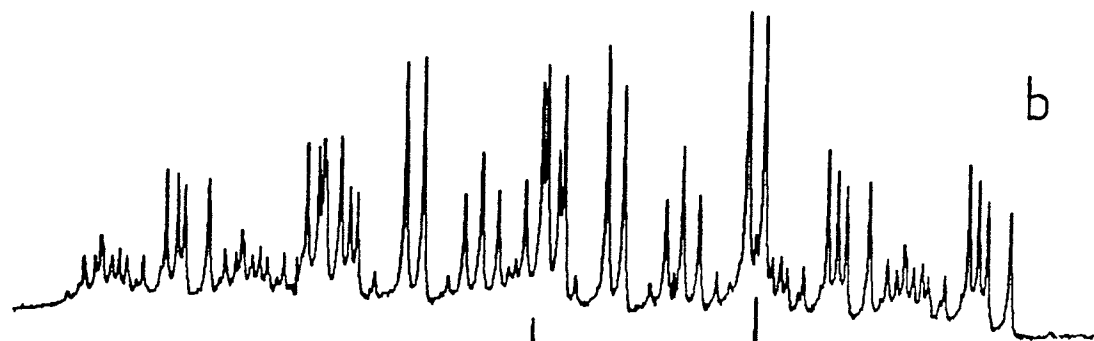
- (a) no decoupling of the methyl protons
- (b) decoupling the methyl protons for the - spin state of  $C_{\alpha}$ .
- (c) decoupling the methyl protons for the + spin state of  $C_{\alpha}$ .

The method used was the same as for 2-iodothioanisole.

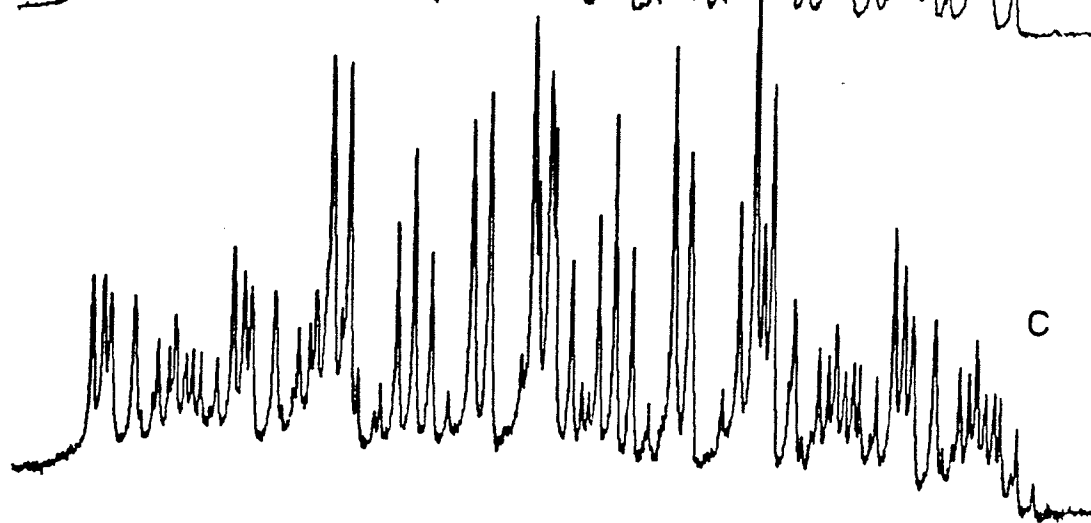
10 Hz



a



b



c

## Figure 20

Determination of the sign of the five-bond carbon-fluorine coupling constants ( $C_{\alpha-m-F}$ ) in tetrafluoro( $\alpha$ - $^{13}\text{C}$ )thioanisole. The meta fluorine resonance is shown at 84.700 MHz.

- (a) no decoupling
- (b) decoupling the methyl protons for the + spin state of  $C_{\alpha}$ .
- (c) decoupling the methyl protons for the - spin state of  $C_{\alpha}$ .



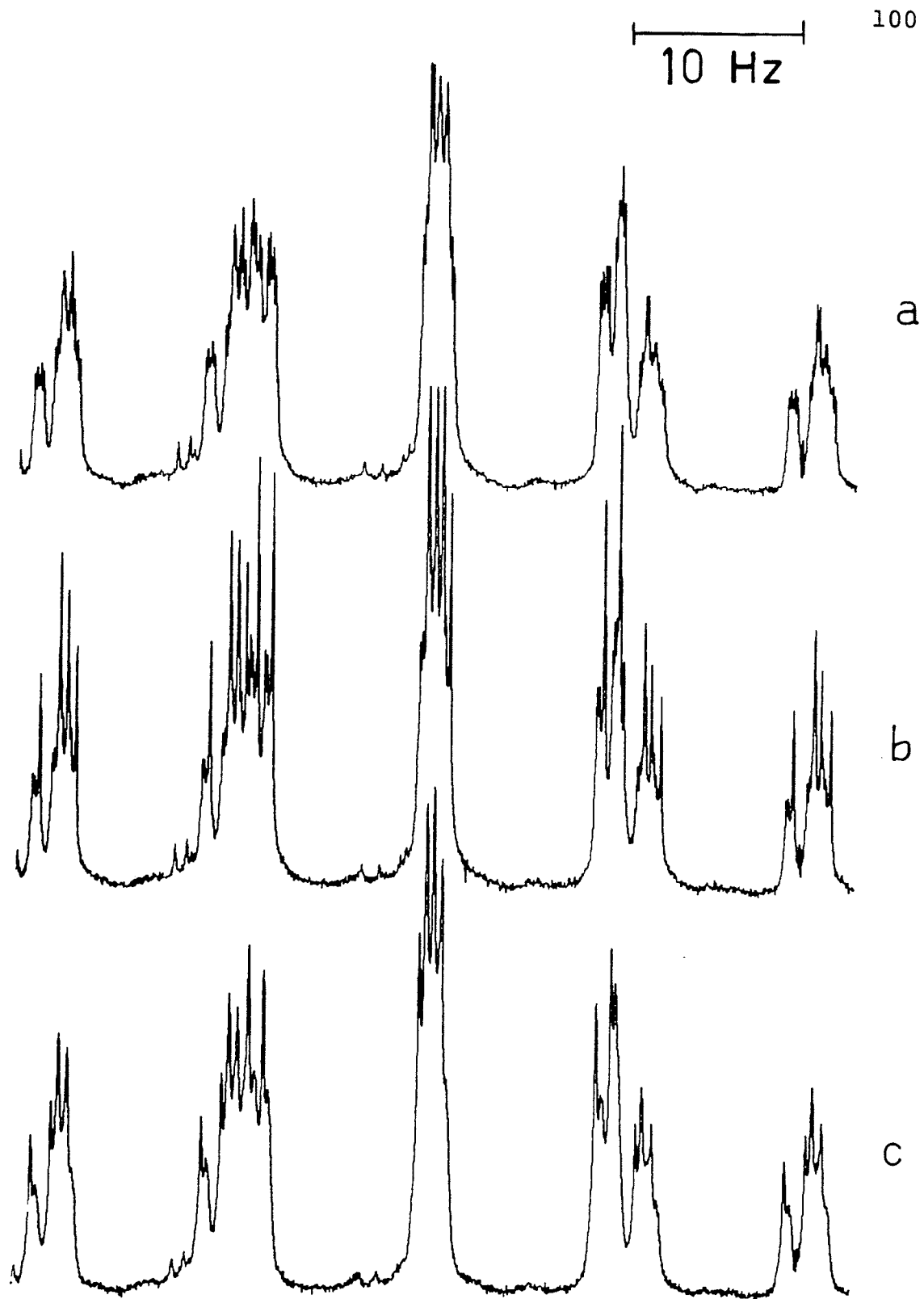
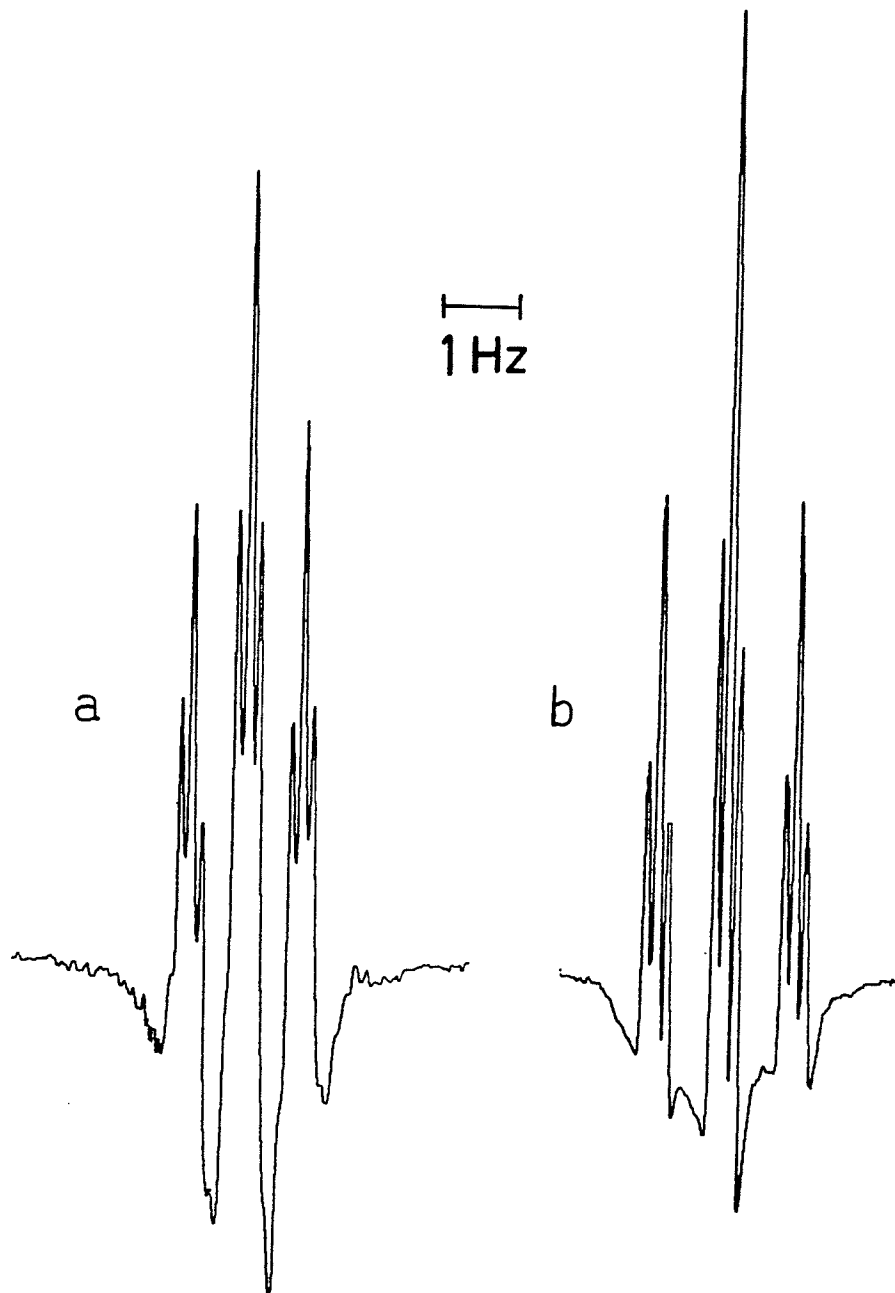


## Figure 21

The methylthio protons spectra of pentafluorothioanisole (a), and 2,3,5,6-tetrafluorothioanisole (b). Sine enhancement of the spectra results in the distorted line shape. The smaller splitting results from the spin-spin coupling between the methyl protons and the meta fluorine and is about 0.14 Hz in both compounds. The spectra were recorded at 90.024 MHz for 2.0 mol % solutions.

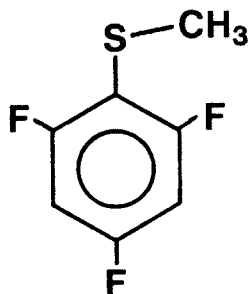


## (xi) 2,4,6-trifluorothioanisole

Spectral parameters for the decoupled methyl carbon spectra and for the coupled proton and fluorine spectra are given below in Table 10a. The proton decoupled carbon spectrum was obtained on a 4 mol % solution in acetone-d<sub>6</sub> at 75.486 MHz. 128 scans were summed into 8K of memory with an acquisition time of about 10 seconds. 0.1 Hz line broadening on the free induction decay improved the signal-to-noise ratio. Proton and fluorine spectra were measured on a 2.0 mol % solution in acetone-d<sub>6</sub>.

Table 10a

Spectral parameters for 2,4,6-trifluorothioanisole in acetone-d<sub>6</sub>.†



$\nu(\text{CH}_3)$	217.827(1)
$\nu_2 = \nu_6$	645.110(1)‡
$\nu_3 = \nu_5$	630.308(1)
$\nu_4$	198.687(1)
$J(\text{CH}_3, \text{F2})$	-0.588(1)
$J(\text{CH}_3, \text{H3})$	0.00
$J(\text{CH}_3, \text{F4})$	0.00
$J(\text{F2}, \text{F6})$	4.342(2)
$J(\text{F2}, \text{H3})$	9.234(1)
$J(\text{F2}, \text{F4})$	7.210(2)
$J(\text{F2}, \text{H5})$	-1.974(1)
$J(\text{H3}, \text{H5})$	2.695(2)
$J(\text{H3}, \text{F4})$	9.067(2)
$J(\text{C}\alpha, \text{F2})$	2.965±0.027
$J(\text{C}\alpha, \text{F4})$	1.198±0.013

...Table 10a continued...

Table 10a..

assigned transitions	424
transitions calcd.	512
assigned fluorine peaks	52
observed fluorine peaks	65
rms deviation	0.0128
largest deviation	0.069

† The parameter values refer to a NUMARIT analysis of the proton and fluorine spectra, obtained at 90.024 and 87.824 MHz, respectively. The parameters referring to  $C\alpha$  are measured from line splittings observed for the methyl carbon resonance.

‡ Proton chemical shifts are relative to the middle peak of acetone- $d_6$ , which is set at 2.054 ppm. The self-consistent chemical shifts, but accurate in an absolute sense only to the second decimal place, are  $\delta=2.00$  for the  $SCH_3$  group and  $\delta=7.00$  for the aromatic protons. The fluorine chemical shifts are arbitrary, but self-consistent to each other. The carbon chemical shift is of less importance, and was not measured.

## (xii) 2,6-difluorothioanisole

The proton spectrum of a 2.0 mol % solution in acetone- $d_6$  was measured at 90.024 MHz. The methyl proton region was analyzed to yield the most important parameter,  $^1J(\text{CH}_3, \text{F})$ , as  $0.746 \pm 0.005 \text{ Hz}$ . The temperature dependence of  $^1J(\text{CH}_3, \text{ortho-F})$  for 2,6-difluorothioanisole, 2,3,5,6-tetrafluorothioanisole, and 2,3,4,5,6-pentafluorothioanisole was measured between 250 and 315K. Results appear as Figure 22.

The fully coupled methyl carbon spectrum of a 15.0 mol % solution of 2,6-difluorothioanisole in acetone- $d_6$  appears as Figure 23 (only one multiplet of the one-bond quartet is shown). The spectrum was acquired at 75.486 MHz into 32K, with an acquisition time of 32.3 seconds. The INEPT pulse sequence was employed. The spectral parameters that are most important here are  $^1J(\text{C}, \text{F})$ ,  $^1J(\text{C}, \text{H})$ , and  $^2J(\text{C}, \text{H})$ , which are  $3.590 \pm 0.005$ ,  $0.210 \pm 0.002$ , and  $0.420 \pm 0.003 \text{ Hz}$  respectively.

## Figure 22

The temperature dependence of  $^5J(\text{CH}_3, \text{F})$  in some fluoro-thioanisoles.

- 2,3,5,6-tetrafluorothioanisole
- x 2,6-difluorothioanisole
- 2,3,4,5,6-pentafluorothioanisole



THE TEMPERATURE DEPENDENCE OF  
 $^5J_{(\text{CH}_3, \text{F})}^\circ$  IN FLUOROTHIOANISOLES

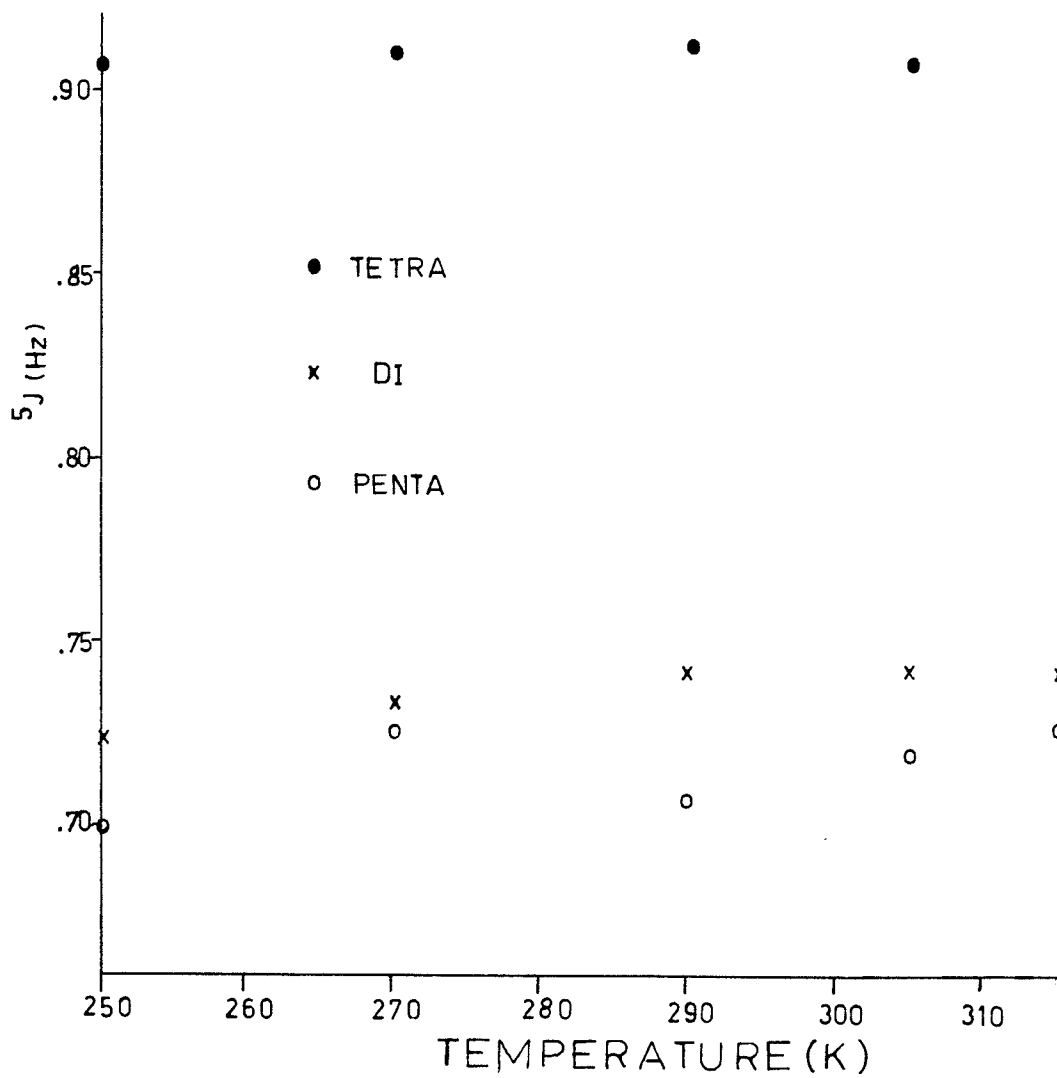
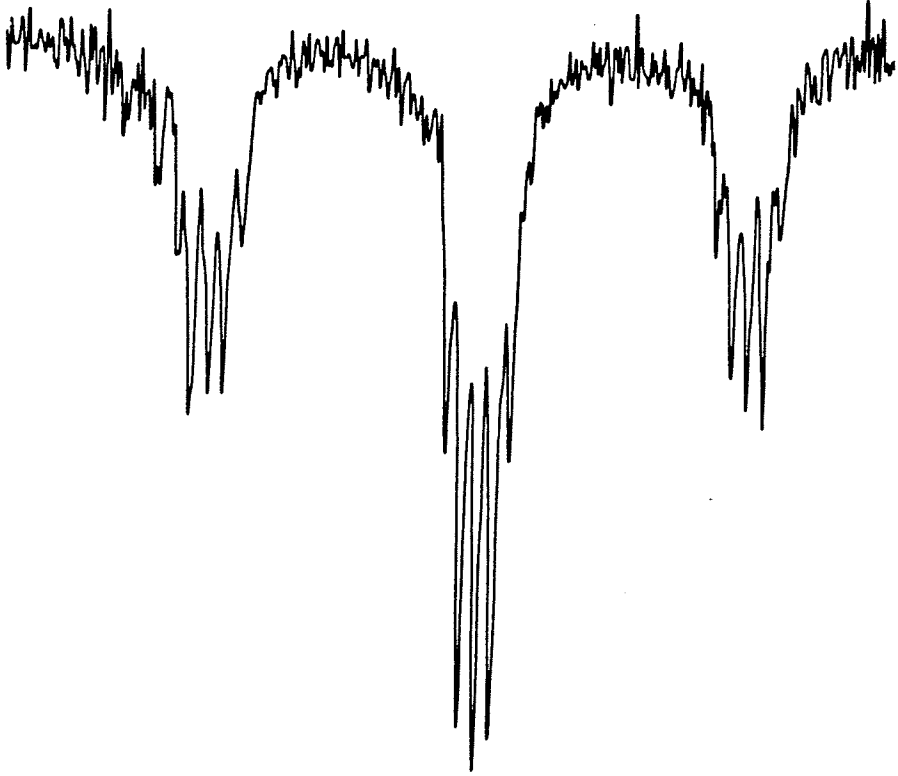


## Figure 23

The lowest field multiplet of the methyl carbon resonance spectrum of 2,6-difluorothioanisole at 75.846 MHz.

1 Hz

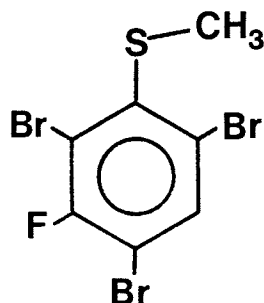


## (xiii) 2,4,6-tribromo-3-fluorothioanisole

The methyl carbon and proton nuclear magnetic resonance spectral parameters for 2,4,6-tribromo-3-fluorothioanisole appear in Table 11. The unisolated compound was approximately 3 mol % in acetone- $d_6$  for both proton and proton-decoupled carbon spectra. The aromatic proton spectral lines are distinguished from those of an impurity by decoupling the SCH<sub>3</sub> protons (which characteristically occur in acetone solution at  $2.5 \pm 0.2$  ppm) and observing line narrowing in the aromatic region of the spectrum. The given 95% confidence intervals are the result of standard deviations observed in peak positions for three spectra.

Table 11

Spectral parameters for 2,4,6-tribromo-3-fluorothioanisole in acetone- $d_6$ .



$\nu(\text{CH}_3)$	$221.935 \pm 0.003$
$\nu_s$	$724.880 \pm 0.004$
$J(\text{F}, \text{H}_5)$	$6.712 \pm 0.003$
$J(\text{CH}_3, \text{H}_5)$	$0.03 \pm 0.01 \dagger$
$J(\text{C}\alpha, \text{F})$	$0.593 \pm 0.010$

$\dagger$  Estimated from line width narrowing upon decoupling. The line width of the decoupled proton spectra, obtained at 90.024 MHz, was 0.10 Hz.

## (xiv) 2-methyl-3-fluorothioanisole

The proton-decoupled methyl carbon spectrum of 2-methyl-3-fluorothioanisole (20 v/v % in acetone-d<sub>6</sub>) gave  $^1J(C\alpha, F)$  as  $0.408 \pm 0.009$  Hz. The spectrum was recorded on a Bruker AM300 spectrometer with a composite decoupling sequence to effectively decouple protons without heating the sample. 78 scans with 20 second acquisition times were summed into 16K of memory. Approximately 85° pulse lengths were employed. The proton spectrum at 300.135 MHz gave  $^1J(CH_3, H6)$  as  $0.334 \pm 0.009$  Hz (2.0 mol % solution in acetone-d<sub>6</sub>).

## (xv) Thiophenols

3,5-dichlorothiophenol, 3,5-dimethylthiophenol, and 4-methylthiophenol  $^1\text{H}$  NMR spectral parameters are collected in Table 12. Concentrations and solvents are noted in the table. Barriers to internal rotation are calculated using the method of reference (5).

Table 12

Spectral parameters for 3,5-dichlorothiophenol(1), 3,5-dimethylthiophenol(2), and 4-methylthiophenol(3)

	(1)	(2)	(3)
$\nu(\text{SH})$	2.77254(4)	3.03938(5)	3.15311(1)
$\nu(\text{CH}_3)$	-	1.96968(1)	2.26954(1)
$\nu_2 = \nu_6$	6.61073(6)	6.52098(7)	7.08952(1)
$\nu_3 = \nu_5$	-	-	6.94854(1)
$\nu_4$	6.79982(4)	6.70527(3)	-
$J(\text{SH}, \text{H}2)$	-0.233(5)	-0.316(5)	-0.456(1)
$J(\text{SH}, \text{H}3)$	-	-	0.272(1)
$J(\text{SH}, \text{H}4)$	-0.221(5)	-0.288(8)	-
$J(\text{SH}, \text{CH}_3)$	-	0.115(6)	0.441(1)

...Table 12 continued...

Table 12...

J(CH <sub>3</sub> ,H2)	-	-	0.357(1)
J(CH <sub>3</sub> ,H3)	-	-	-0.713(1)
J(CH <sub>3</sub> ,H4)	-	-0.711(6)	-
J(H2,H3)	-	-	7.935(2)
J(H2,H4)	1.823(5)	1.567(5)	-
J(H2,H5)	-	-	0.507(1)
J(H2,H6)	-	-	2.112(2)
J(H3,H5)	-	-	2.110(2)
assigned peaks	14	-	113
observed peaks	17	10	125
transitions calcd.	24	-	512
transitions assigned	19	-	391
rms deviation	0.0097	-	0.0089
largest difference	0.015	-	0.031
barrier to internal rotation (kJ/mole)	6.9±0.7	4.4±0.4	1.7±0.3

(1) 5.0 mol % in benzene-d<sub>6</sub> at 305K at 90 MHz.

(2) J(SH,H2), J(SH,H4), and J(H2,H4) are measured under conditions of methyl proton irradiation. J(SH,CH<sub>3</sub>) is measured while irradiating ortho ring protons. The parameters listed are for a ca. 1 mol % solution in benzene-d<sub>6</sub> at 300K and at 300 MHz. Values in parentheses denote 95 % confidence intervals for the parameters.

(3) NUMARIT analysis of a 2.0 mol % solution in CCl<sub>4</sub>/cyclohexane-d<sub>12</sub> at 293K and at 300 MHz.

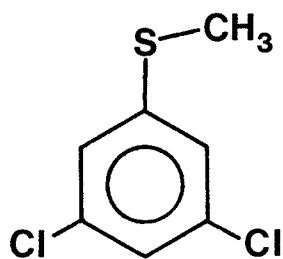


## (xvi) 3,5-dichlorothioanisole

The spectral parameters for a 5 mol % solution of 3,5-dichlorothioanisole in  $C_6D_6/TMS$  appears in Table 13 (analysis by S. R. Salman). Figure 24 shows parts of the aromatic region of the methyl proton decoupled spectrum of the aromatic region of a 2.0 mol % solution of 3,5-dichloro( $\alpha$ - $^{13}C$ )thioanisole in acetone- $d_6$ . The coupling between H4 and the methyl carbon is  $-0.087 \pm 0.005$  Hz.

Table 13

Spectral parameters for 3,5-dichlorothioanisole in  $C_6D_6/TMS$ .

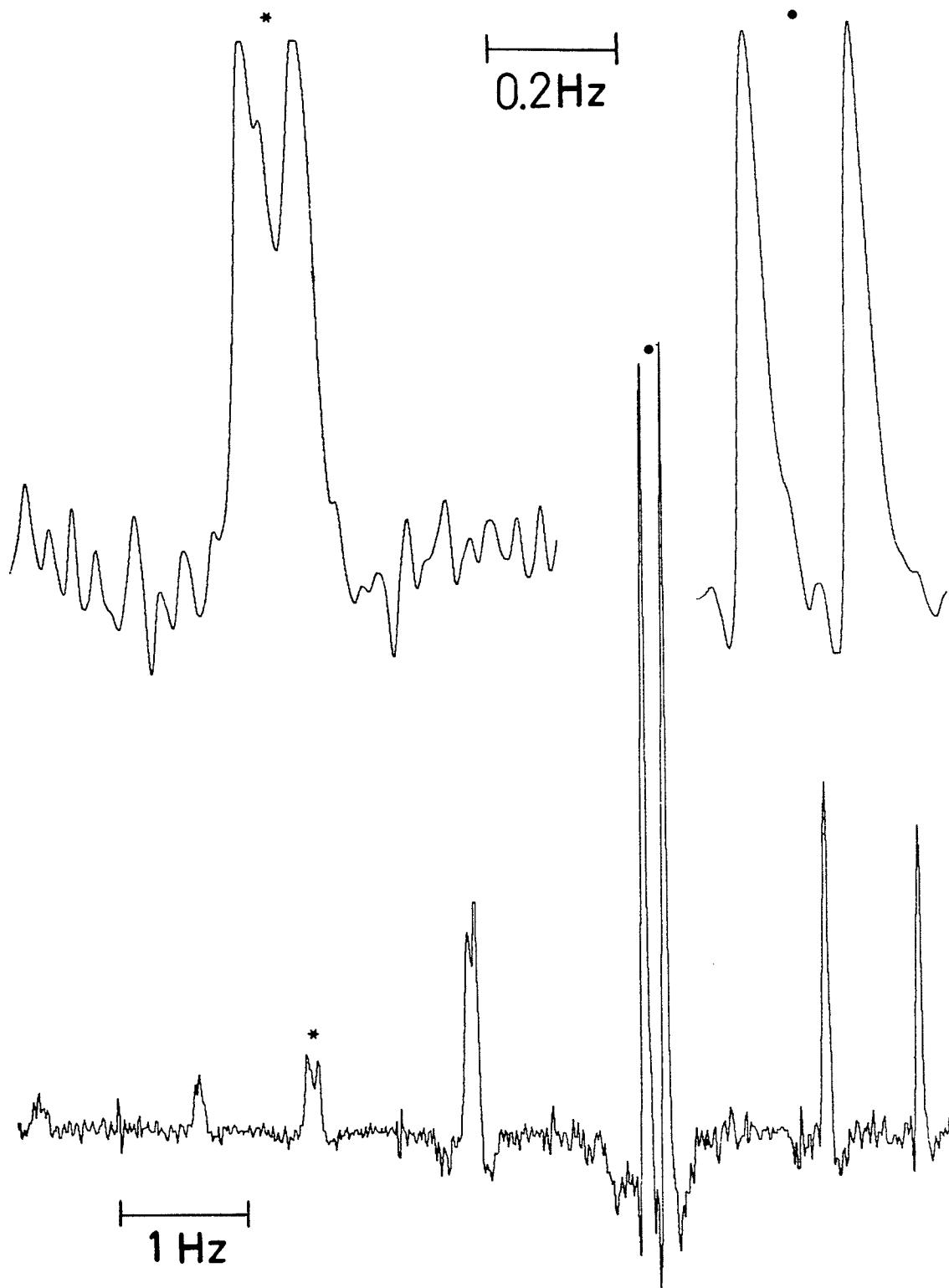


	100.002 MHz
$\nu(CH_3)$	170.512
$\nu_2 = \nu_6$	680.523(2)
$\nu_4$	687.888(2)
$J(H2, H4)$	1.815(2)
$J(CH_3, H2)$	-0.147(2)
$J(CH_3, H4)$	-0.05±0.01†
observed peaks	10
assigned peaks	10
transitions calcd.	48
assigned transitions	38
rms deviation	0.0066
largest deviation	0.016

† Estimated from line widths in the para proton region.

## Figure 24

The methyl decoupled aromatic spectrum of 3,5-dichloro( $\alpha$ - $^{13}\text{C}$ )thioanisole in acetone- $d_6$  at 90.024 MHz. Two sections of the lower spectrum, plotted at 0.5 Hz/cm, are expanded to 0.1 Hz/cm above. The spectral regions are denoted by asterisks and closed circles.



## (xvii) 3,5-dimethylthioanisole

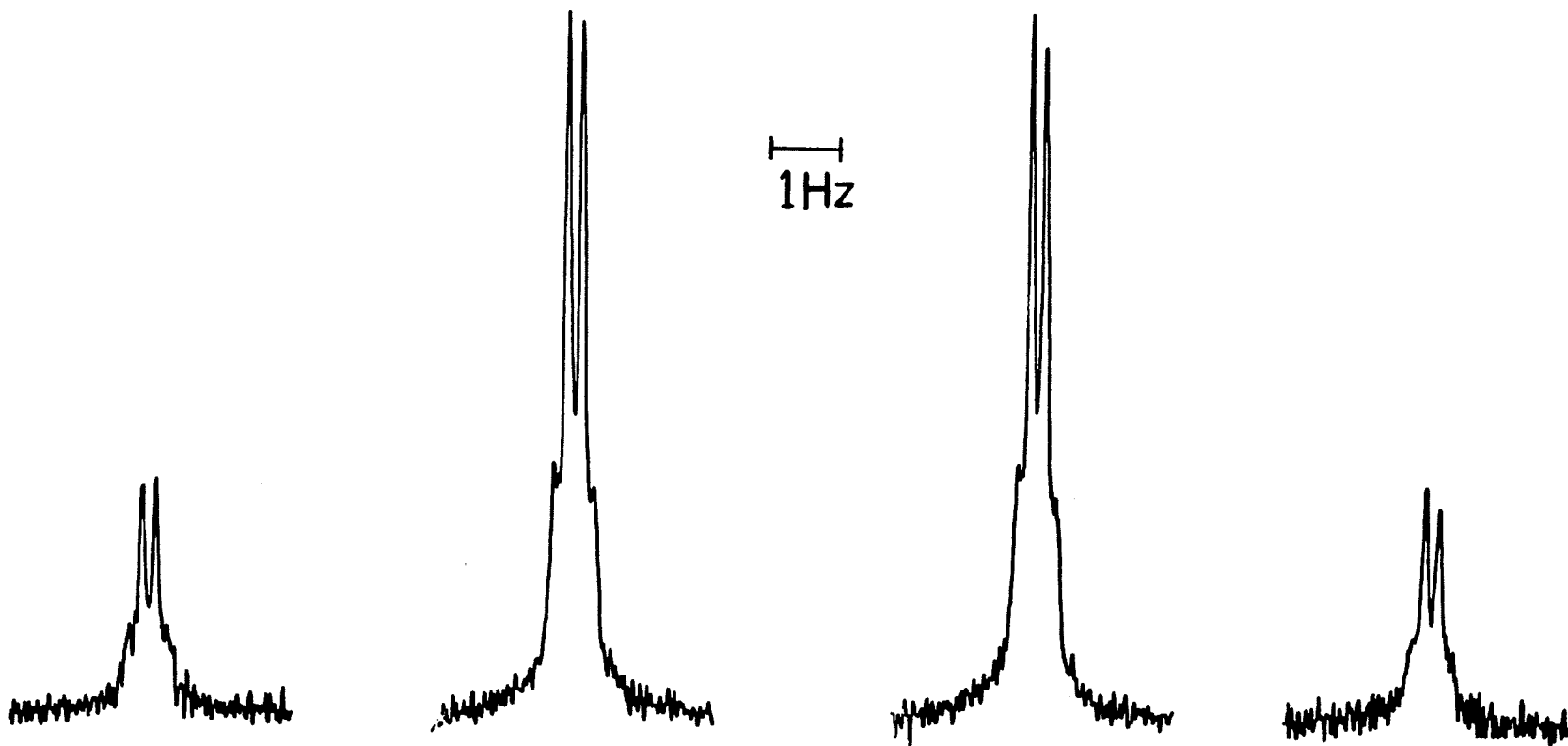
The SCH<sub>3</sub> carbon spectrum of a ca. 2 mol % solution of 3,5-dimethyl( $\alpha$ -<sup>13</sup>C)thioanisole in acetone-d<sub>6</sub> was measured at 74.486 MHz. The ring methyl protons were decoupled in order to simplify the spectrum. 1000 scans were devoted to a spectral width of 800 Hz, and an acquisition time of 30.7 seconds. The temperature was 300K. Apodization of the free induction decay with -0.08 Hz line broadening and a Gaussian multiplication factor of 0.6 and Fourier transformation gave a spectrum showing the one-bond quartet (<sup>1</sup>J = ca. 140 Hz) with further splittings due to coupling to the para proton of 0.132±0.004 Hz.

## (xviii) 4-methylthioanisole

The SCH<sub>3</sub> carbon spectrum of a 50 v/v % solution of 4-methylthioanisole in acetone-d<sub>6</sub> is shown in Figure 25. The aromatic region corresponding to the protons meta to the ring methyl is decoupled in order to simplify the spectra. The SCH<sub>3</sub> carbon probably couples to the meta protons by approximately 0.075 Hz, and presumably couples very little to the ortho protons. The spectra are recorded at 75.486 MHz with 128 scans accumulated into 64K of memory. The acquisition time is about 28 seconds and the temperature is 300K. The seven-bond coupling constant between the methylthio carbon and the ring methyl protons is 0.190±0.004 Hz.

## Figure 25

The methylthio carbon spectrum of 4-methylthioanisole under conditions of aromatic proton decoupling. The scale shown refers to each multiplet separately.





## B. Molecular Orbital Calculations

Some results of the partial geometry optimization of thioanisole at the STO-3G level appear as Figure 26. This geometry optimization is almost total, with the exception of carbon-carbon-carbon bond angles in the ring, which are held at  $120^\circ$ , and that the aromatic ring is constrained to lie in a plane. The inclusion of 3d orbitals on sulfur or complete optimization makes little difference in the calculated barrier to internal rotation over that calculated by the partial geometry optimization procedure (Table 14). Barriers to internal rotation, as calculated by the partial geometry optimization procedure at the STO-3G level, for several derivatives of thioanisole are included in the same table. The calculated potential curves for thioanisole, 2,6-difluorothioanisole, 2,6-dichlorothioanisole, and 3,5-difluorothioanisole appear as Figures 27 to 30. The inset equation is the best curve fitted to the potential function obtained by non-linear regression analysis.

Some results from INDO calculations for thioanisole, 3,5-difluorothioanisole, and 4-fluorothioanisole are given in Table 15. Figure 31 shows the INDO calculated  ${}^6J(C,H)$  as a function of the dihedral angle.

## Figure 26

Calculated planar geometry of thioanisole from optimization at the STO-3G level.

The 90° conformer calculated geometry is very nearly the same as that for the 0° conformer except that the C-S-C bond angle decreases to 97.9°, the S-Cl-C(ortho) and all C-C-H bond angles become 120°, all aromatic C-H bond lengths become 1.083 Å, the sulfur atom is no longer in the aromatic plane by 1.25°, the S-Cl bond length increases to 1.787Å, and the C $\alpha$ -S bond length increases to 1.803Å.

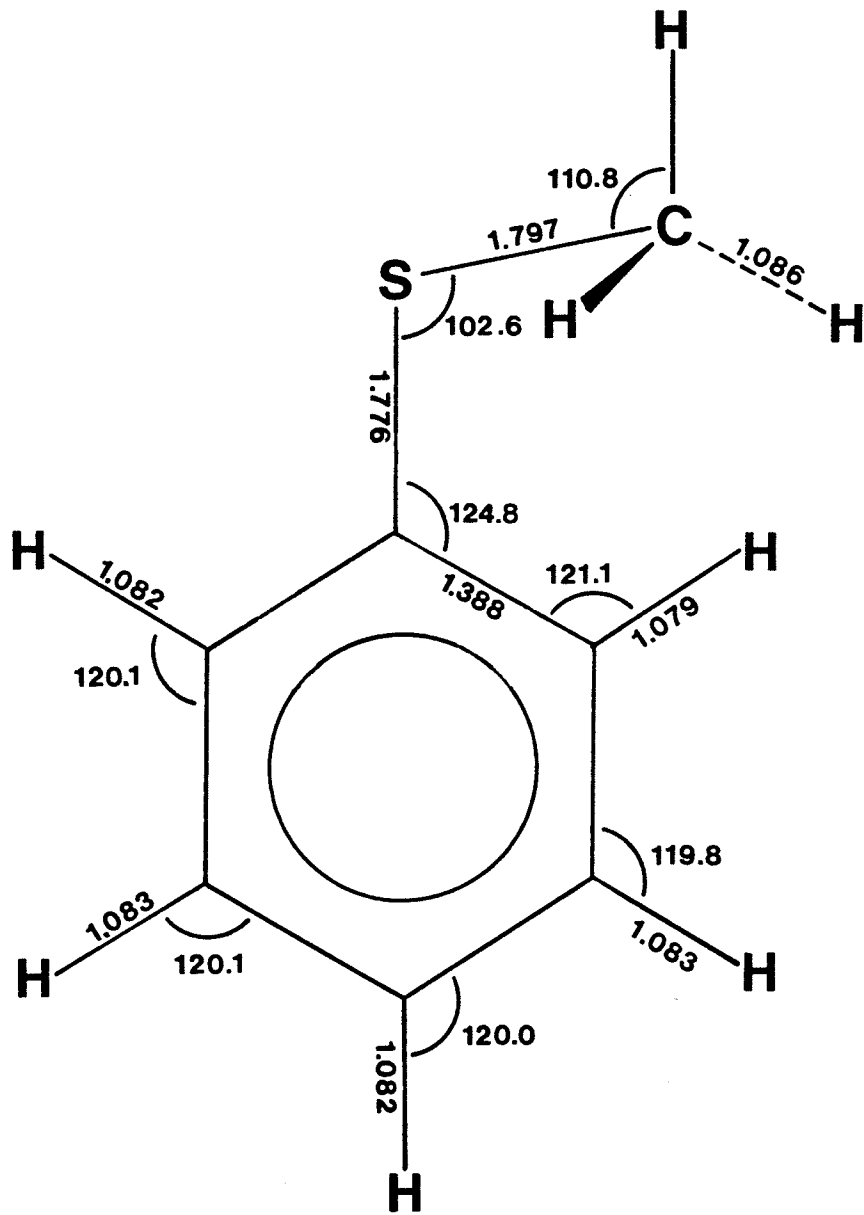


Table 14

Barriers to internal rotation as calculated by optimization at the STO-3G level†.

molecule	barrier(kJ mol <sup>-1</sup> )
thioanisole	5.9
thioanisole, with 3d orbitals	7.9
thioanisole, complete optimization	5.9
4-fluorothioanisole	4.6
4-methylthioanisole	4.9
3,5-dimethylthioanisole	6.6
3,5-difluorothioanisole	8.6
3,5-dichlorothioanisole	7.5
2,6-difluorothioanisole	9.7
2,6-dichlorothioanisole	31.3
2-chlorothioanisole	5.3

† The barriers listed are the difference in energies between 0 and 90° conformers. The energy for the 180° (cis) conformer of 2-chlorothioanisole is 29.4 kJ mol<sup>-1</sup> above the most stable trans conformer. Energies were calculated by partial geometry optimization at the STO-3G level (see text for details), unless otherwise stated.

## Figure 27

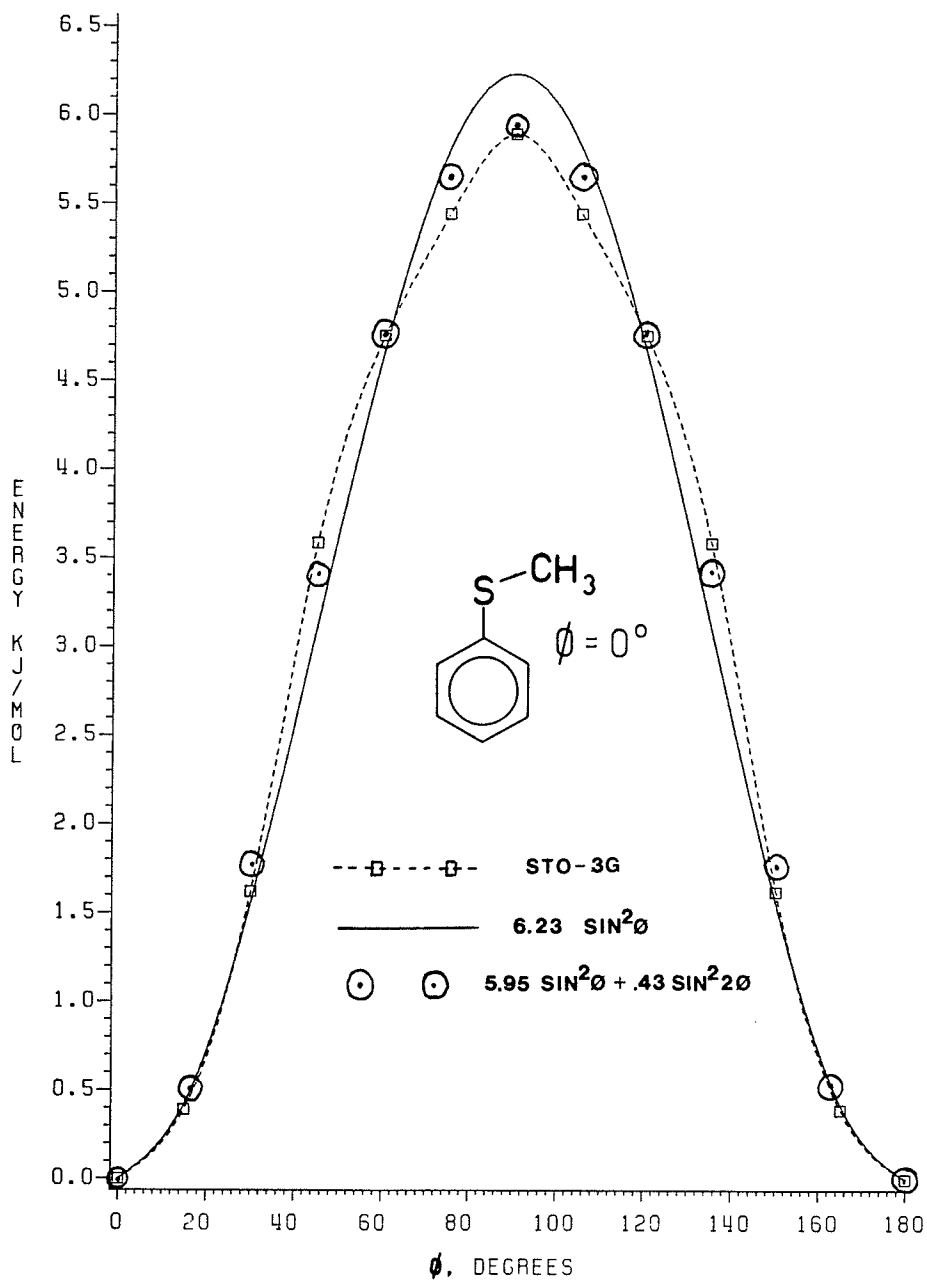
The STO-3G potential curve for internal rotation in thioanisole.

The best fit equation for a two-fold potential function:

$$\Delta E = 6.23 \pm 0.24 \sin^2 \phi$$

The best fit equation for a two- and four-fold potential:

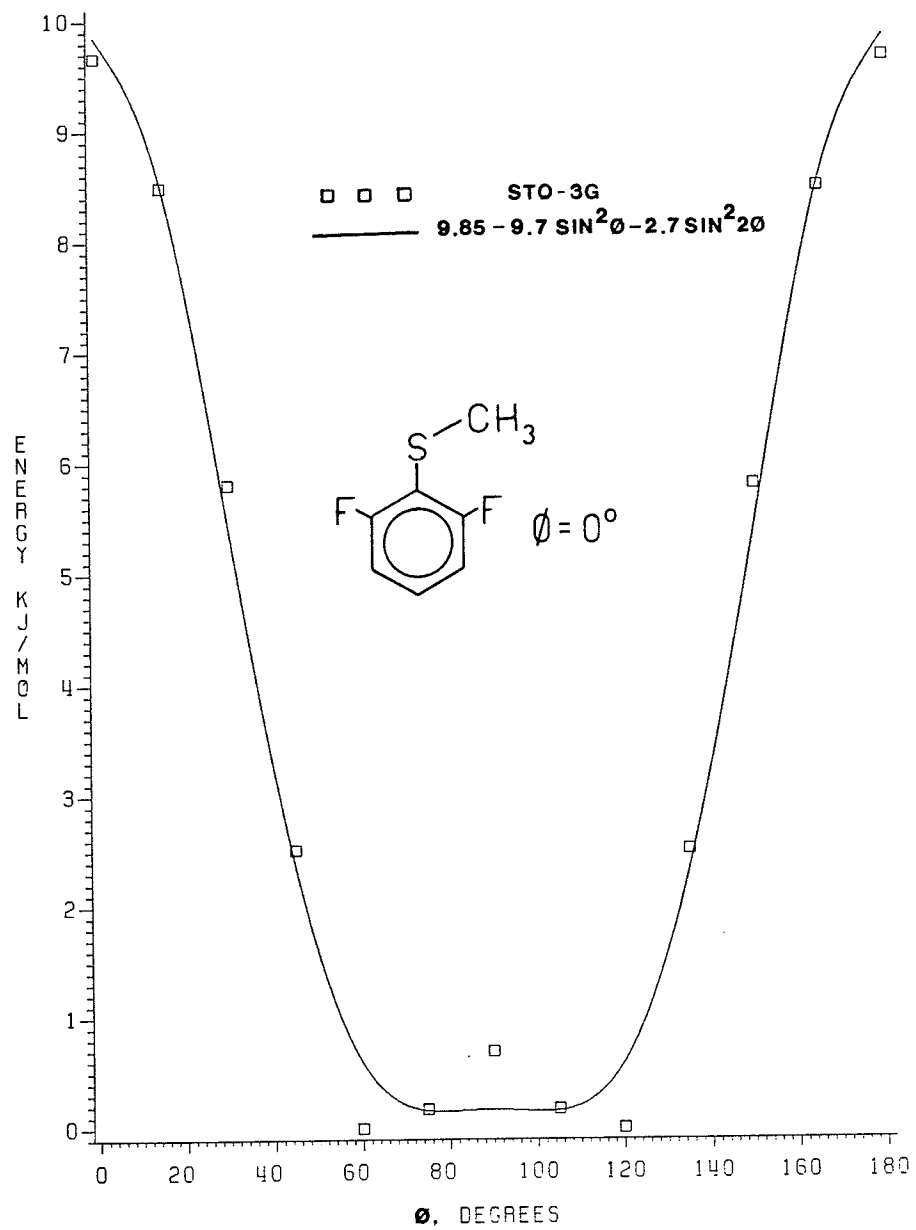
$$\Delta E = 5.95 \pm 0.18 \sin^2 \phi + 0.43 \pm 0.17 \sin^2 2\phi$$

STO-3G CALCULATED POTENTIAL CURVE FOR INTERNAL ROTATION  
IN THIOANISOLE

## Figure 28

The STO-3G potential curve for internal rotation in 2,6-difluorothioanisole. The best fit equation for a two- and four-fold potential function:

$$\Delta E = 9.85 - 9.7 \pm 0.6 \sin^2 \theta - 2.7 \pm 0.6 \sin^2 2\theta$$

STO-3G CALCULATED POTENTIAL CURVE FOR INTERNAL ROTATION  
IN 2,6-DIFLUOROTHIOANISOLE

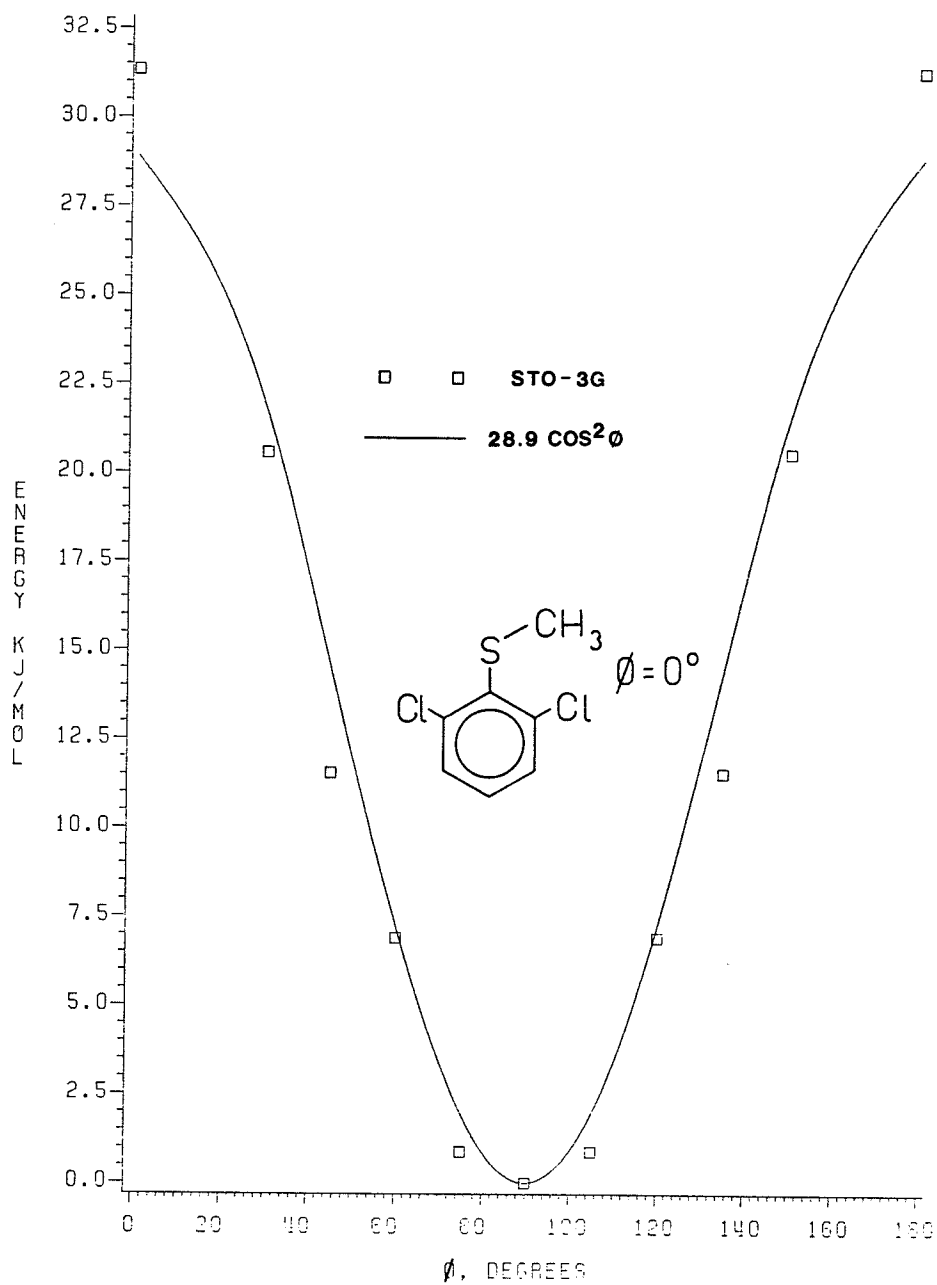


## Figure 29

The STO-3G potential curve for internal rotation in 2,6-dichlorothioanisole.

The best fit equation for a two-fold potential function:

$$\Delta E = 28.9 \pm 2.1 \cos^2 \theta$$

STO-3G CALCULATED POTENTIAL CURVE FOR INTERNAL ROTATION  
IN 2,6-DICHLOROTHIOANISOLE

## Figure 30

The STO-3G potential curve for internal rotation in 3,5-difluorothioanisole. The best fit equation for a two-fold potential function:

$$\Delta E = 8.84 \pm 0.26 \sin^2 \phi$$

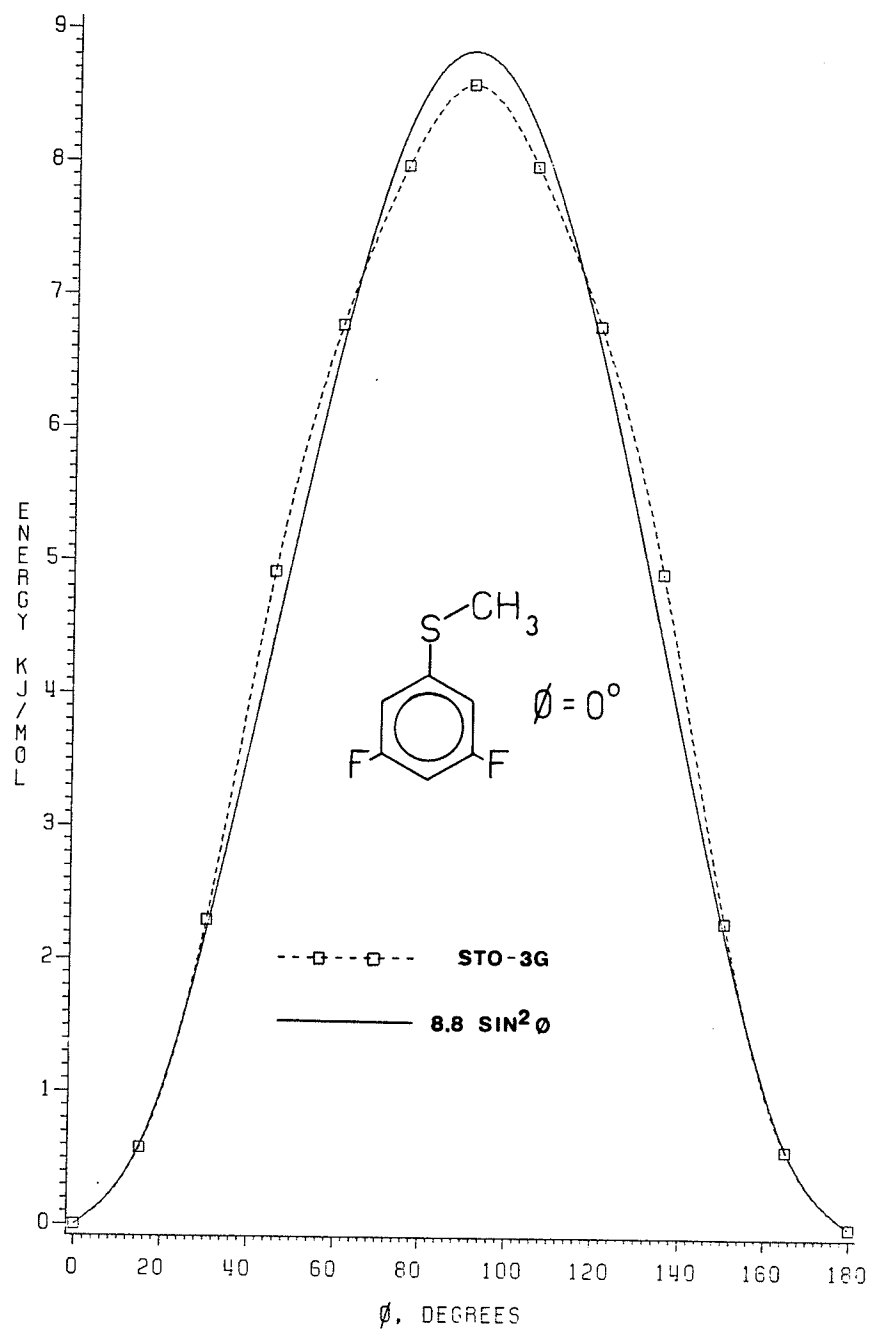
STO-3G CALCULATED POTENTIAL CURVE FOR INTERNAL ROTATION  
IN 3,5-DIFLUOROTHIOANISOLE

Table 15

Some coupling constants, as calculated by INDO MO FPT for thioanisole, 3,5-difluorothioanisole, and 4-fluorothioanisole†.

J(C $\alpha$ , X)	$\phi$ (degrees)						90°
	0° (180°)	15° (175°)	30° (150°)	45° (135°)	60° (120°)	75° (105°)	
H2,H6	-0.73 (-0.73)	-0.74 (-0.74)	-0.78 (-0.76)	-0.84 (-0.79)	-0.86 (-0.85)	-0.90 (-0.90)	-0.93
H3,H5	-0.07 (0.10)	-0.06 (0.10)	-0.02 (0.11)	0.04 (0.13)	0.09 (0.14)	0.14 (0.15)	0.16
H4	-0.06	-0.09	-0.17	-0.30	-0.40	-0.50	-0.54
C2,C6	2.15 (2.80)	2.14 (2.74)	2.15 (2.58)	2.14 (2.32)	2.04 (2.05)	1.90 (1.89)	1.84
C3,C5	-0.37 (-0.15)	-0.45 (-0.28)	-0.66 (-0.51)	-0.97 (-0.90)	-1.31 (-1.31)	-1.61 (-1.62)	-1.73
C4	0.01	0.10	0.37	0.77	1.12	1.51	1.64
F3,F5	-0.11 (0.11)	-0.14 (0.06)	-0.25 (-0.13)	-0.42 (-0.34)	-0.61 (-0.60)	-0.77 (-0.78)	-0.84
F4	-0.34	-0.30	-0.15	0.10	0.89	0.47	0.54
J(CH <sub>3</sub> , H)							
H2,H6	-0.14 (0.10)	-0.11 (0.11)	-0.03 (0.11)	0.07 (0.11)	0.10 (0.10)	0.11 (0.10)	0.10
H3,H5	0.07 (0.23)	0.07 (0.23)	0.07 (0.22)	0.08 (0.21)	0.09 (0.20)	0.12 (0.17)	0.14
H4	-0.02	-0.01	-0.01	-0.01	-0.03	-0.05	-0.06

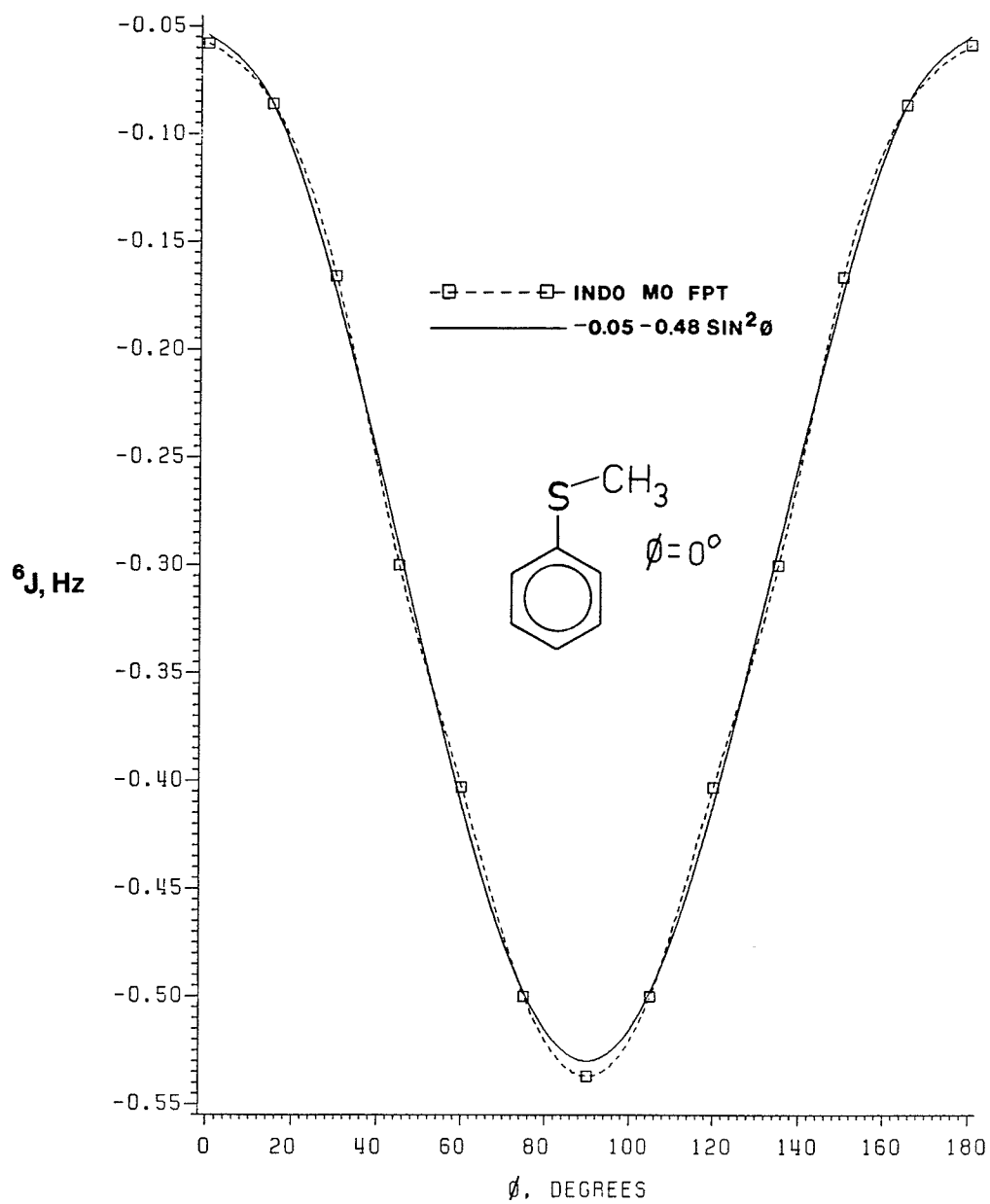
† The data tabulated is for thioanisole, except data for coupling constants involving fluorine nuclei. The assumed geometries are from optimization at the STO-3G level of MO theory.

Figure 31

The INDO MO FPT calculated  ${}^6J(C,H)$  for thioanisole.

The best fit equation for the experimental curve is:

$${}^6J(C,H) = -0.05 \pm 0.01 - 0.49 \pm 0.01 \sin^2 \theta$$

INDO CALCULATED  ${}^6J$  C,H FOR  
THIOANISOLE

DISCUSSION



### A. The hindered rotor model and the J method

Internal rotation in molecules usually describes the rotation of one part of a molecule relative to another part about a bond that joins the two parts. The heavier part is designated the molecular frame, while the motion of the top, the lighter part, is considered about the adjoining bond. As the top rotates in the frame, an infinite number of conformations will be formed, and re-formed, as the internal rotation proceeds through  $360^\circ$ . If there are no interactions between the two parts that favour any one conformation, or conformations, the internal rotation is called free. However, if any conformation is more likely to occur, a hindering potential must exist that biases the conformer distribution. The difference in potential energy between the conformer of greatest stability and the conformer of least stability is known as the barrier to internal rotation.

A mathematical description of the hindering potential,  $V$ , begins with the observation that internal rotation is periodic. Therefore, a logical choice for a function would be one that is trigonometric. The equation most often used<sup>1</sup> to describe the potential for internal rotation is

$$V(\varnothing) = \sum_n V(n)/2 (1 - \cos n\varnothing) \quad (3)$$

where  $\varnothing$  is the angle describing the orientation of the top, relative to the frame of the molecule. The coefficients,  $V(n)$ , are determined experimentally, and are the algebraic symbols for the hindering potential of that symmetry. For an  $n$ -fold symmetric potential, coefficients which are integral multiples of  $n$  are non-zero. Experimental values<sup>9,1</sup> show that  $V(n) \gg V(n+1) \gg V(n+2) \dots$ , i.e. that the preceding term is larger than that of the following term in the series. Therefore, to a good approximation for a predominantly two-fold symmetric potential, one may write

$$V(\varnothing) = V(2)/2 (1 - \cos 2\varnothing) + V(4)/2 (1 - \cos 4\varnothing) \quad (4)$$

and many experimental investigations of such potentials assume that

$$V(\varnothing) = V(2)/2 (1 - \cos 2\varnothing) \quad (5)$$

This work concerns itself, in part, with the determination of rotational barriers and preferred conformations by high-resolution nuclear magnetic resonance spectroscopy and the J method<sup>5,5</sup>. Experimentally, the method requires the measurement of long-range spin-spin coupling constants between a nucleus in the para position (carbon, proton, or fluorine) and a nucleus bonded to the carbon or heteroatom in the  $\alpha$  position of the side chain. Such coupling constants are transmitted by

the  $\pi$ -electrons via a  $\sigma$ - $\pi$  mechanism<sup>5,6</sup> and as such are expected to exhibit a  $\sin^2\theta$  dependence.

Therefore, if the appropriate reference coupling constants exist, the expectation value for  $\sin^2\theta$  may be calculated. More specifically, from equation(1), p. 22

$$\langle \sin^2\theta \rangle = {}^6J(\text{observed})/{}^6J_{,0} \quad (6)$$

where  ${}^6J_{,0}$  is the value of the coupling constant at  $\theta=90^\circ$ . Furthermore,  $\langle \sin^2\theta \rangle$  is the ensemble average of  $\sin^2\theta$  over the hindered rotor states. The hindered rotor states, and their energies, have been calculated by solving the Schrödinger equation

$$\hat{H} \Psi(m) = E(m) \Psi(m) \quad (7)$$

$E(m)$  is the energy of the  $m^{\text{th}}$  state with wavefunction  $\Psi(m)$ .  $\hat{H}$  is the Hamiltonian operator which is itself a sum of the potential and kinetic energy operators  $\hat{V}$  and  $\hat{T}$ , respectively. Equation (7) may be re-written to include the individual operators and as given in reference (55), and with reference to equation (4):

$$(-\hbar^2/2I) (d^2\Psi/d\theta^2) + (V_2/2) (1 - \cos 2\theta) \Psi = E \Psi \quad (8)$$

The principal parameters are  $I$ , the reduced moment of inertia, and  $V_2$ , the magnitude of the two-fold barrier to internal rotation. Once the hindered rotor states and their energies have been obtained and the value of  $\langle \sin^2\theta \rangle$  has been calculated by weighting its expectation

value for each state with the usual Boltzmann factor, tables of  $\langle \sin^2 \varphi \rangle$ , temperature, two-fold barrier height, and reduced moments of inertia may be constructed. This has been done by Dančura<sup>9,2</sup>. The tables illustrate that  $\langle \sin^2 \varphi \rangle$  is a very weak function of the reduced moment of inertia.

## B. MO calculations of the internal barrier in thioanisoles

Thioanisole is a benzene derivative in which it is assumed that the barrier is two-fold, and that the most stable conformation is that with coplanar heavy atoms ( $\theta=0^\circ$ ). Although experimental studies have shown that the methylthio group prefers to lie in the plane of the aromatic ring, the shape, and notably, the height, of the internal barrier is uncertain.

The STO-3G level of MO theory implies that the barrier to internal rotation in thioanisole is  $5.9 \text{ kJ mol}^{-1}$  and is predominantly two-fold (Figure 27). However, a small four-fold component added into the expression for the potential energy perhaps gives better agreement with the STO-3G calculated energies. The total energy for the most stable, geometry optimized, conformer is  $-659.6543 \text{ a. u.}$ , which is approximately  $15 \text{ kJ mol}^{-1}$  lower than that given in a previous calculation with partial optimization ( $-659.6485 \text{ a. u.}$ )<sup>50</sup>. With the addition of d orbitals in the basis set, the energy drops to  $-659.6918 \text{ a. u.}$ , or  $98 \text{ kJ mol}^{-1}$  lower than the energy calculated without the inclusion of d orbitals. Since the barrier to internal rotation, as calculated by STO-3G, does not change considerably with the addition

of d orbitals, and since the addition increased the computation time for geometry optimization by six- or seven-fold, d orbitals were not generally included for STO-3G calculations on thioanisoles. STO-3G potential energy curves for internal rotation in 3,5-difluorothioanisole (Figure 30) and 4-fluorothioanisole (data not shown) are similar to that of thioanisole.

The methyl C-H bonds are in a conformation of lowest energy when the dihedral angles with respect to the plane defined by Cl-S-C $\alpha$  are 60, 180, and 300° for both planar and perpendicular conformers of thioanisole. As the methylthio group twists out of the ring plane, the methyl group twists so as to keep two proton-ortho proton distances equal. At  $\phi=45^\circ$ , the respective dihedral angles are 45, 165, and 285°. Such a motion is four-fold and may account for the four-fold component seen in the potential energy curve describing the disposition of the methylthio group about the Csp<sup>2</sup>-sulfur bond.

However, a reasonable explanation of the data presented in this work is possible, if the four-fold component of the barrier is considered negligible for the compounds in which both ortho positions are occupied by protons.

### C. The stereospecificity of coupling constants

#### (i) The stereospecific coupling constant ${}^6J(C\alpha, H4)$

In the presence of two ortho chlorine or bromine substituents,  ${}^6J(C\alpha, H4)$  is  $-0.510 \pm 0.005$ † and  $-0.541 \pm 0.005$  Hz, respectively. In 4-methyl-2,6-dibromothioanisole,  ${}^7J(C\alpha, CH_3)$  is  $0.606 \pm 0.005$  Hz. In the presence of two sizeable ortho substituents, X-ray diffraction data indicate a perpendicular conformation of the methoxy group in anisole<sup>93-95</sup>. The barrier to internal rotation in thioanisole is likely much less than that in anisole<sup>96</sup>. Since the planar conformations of anisole and thioanisole are preferred, it follows that in the presence of two bulky ortho substituents, a perpendicular conformation for the thioanisole derivative is also likely. STO-3G results on 2,6-dichlorothioanisole (Figure 29) are confirmatory. The perpendicular conformer is calculated to be nearly  $32 \text{ kJ mol}^{-1}$  more stable than a planar conformation.

---

† From the proton spectrum of a 4 mol % solution of 2,6-dichloro( $\alpha$ - $^{13}\text{C}$ )thioanisole in acetone- $d_6$ , the measured coupling constant is  $-0.519(4)$  Hz. The value from the carbon spectrum for a 22 mol % solution in benzene- $d_6$  is  $-0.500 \pm 0.005$  Hz. The quoted value is the average of these two measurements.

For a  $\sigma$ - $\pi$  mechanism, in which the coupling constant is transmitted via the  $\pi$  orbitals of the benzene ring, it is expected that  ${}^6J(C\alpha, H)$  is approximately equal to  $-{}^7J(C\alpha, H)$ . Although the sign of the latter coupling is not known in the thioanisole derivative, INDO MO FPT computations (Table 17) agree that the six- and seven-bond couplings are nearly equal in magnitude, and opposite in sign; and that  ${}^6J(C\alpha, H)$  has a  $\sin^2\theta$  dependence, as expected for a  $\sigma$ - $\pi$  mechanism (Figure 31). In particular, the equation fitted to the INDO results is

$${}^6J = -0.05 - 0.49 \sin^2\theta \quad (9)$$

For  $\theta = 90^\circ$ , the calculated value of  ${}^6J$  is  $-0.54$  Hz, which agrees very well with the observed value of  $-0.541 \pm 0.005$  Hz in 2,6-dibromothioanisole. The nearly exact agreement is most likely fortuitous since the value of  $-0.05$  Hz is most likely an artifact of the calculation<sup>8</sup>. The sign determination of  ${}^6J(C\alpha, H)$  in 2,6-dichlorothioanisole (Figures 12 and 13) agrees with the sign calculated by INDO MO FPT. In a similar INDO calculation for a perpendicular conformation of 4-methylthioanisole, the calculated value is  $+0.61$  Hz, which agrees well with the magnitude observed in 2,6-dibromo-4-methylthioanisole (0.607 Hz).

By analogy with  ${}^6J(C\alpha, H4)$  in anisole<sup>9,6</sup>, and  ${}^6J(SH, H4)$  in thiophenol<sup>24</sup>,  ${}^6J(C\alpha, H4)$  in thioanisole is likely a



$\sigma$ - $\pi$  coupling with a simple conformational dependence. Calculations on 2,6-difluorothioanisole and 3,5-difluorothioanisole suggest that  ${}^6J$  may decrease by approximately 0.05 Hz in the presence of the ortho or meta substituents, implying that intrinsic ring substituent perturbations of this coupling are small, but perhaps not negligible.  ${}^6J_{,0}(C\alpha, H4)$  in thioanisole and its derivatives will be taken as  $0.54 \pm 0.01$  Hz in magnitude and  ${}^7J_{,0}(C\alpha, CH_3)$  in 4-methylthioanisole as  $0.61 \pm 0.01$  Hz.

The increase in  ${}^7J$  relative to  ${}^6J$  seen (ca. 12%) with the methyl group replacement technique for the establishment of a  $\sigma$ - $\pi$  mechanism is similar to the increase seen in alkenes<sup>97</sup> and that observed for 4-methylthiophenol. In thiophenols analogous conformational dependences of SH couplings into the ring are<sup>24</sup>

$$\begin{aligned} {}^4J(H,H) &= -1.10 (\sin^2\theta) && \text{and} \\ {}^6J(H,H) &= -0.97 (\sin^2\theta) && (10a, 10b) \end{aligned}$$

From table 14,  ${}^4J(H,H) = -0.456$  Hz. It follows that  $\langle \sin^2\theta \rangle$  is 0.414 and that the non-existent  ${}^6J$  should be -0.402. The observed coupling is  ${}^7J(SH, CH_3) = +0.441$ , which is approximately 10% larger than would be expected if  ${}^6J = -{}^7J$ . In toluene derivatives, however,  ${}^6J$  is equal to  ${}^7J$  in magnitude, to within experimental error.

(ii) The six-bond carbon-fluorine coupling constant.

If  ${}^6J(C\alpha, F)$  is taken as a  $\sigma$ - $\pi$  coupling, then the discussion below is self-consistent and also consistent with the trends observed in the corresponding anisole derivatives. In 4-fluoroanisole, INDO MO FPT calculations do substantiate its  $\sin^2\theta$  dependence, but underestimate its maximum value (observed as  $1.480 \pm 0.02$  Hz) as 0.7 Hz. In 4-fluorothioanisole, INDO calculates  ${}^6J(C\alpha, F)$  to be a maximum at  $\theta = 60^\circ$  with a value of 0.86 Hz (Table 15). However, if this value is ignored, equation (11) reproduces  ${}^6J(C\alpha, F)$  to within 0.02 Hz.

$${}^6J(C\alpha, F) = 0.89 \sin^2\theta - 0.35 \quad (11)$$

If the non-stereospecific contribution to equation (11) is considered an artifact, the calculated coupling constant for  ${}^6J_{,0}$  is +0.89 Hz. The measured value in 2,6-dibromo-4-fluorothioanisole is  $1.480 \pm 0.013$  Hz.

The methyl group replacement technique<sup>3</sup> is inapplicable as a test of the  $\sigma$ - $\pi$  mechanism. Here, the presence of a contribution to  ${}^6J(C\alpha, F)$  from a mechanism other than a  $\sigma$ - $\pi$  mechanism or an intrinsic ring substituent perturbation of its magnitude cannot yet be ruled out.

In spite of its problematical basis, for

4-fluorothioanisoles equation (12) will be used

$$\langle \sin^2\theta \rangle = {}^6J(C\alpha, F)_{\text{observed}} / 1.48 \pm 0.02 \quad (12)$$

where  $\langle \sin^2\theta \rangle$  is the expectation value of  $\sin^2\theta$  for the hindered motion.

- (iii) The rotational angle dependence of  ${}^5J(C\alpha,H)$  in thioanisole

In thiophenol, the five-bond spin-spin constant between the sulfhydryl proton and the ring proton in the meta position<sup>5</sup> is given by equation (13),

$${}^5J = {}^5J_{\rho_0}(\pi)\langle\sin^2\emptyset\rangle + {}^5J_{1,\rho_0}(\sigma)\langle\sin^2(\emptyset/2)\rangle \quad (13)$$

where  $\emptyset$  is the angle by which the SH bond twists out of the benzene plane,  ${}^5J_{\rho_0}(\pi)$  is the  $\pi$  electron contribution having a maximum at  $\emptyset = 90^\circ$ , and  ${}^5J_{1,\rho_0}(\sigma)$  is the  $\sigma$  electron contribution with a maximum at  $\emptyset = 180^\circ$  (zig-zag orientation). The analogous coupling  ${}^5J(C\alpha,H)$  in thioanisole may well have the same angle dependence. The equation

$${}^5J = -0.06 + 0.14 \sin^2\emptyset + 0.15 \sin^2\emptyset/2 \quad (14)$$

fits the INDO MO FPT calculated results given in Table 15 to within 0.02 Hz.

In 2,6-dibromothioanisole, where  $\langle\sin^2\emptyset\rangle$  is nearly unity and  $\langle\sin^2\emptyset/2\rangle$  is 1/2, the observed coupling is  $0.217 \pm 0.005$  Hz. In thioanisole, the data below indicate  $\langle\sin^2\emptyset\rangle$  as 0.272 and here the observed coupling is 0.078 Hz. Assuming that the conformationally independent coefficient of equation (14) is an artifact of the INDO calculation, the empirical equivalent to (14) is

$${}^5J = 0.19 \sin^2\theta + 0.052 \langle \sin^2\theta/2 \rangle \quad (15)$$

Although ring substituents do not dramatically alter the total  $\pi$  population of the benzene ring, there may be a redistribution of this population, especially since the substituent will polarize the  $\sigma$  framework<sup>5,5</sup>. Therefore, since  ${}^6J(C\alpha, H)$  is probably determined by the net  $\pi$  electron distribution, its magnitude need not be altered since multiple coupling paths are followed. However, the  $\sigma$  component may well be affected by the presence of halogen substituents. In 2-iodothioanisole and in 2,4,5-trichlorothioanisole, where  $\langle \sin^2\theta \rangle$  is small, and  $\langle \sin^2\theta/2 \rangle$  is nearly unity, the observed all trans coupling constants ( ${}^5J(C\alpha, H3)$ ) are  $0.133 \pm 0.013$  and  $0.194 \pm 0.011$  Hz, respectively, indicating that substituent perturbations are important for this coupling.

(iv) The rotational angle dependence of  $^5J(C\alpha,F)$  in meta-fluorothioanisoles

In a manner similar to  $^5J(C\alpha,H)$ ,  $^5J(C\alpha,F)$  may be a composite of  $\sigma-\pi$  and  $\sigma$  electron coupling mechanisms. Equation (12) reproduces the INDO MO FPT results given in Table 15 to within 0.05 Hz

$$^5J(\text{INDO}) = -0.06 - 0.84(\sin^2\theta) + 0.15(\sin^2\theta/2) \quad (16)$$

What is different and interesting here is that the two mechanisms give contributions of opposite sign.

The measured values of  $^5J(C\alpha,F)$  for 2,4,6-tribromo-3-fluorothioanisole ( $\langle \sin^2\theta \rangle = 1$ ), pentafluorothioanisole ( $\langle \sin^2\theta \rangle = 0.805$ , see discussion below), and 2,3,5,6-tetrafluorothioanisole ( $\langle \sin^2\theta \rangle = 0.685$ ) are  $-0.593 \pm 0.01$ ,  $-0.463 \pm 0.008$ , and  $-0.376 \pm 0.006$  Hz, respectively. The sign has been determined for tetrafluorothioanisole (Figure 20), and is in agreement with that predicted from the INDO MO FPT results. A best fit equation for these three compounds yields an empirical equivalent to equation (16)

$$^5J(\text{observed}) = -0.82\langle \sin^2\theta \rangle + 0.41\langle \sin^2\theta/2 \rangle \quad (17)$$

This equation reproduces the observed coupling constants to within 0.02 Hz. For all of these compounds,  $\langle \sin^2\theta/2 \rangle$  is 0.5. A non-stereospecific contribution ( $-0.06$  in equation (16)) is probably absent.

A check of the proposed mechanisms is available with 2-methyl-3-fluorothioanisole. Here, the observed all trans coupling is  $0.408 \pm 0.009$  Hz. Assuming  $\langle \sin^2 \theta \rangle = 0.0$  and  $\langle \sin^2 \theta / 2 \rangle = 1.0$ , the calculated coupling is  $+0.410$  Hz. However, since the ortho methyl group is not very large, the methylthio group is not held rigidly in plane at  $180^\circ$  to the C3-F bond, but librates considerably about this position. Therefore  $\langle \sin^2 \theta \rangle$  is most likely small, but not zero, and  $\langle \sin^2 \theta / 2 \rangle$  is nearly unity, but not equal to it. Then, the calculated coupling from equation (17) is too small.

Before equation (17) is accepted as the conformational dependence of  $^3J(C\alpha, F)$ , contributions from other mechanisms should be taken into account, and ring substituent perturbations of the coupling constant magnitude should be accounted for.

(v)  ${}^4J(C\alpha,H)$  and  ${}^4J(C\alpha,F)$ 

In 2-iodothioanisole,  ${}^4J(C\alpha,H)$  is  $+0.172\pm 0.012$  Hz. INDO MO FPT calculates the coupling to be  $-0.73$  Hz for a planar conformation of thioanisole. In the methyl-proton decoupled spectrum of 3,5-dichloro( $\alpha$ - ${}^{13}C$ )thioanisole, the observed line width in the ortho region (0.045 Hz) is no larger than that observed in the para proton region (Figure 24). Clearly, here  ${}^4J(C\alpha,H)$  is vanishingly small. Therefore, the observed coupling in 2-iodothioanisole indicates that this coupling is likely proximate<sup>87</sup> in nature.

${}^4J(C\alpha,F)$  is considerably larger in magnitude (between +3 and +4 Hz in 2,6-difluorothioanisole derivatives) and the discussion which follows below indicates that it also could be a proximate coupling. INDO MO FPT calculations for  ${}^4J(C\alpha,F)$  are as disappointing as for  ${}^4J(C\alpha,H)$  and indicate that  ${}^4J(C\alpha,F)$  is negative (whereas it is found experimentally to be positive, Figure 19) and that it has no simple conformational dependence.



D. Barriers to internal rotation and coupling constants between  $C\alpha$  and ring nuclei as indicators of methylthio group conformation.

(i) The barriers to internal rotation in thioanisole, 4-fluorothioanisole, 4-methylthioanisole, 3,5-dimethylthioanisole, and 3,5-dichlorothioanisole.

The barriers to internal rotation in five thioanisole derivatives with no substituents ortho to the methyl are given in Table 16. Equation 6 and data from equation 8<sup>5,9,2</sup> are most pertinent.

Table 16 Barriers to internal rotation

Substituents	${}^6J(C\alpha, X)$	${}^6J_{\theta}$	$\langle \sin^2\theta \rangle$	$V_2$ (kJ mol <sup>-1</sup> )
4-fluoro	0.474(7)	1.48(2)	.320(20)	3.7±.6
4-methyl	0.190(4)	0.61(1)	.311(12)	3.9±.1
4-H	-0.147(3)	-0.54(1)	.272(15)	5.1±.2
3,5-dimethyl	-0.132(4)	-0.54(1)	.244(12)	6.1±.4
3,5-dichloro	-0.087(5)	-0.54(1)	.161(13)	9.6±.7

Values in parentheses for the coupling constants correspond to three times the standard deviation calculated by NUMARIT or are the 95% confidence intervals for the last one (or last two) places. The error estimates for the barrier to internal rotation are calculated on the basis of the highest and lowest  $\langle \sin^2\theta \rangle$  values, which

come, in turn, from measurement errors in the coupling constants.

The barrier to internal rotation in thioanisole is  $5.1 \pm 0.2$  kJ mol<sup>-1</sup>. This value is higher than the value estimated by Schweig and Thon<sup>29</sup> for thioanisole vapour ( $3.5 \pm 0.3$  kJ mol<sup>-1</sup>), using a two-site model. In anisole, the barrier in the liquid is substantially higher than that of the vapour<sup>7,2</sup>.

The barrier in thioanisole is somewhat larger than in thiophenol ( $3.4$  kJ mol<sup>-1</sup>)<sup>24</sup>. In both molecules, the planar form is most stable. Methylation of the sulfhydryl group might increase steric interactions with ortho protons and might destabilize the planar conformer relative to the perpendicular conformer. This would lead to a lower barrier. Since the barrier increases, it seems plausible that the methyl group on the sulfur donates electrons more easily than does hydrogen, and increases conjugation with the ring.

In 4-fluorothiophenol, the barrier to internal rotation is measured to be  $0.4$  kJ mol<sup>-1</sup>, lower than in thiophenol<sup>24</sup>. The measured barrier in 4-fluorothioanisole is also lower than in thioanisole and is  $3.7 \pm 0.2$  kJ mol<sup>-1</sup>. The barrier in 4-fluoroanisole is found<sup>9,6</sup> to be  $23.4$  kJ mol<sup>-1</sup>, which is likely lower than in anisole. A previous determination of 4-fluorothioanisole at room

temperature by microwave spectroscopy<sup>25</sup> gives the barrier as  $3.0 \pm 1.0$  kJ mol<sup>-1</sup>, which is in agreement with the experimental determination in this thesis.

In order to compare the barriers to internal rotation in thioanisoles to those in the corresponding thiophenols, 3,5-dimethylthiophenol, 3,5-dichlorothiophenol, and 4-methylthiophenol were also investigated. The barriers to internal rotation for the thioanisole derivatives listed in Table 16 are reproduced in Table 17, with the rotational barriers of the corresponding thiophenols (from Table 14 and reference 24). Barriers to internal rotation calculated by STO-3G are also included for the thioanisoles.

Table 17 Barriers to internal rotation in thioanisoles and thiophenols

Substituents	Barrier (kJ mol <sup>-1</sup> )		
	STO-3G calculated (thioanisole)	thioanisole derivative	thiophenol derivative
4-fluoro	4.6	3.7	0.4 <sup>24</sup>
4-methyl	4.9	3.9	1.7
4-H	5.9	5.1	3.4 <sup>24</sup>
3,5-dimethyl	6.6	6.1	4.4
3,5-dichloro	7.5	9.6	6.9

What is apparent from the table is that trends in the

experimentally determined barriers for the thioanisoles are reproduced by STO-3G calculations, and mimic the increasing barrier in the thiophenols. Electron releasing and withdrawing groups can decrease and increase, respectively, the conjugation with the ring and the barrier to internal rotation.

Parenthetically,  ${}^6J(C\alpha,H)$  in 2,6-dichlorothioanisole is  $-0.51 \pm 0.01$  Hz, indicating that the perpendicular conformation of the methylthio group is preferred by at least  $19 \text{ kJ mol}^{-1}$  over a planar conformation. This is the lower limit; the mean value is  $25 \text{ kJ mol}^{-1}$ . This result is comparable to the STO-3G calculated result of  $31.3 \text{ kJ mol}^{-1}$  (Figure 29).

(ii) Barriers to internal rotation in fluorothioanisoles

If both positions ortho to the methylthio group are occupied by fluorine, STO-3G MO and coupling constant data are consistent with a preferred perpendicular conformation of the methylthio group. However, here the four-fold component to internal rotation may not be negligible, as indicated by STO-3G MO theory for 2,6-difluorothioanisole (Figure 28). Further support for a four-fold component comes from Figure 22. Here plots of  ${}^3J(\text{CH}_3, \text{F})$  for 2,6-difluorothioanisoles show little variation with temperature. This coupling has been shown to be proximate in nature in anisoles (from unpublished work in this laboratory). Its value is +0.2 to 0.3 Hz when the methoxy group is orientated in the plane of the ring with the methyl group lying trans to an ortho C-F bond. As the methyl group approaches this C-F bond, the coupling becomes larger than +3 Hz<sup>96</sup>. The analogous coupling in thioanisoles most likely has a similar conformational dependence. For a two-fold barrier, the invariance with temperature can be explained by either no preference for any conformation, i.e. a zero barrier, or a very large barrier for which the methylthio moiety is held in place. For the compounds studied, the barriers are intermediate (see below). These compounds are most stable with the S-Csp<sup>3</sup> bond

oriented perpendicular to the ring plane. In 2,6-difluoroanisole derivatives a temperature dependence of the proximate coupling is seen for derivatives with non-zero barriers<sup>7,2</sup>. The absence of a measurable temperature dependence for the 2,6-difluorothioanisoles can be rationalized if a substantial four-fold component exists which tends to flatten the potential curve about 90°, or if the increasing density of the solution at lower temperatures stabilizes the perpendicular conformations<sup>9,6</sup>.

Presumably, the barrier to internal rotation is dictated by steric interactions between the methylthio C-H bonds and the ortho C-F bonds. When fluorine is replaced by a larger halogen, such as chlorine (Figure 29) or bromine, the four-fold component of the barrier becomes negligible again. Therefore, because there are likely contributions from steric hindrance favouring a perpendicular conformation, from conjugation into the plane of the ring, and from a four-fold component to internal rotation in 2,6-difluorothioanisoles, it seems likely that barriers to internal rotation in this class of compounds may be sensitive to other substituents on the ring.

Assuming that the STO-3G calculations overestimate the four-fold component, barriers to internal rotation

can be derived using equation (6) and data<sup>9,2</sup> from equation (8). Using this approach, a reasonable explanation of the data is possible. The relevant coupling constants for 2,6-difluorothioanisole, 2,4,6-trifluorothioanisole, 2,3,5,6-tetrafluorothioanisole, and 2,3,4,5,6-pentafluorothioanisole are collected in Table 18.

Table 18 Conformationally dependent coupling constants for 2,6-difluorothioanisoles

Fluorine positions	${}^4J(C\alpha, F)$	${}^5J(C\alpha, F)$	${}^6J(C\alpha, F)$	${}^6J(C\alpha, H)$	${}^5J(CH_3, F)$
2,6	3.590(5)	-	-	0.420(3)	0.746(5)
2,4,6	2.965(27)	-	1.198(13)	-	0.588(1)
2,3,5,6	3.984(6)	0.376(6)	-	0.370(5)	0.907(2)
2,3,4,5,6	3.275(15)	0.463(8)	1.192(16)	-	0.722(3)

Values in parentheses are the standard deviations calculated by NUMARIT or the 95% confidence intervals in the last one (or last two) decimal places.

## (a) 2,6-difluorothioanisole

${}^6J(C\alpha, H4)$  is  $0.420 \pm 0.003$  Hz, and, as before,  $\langle \sin^2\theta \rangle$  is  $0.420 \pm 0.003 / 0.54 \pm 0.01$  or 0.778. In terms of a two-fold barrier, the magnitude is  $6.9 \pm 0.8$  kJ mol $^{-1}$  as obtained from tables<sup>9,2</sup> of  $\langle \sin^2\theta \rangle$  as a function of the barrier, the temperature, and the reduced moment of inertia. Since  $\langle \sin^2\theta \rangle$  is greater than 0.5, the preferred conformation is perpendicular. STO-3G theory (Figure 28) supports these conformational deductions, but overestimates the barrier by almost 3 kJ mol $^{-1}$ .

## (b) 2,4,6-trifluorothioanisole

A para substituent decreases the extent of conjugation with the ring for thiophenol and thioanisole. Therefore, one would expect the same phenomenon for 2,4,6-trifluorothioanisole relative to 2,6-difluorothioanisole. In the former,  ${}^6J(C\alpha, F)$  is  $1.198 \pm 0.013$ , so that the value of  $\langle \sin^2\theta \rangle$  is  $1.198 \pm 0.013 / 1.48 \pm 0.02$  or 0.809. In terms of a two-fold barrier, its magnitude is  $8.1 \pm 1.0$  kJ mol $^{-1}$ . Further evidence for a more stable perpendicular conformer comes from examinations of  ${}^6J(CH_3, F)$  and  ${}^6J(C\alpha, F)$ . Both couplings have been shown to be mainly proximate in origin for 2-fluoroanisole<sup>7,2</sup>. Here, the same will be assumed for ortho-fluorothioanisoles. As such, the magnitude of both couplings should decrease as the methylthio group is more often out-of-



plane for 2,4,6-trifluorothioanisole relative to 2,6-difluorothioanisole. From the numbers given in table 18, the decrease is apparent.

(c) 2,3,5,6-tetrafluorothioanisole

The value of  $\langle \sin^2\theta \rangle$  for 2,3,5,6-tetrafluorothioanisole is  $0.370 \pm 0.005 / 0.54 \pm 0.01$  or 0.685. In terms of a two-fold barrier, its magnitude is therefore  $4.1 \pm 0.6$  kJ mol<sup>-1</sup>, as determined from the tables of  $\langle \sin^2\theta \rangle^{1/2}$ . Here, the meta fluorines appear to increase conjugation with the ring and to stabilize the planar conformation relative to 2,6-difluorothioanisole. The more planar conformation for 2,3,5,6-tetrafluorothioanisole relative to the other compounds in table 18 is supported by the large magnitudes of the predominantly proximate coupling constants  $^4J(C\alpha, F)$  and  $^5J(CH_3, F)$ .

(d) Pentafluorothioanisole

In a series of para substituted 2,3,5,6-tetrafluorothioanisoles<sup>47</sup>, the magnitudes of  $^5J(CH_3, F)$  are dependent on the electron withdrawing ability of the substituents. The value for pentafluorothioanisole is smaller than that for tetrafluorothioanisole, indicating a more stable perpendicular conformation for the penta-substituted compound. The four bond carbon-fluorine coupling constant supports this conclusion.

In pentafluorothioanisole,  $\langle \sin^2\theta \rangle$  is  $1.192 \pm 0.016 / 1.48 \pm 0.02$  or 0.805, indicating a barrier, presumed two-fold, of  $7.9 \pm 1.1$  kJ mol<sup>-1</sup>. X-ray fluorescence spectra also indicate a non-planar conformation for pentafluorothioanisole<sup>33</sup>.

In comparison with 2,4,6-trifluorothioanisole,  ${}^4J(C\alpha, F)$  and  ${}^5J(CH_3, F)$  show that the presence of meta fluorines in pentafluorothioanisole increase the conjugation with the ring such that the methylthio group lies more in plane. The magnitudes of  ${}^4J(C\alpha, F)$ , and therefore of  $\langle \sin^2\theta \rangle$ , are nearly the same, however, suggesting either a possible substituent dependence for this coupling, or that the proximate couplings are more sensitive to methylthio group conformation. Of course, within experimental error, the barrier to internal rotation in 2,4,6-trifluorothioanisole could easily be 1 kJ mol<sup>-1</sup> higher than that in pentafluorothioanisole.

Comparing pentafluorothioanisole with 2,6-difluorothioanisole, the increase in conjugation caused by the two meta fluorines is more than offset by the decrease caused the para fluoro substituent. The magnitudes of  ${}^4J(C\alpha, F)$ ,  ${}^5J(CH_3, F)$ , and the barriers to internal rotation, are all consistent with this conformational deduction.

## (e) 2-bromo-4-fluorothioanisole

In 2-bromo-4-fluorothioanisole a single measurement of  ${}^6J(C\alpha, F)$  is 0.252 Hz. Then  $\langle \sin^2\theta \rangle$  is 0.252/1.48 or 0.17. Although the methylthio group prefers to lie trans to the bromine, a considerable population of non-planar conformations exists, in order to give a non-zero value of  $\langle \sin^2\theta \rangle$ .

E. Measurements of  $^5J(\text{CH}_3, \text{H})$  in thioanisoles and their conformational implications.

The proximate or "through-space" coupling between methyl and ortho protons,  $^5J(\text{CH}_3, \text{H})$ , is established as useful in conformational analysis in anisole and its derivatives<sup>99, 100</sup>. This coupling is sensitive to the distance between the coupled nuclei. In some ortho substituted thioanisoles it is suggested<sup>45</sup> that the magnitude of the coupling depends upon the size of the substituent. Such a suggestion is reasonable if  $^5J(\text{CH}_3, \text{H})$  in thioanisole and its derivatives is also a proximate coupling constant.

One can thus equate increasing planarity with increasing magnitude of this coupling. Assuming that the planar conformation is most stable, and that the barrier to internal rotation is two-fold, a lower value of  $\langle \sin^2\theta \rangle$  is associated with the increasing magnitude of this coupling. Then the magnitude of the coupling increases through the series thioanisole (0.141), 3,5-dichlorothioanisole (0.147), 4-nitrothioanisole (0.178), 2-methyl-3-fluorothioanisole (0.334), 2-bromo-4-fluorothioanisole (0.347), 2-bromothioanisole (0.387), 2-iodothioanisole (0.394), and 2,4,5-trichlorothioanisole (0.412), with the magnitude of the coupling

constants in Hz given in parentheses. Typical 95% confidence intervals for the coupling constants were less than  $\pm 5$  mHz. The sign has been determined for 2,5-dichlorothioanisole<sup>46</sup> and is negative.

Since the barrier to internal rotation is higher in 3,5-dichlorothioanisole ( $9.5 \text{ kJ mol}^{-1}$ ) than in thioanisole ( $5.1 \text{ kJ mol}^{-1}$ ), the observed larger magnitude of  $^5J(\text{CH}_3, \text{H})$  for the 3,5-dichloro compound is expected.

In 4-nitrothioanisole, the magnitude of this coupling is 0.178 Hz, which is consistent with an increased conjugational barrier about the  $\text{Csp}^2\text{-S}$  bond. In 4-nitrothiophenol, the barrier to internal rotation<sup>24</sup> is  $9.0 \pm 0.8 \text{ kJ mol}^{-1}$ . Extrapolation from table 17 indicates that the rotational barrier in 4-nitrothioanisole is likely  $13 \pm 2 \text{ kJ mol}^{-1}$ .

The INDO MO FPT data for  $^5J(\text{CH}_3, \text{H})$  in anisole are reproduced by  $\cos^4\theta$  up to  $60^\circ$  whereupon the coupling becomes nearly zero. The coupling to the ortho proton lying trans to the coplanar methoxy group apparently vanishes. The coupling in thioanisole may behave similarly, as suggested by INDO MO FPT (table 15). Here, the maximum value is calculated to be  $-0.28 \text{ Hz}$ , and the value drops to  $+0.10 \text{ Hz}$  at approximately  $60^\circ$  and remains relatively constant through  $180^\circ$ . Although observed couplings for ortho substituted thioanisoles indicate

that the INDO estimate for  $\phi = 0^\circ$  is likely low, the value for  $\phi = 180^\circ$  may be quite real. The methyl protons appear to couple to protons one bond further removed (meta) by  $0.06 \pm 0.02$  Hz. This six-bond coupling is apparently non-stereospecific<sup>9</sup>, and is positive whether the methyl group is oriented cis or trans to the C-H(meta) bond. Parenthetically, the methyl proton coupling,  ${}^7J(\text{CH}_3, \text{H})$  to para protons is  $-0.053(1)$  Hz in thioanisole,  $-0.058(2)$  Hz in 2-bromothioanisole, and  $-0.034 \pm 0.026$  Hz in 2,5-dichlorothioanisole. In 2,6-dichlorothioanisole and 2-hydroxythioanisole, its presence cannot be detected, indicating a stereospecificity opposite to that predicted by INDO MO FPT.

Assuming known two-fold internal barriers in thioanisole and 3,5-dichlorothioanisole, population distribution curves can be derived for both compounds. For every dihedral angle,  ${}^5J(\text{CH}_3, \text{H})$  follows from equation 18a),

$$J(\phi) = J(\phi = 0^\circ) \cdot \cos^4 \phi \quad (18a)$$

The averaged coupling constant may be estimated from

$$J = \sum_{\phi} J(\phi) \cdot P(\phi) \quad (18b)$$

where  $P(\phi)$  is the normalized population for the angle  $\phi$  obtained from a Boltzmann distribution. The  ${}^5J(\text{CH}_3, \text{H})$  for thioanisole and 3,5-dichlorothioanisole may be reproduced to within 0.01 Hz if  $J(\phi=0^\circ)$  is set to  $-0.407$

Hz (Table 19). For ortho substituted thioanisoles, this value tends to  $-0.43$  Hz, that observed in 2-nitrothioanisole. Although a larger ortho substituent will decrease  $\langle \sin^2 \theta \rangle$ , i.e. induce a more planar conformation, the substituent will also increase the C2-C1-S angle because of steric repulsion between the sulfur and the substituent. With other geometries held constant, an increase in this angle alone will bring the methyl protons closer to the ortho proton even with torsion in the plane about the the ortho proton. Therefore, for thioanisole derivatives with no substituent in the ortho position, a  ${}^3J(\text{CH}_3, \text{H})$  of  $-0.407$  for a planar conformation is reasonable. Unfortunately, more work needs to be done in order to establish  ${}^3J(\text{CH}_3, \text{H})$  for  $\theta = 0^\circ$ .

A two-fold barrier in 4-nitrothioanisole of  $13 \text{ kJ mol}^{-1}$  yields  ${}^3J$  by equations (18) to be  $-0.170$  Hz, in approximate agreement with the experimentally determined value of  $0.178(4)$  Hz.

In 2-bromothioanisole,  ${}^3J(\text{CH}_3, \text{H})$  is  $-0.387$  Hz, whereas in the 4-fluoro derivative,  ${}^3J(\text{CH}_3, \text{H})$  is  $-0.347$  Hz, consistent with the idea that para fluoro substituents decrease the conjugation with the ring and non-planar conformers are more populated. When the ortho position is occupied by iodine, rather than bromine, steric compression is greater due to the greater van der

Waals radius of the substituent, and the observed coupling is  $-0.394$  Hz.

In 2-chlorothioanisole, the reported<sup>45</sup> coupling constant is  $0.17$  Hz. This dated measurement is most likely an underestimate since underestimates were found for 2-iodothioanisole ( $0.36, 0.394$  Hz), 2-bromothioanisole ( $0.31, 0.367$ ), 2-methoxythioanisole (no coupling observed,  $0.22$ ), and for thioanisole (no coupling observed,  $0.141$ ), where the first number in parentheses represents data from reference 45, and the second refers to recent data from this laboratory. Using the STO-3G calculated energy profile for 2-chlorothioanisole (full data not shown), and equations 18a and 18b, the calculated coupling constant is  $-0.29$  Hz. In 2,5-dichlorothioanisole, where the meta chlorine substituent increases the barrier to internal rotation and hence should increase the magnitude of  $^5J$ , the observed<sup>46</sup> coupling constant is  $-0.35 \pm 0.02$  Hz. Introduction of another chlorine at the para position increases  $^5J(\text{CH}_3, \text{H})$  further to  $-0.412$  Hz. The apparent increase in the barrier is not unexpected since the barrier to internal rotation in thiophenols is likely increased by a 4-chloro substituent<sup>5</sup>.

All thioanisole derivatives discussed in this section were studied as 2-2.4 mol % solutions in acetone- $d_6$ ,



except thioanisole and 3,5-dichlorothioanisole, which were 2 mol % solutions in benzene- $d_6$ . Solvent effects can be responsible for small changes in the barrier to internal rotation and the observed coupling constant between the methyl protons and ortho proton(s). Data for 4-aminothiophenol<sup>2</sup> indicate that the rotational barrier ( $2.9 \text{ kJ mol}^{-1}$ ) may vary by perhaps as much as  $0.4 \text{ kJ mol}^{-1}$  in going from  $\text{CCl}_4$  to  $\text{C}_6\text{D}_6$  or  $\text{CDCl}_3$  as solvents. For pentafluorothioanisole,  $^5\text{J}(\text{CH}_3, \text{F})$  is  $0.722 \pm 0.003 \text{ Hz}$ , as a 2 mol % solution in acetone- $d_6$ ,  $0.734 \pm 0.002 \text{ Hz}$  for a 23 mol % solution in acetone- $d_6$ , and  $0.746 \pm 0.022 \text{ Hz}$  as a 5 mol % solution in  $\text{CCl}_4$ .

Table 19 Comparisons of  $^5\text{J}(\text{CH}_3, \text{H})$

Molecule	$^5\text{J}(\text{CH}_3, \text{H})$	
	observed	calculated
thioanisole	-0.141	-0.131
3,5-dichlorothioanisole	-0.147	-0.156
4-nitrothioanisole	-0.178	-0.170
2-chlorothioanisole	likely < $ -0.35 $	-0.290

SUMMARY AND CONCLUSIONS

The barrier to internal rotation in thioanisole in solution is  $5.1 \pm 2$  kJ mol<sup>-1</sup>. Various substituents modify the extent of conjugation of the methylthio group with the ring and therefore influence the rotational barrier. A compilation of the barriers determined and estimated in this work appears as Figure 32. The technique used, for the most part, is the J method<sup>55</sup>, in which a long-range nuclear spin-spin coupling with a known conformational dependence is related to the hindering potential and other parameters.

The couplings  ${}^6J(C\alpha, H)$  and  ${}^6J(C, F)$  most likely have  $\sigma$ - $\pi$  mechanisms, whereas  ${}^5J(C\alpha, H)$  and  ${}^5J(C\alpha, F)$  interactions arise from  $\sigma$ - $\pi$  and  $\sigma$  mechanisms. For the latter coupling, the two mechanisms give contributions of opposite sign.

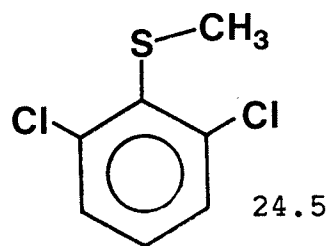
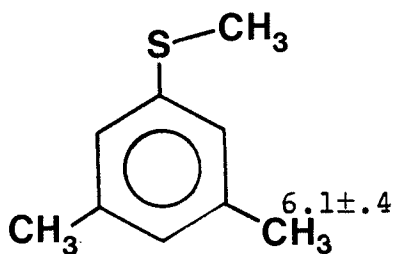
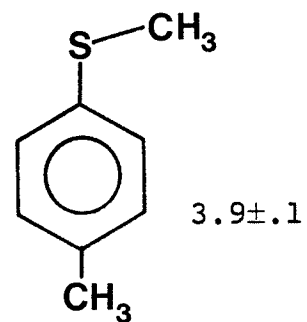
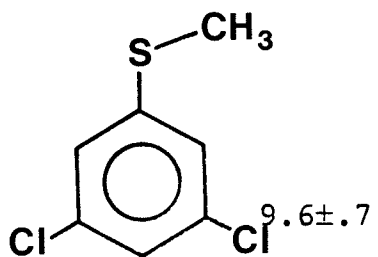
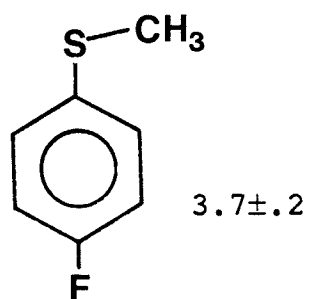
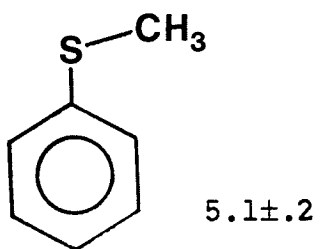
The barriers to internal rotation in thioanisole and its derivatives are a composite of steric and conjugative interactions. In thioanisole, the preferred conformation is planar. Two ortho C-F bonds increase the steric repulsions between the methyl group and ortho substituents, destabilizing the planar conformation relative to the non-conjugative perpendicular conformation. As well, because fluorine is a  $\pi$  donor, the ortho (or para) fluorines will decrease the conjugation, or double-bond character, of the Csp<sup>2</sup>-S bond and therefore

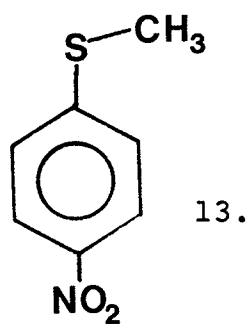
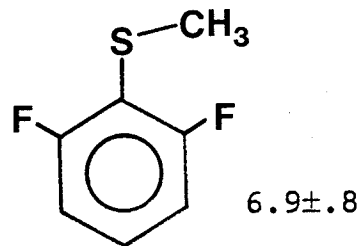
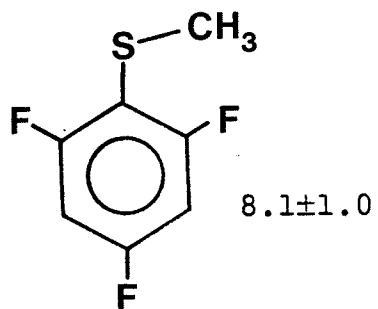
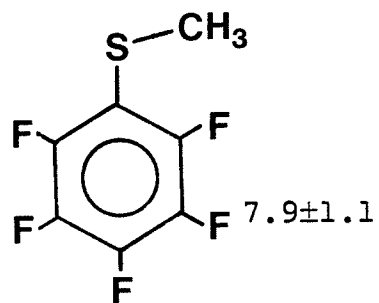
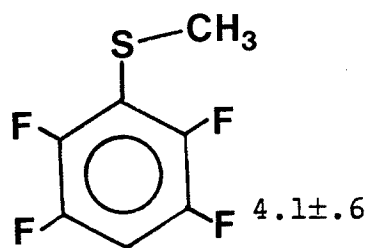
cause a further destabilization of the conjugative ground state.

The magnitude of the coupling between the methyl protons and ortho proton(s) in some thioanisole derivatives and in ortho substituted thioanisoles is an indication of the conformation of the methylthio group. As the magnitude of the coupling increases, the planar conformation becomes more preferred. The bulkier the single ortho substituent is, the larger the observed coupling, as expected.

## Figure 32

Barriers to internal rotation for thioanisole and some of its derivatives (in  $\text{kJ mol}^{-1}$ ). The barriers for 4-nitrothioanisole and 2,6-dichlorothioanisole are estimates only.





FUTURE CONSIDERATIONS



The proximate couplings,  ${}^5J(\text{CH}_3, \text{H})$  and  ${}^5J(\text{CH}_3, \text{F})$  may well be empirically reproduced by a  $\cos^4\theta$  dependence where  $\theta$  is the angle between the  $\text{Csp}^3\text{-S}$  bond and the ring plane. A known potential function for internal rotation can be used to calculate values of  $\langle \cos^4\theta \rangle$ . If the function is assumed to be a multiple of  $\sin^2\theta$ , a barrier height may be estimated from the value of  ${}^5J(\text{CH}_3, \text{X})$ . In this manner, perhaps the determination of the barrier to internal rotation in benzene derivatives via long-range coupling constants may be extended past the present 13  $\text{kJ mol}^{-1}$  upper limit of the J method<sup>5,5</sup>.

STO-3G calculations indicate that the barrier to internal rotation in 3,5-difluorothioanisole is 8.6  $\text{kJ mol}^{-1}$ . STO-3G generally overestimates the barrier in other thioanisole derivatives (table 14), so that the true barrier is more likely 8  $\text{kJ mol}^{-1}$ . If so, from equation (17), and since  $\langle \sin^2\theta/2 \rangle$  is 0.5 for a two-fold barrier, the magnitude of  ${}^5J(\text{C}\alpha, \text{F})$  should be 0.04 Hz. Furthermore, the sign should be positive.

A series of MO calculations on phenol derivatives<sup>10,1</sup> indicated that meta-nitro substituents should decrease conjugation of the methylthio group into the ring. Experimental investigations, by the J method, of 3,5-dinitrothiophenol and 3,5-difluorothiophenol and their methylated counterparts, would help to determine

meta substituent effects in thiophenols and thioanisoles. INDO MO FPT calculations (table 15) indicate that the five bond carbon-carbon coupling constant,  ${}^5J(C\alpha, C4)$ , is  $\sigma$ - $\pi$  mediated. If  ${}^5J$  for the perpendicular conformer were to be established, the para substituent effect for thioanisoles could be investigated more extensively than in the three compounds studied in this work. Of special interest is 4-nitrothioanisole, for which extrapolation of thiophenol and thioanisole barriers and the proximate coupling,  ${}^5J(CH_3, H)$ , indicate a barrier to internal rotation of about  $13 \text{ kJ mol}^{-1}$ .

In addition to the many thioanisole derivatives whose methods of syntheses are adumbrated in the experimental methods section of this thesis, an additional nineteen derivatives have also been made. The para-X-thioanisoles include X = bromo, chloro, t-butyl, methylthio, ethyl, cyano, acetimido, and ethoxy. Other compounds are 4,4'-di(methylthio)biphenyl, 2,4-dibromo-6-fluorothioanisole, 1-(methylthio)naphthalene, 1-(methylthio)-4-nitronaphthalene, 3-methoxythioanisole, o-bis(methylthio)benzene, 2,4-dichloro-5-methylthioanisole, 2-fluorothioanisole, 3-fluorothioanisole, and 3-methyl-4-bromothioanisole. The proton and carbon high resolution NMR spectra of these compounds should be run and analyzed. Of particular interest are  ${}^5J(CH_3, H)$  and  ${}^5J(C\alpha, H)$  in the para substituted series. Perhaps then

the substituent effects for  ${}^5J(C\alpha,H)$  could be known. Since  $\langle \sin^2\theta/2 \rangle$  is 0.5 in compounds of two-fold symmetry<sup>24</sup>, the barriers to internal rotation in the para substituted thioanisoles could then be measured from  ${}^5J(C\alpha,H)$ .

A check for the measured barriers from  ${}^5J(C\alpha,H)$  could come from  $C\alpha-C4$  coupling constants.

The methyl group replacement technique for benzene derivatives usually shows that for a  $\sigma-\pi$  mechanism for couplings from a side chain to a para proton and methyl group,  ${}^6J = -{}^7J$ . In thiophenol and thioanisole, a ca. ten per cent discrepancy is noted. The question raised is whether this is a property of the heteroatom or whether the phenomenon is more general and extends to the corresponding Group VI elements selenium and tellurium. Presumably, the 10 % increase will be also noted in other phenyl alkyl sulfides. Molecular orbital calculations may give some clues.

REFERENCES

1. W.J.E. Parr and T. Schaefer, *J. Magn. Reson.* 25,171 (1977).
2. T. Schaefer and W.J.E. Parr, *Can. J. Chem.* 55,552 (1977).
3. T. Schaefer, T.A. Wildman, and S.R. Salman, *J. Am. Chem. Soc.* 102,107 (1980).
4. T. Schaefer, L. Kruczynski, and W. Niemczura, *Chem. Phys. Lett.* 38,498 (1976).
5. T. Schaefer, T.A. Wildman, and R. Sebastian, *Can. J. Chem.* 60,1924 (1982).
6. T. Schaefer, W.J.E. Parr, and W. Danchura, *J. Magn. Reson.* 25,167 (1977).
7. T. Schaefer and R. Laatikainen, *Can. J. Chem.* 61,2785 (1983).
8. T. Schaefer, J. Peeling, and G.H. Penner, *Can. J. Chem.* 61,2773 (1983).
9. T. Schaefer, R. Sebastian, R.P. Veregin, and R. Laatikainen, *Can. J. Chem.* 61,29 (1983).
10. R.K. Harris, Nuclear Magnetic Resonance Spectroscopy, (Pitman, London, 1983).
11. C.P. Slichter, Principles of Magnetic Resonance, (Springer-Verlag, Berlin, 2nd edition, 1978).
12. E. Fukushima, and S.B.W. Roeder, Experimental Pulse NMR, (Addison-Wesley, Don Mills, 1981).
13. H. Günther, NMR Spectroscopy, (John Wiley & Sons, Toronto, 1980).
14. R.J. Abraham, The Analysis of High Resolution NMR Spectra, (Elsevier, Amsterdam, 1971).
15. A. Abragam, The Principles of Nuclear Magnetism, (Oxford University Press, Oxford, 1961).
16. J.A. Pople, W.G. Schneider, and H.J. Bernstein, High-Resolution Nuclear Magnetic Resonance, (McGraw-Hill, New York, 1959).

17. A. Carrington and A.D. McLachlan, Introduction to Magnetic Resonance, (Harper and Row, New York, 1967).
18. P. Palmieri, F. Tullini, B. Velino, and C. Zauli, *Gazz. Chim. Ital.* 105,919 (1975).
19. J.H. Green, *Spectrochim. Acta*, 24A,1627 (1968).
20. K.T. Trueblood, and J.D. Dunitz, *Acta Cryst.* B39:1,120 (1983)
21. H. Lumbroso, J. Curé, and C.G. Andrieu, *J. Mol. Struct.* 43,87 (1978).
22. M.J. Aroney, R.J.W. LeFèvre, R.K. Pierens, and M.G.N. The, *J. Chem. Soc. B*, 1132, (1971).
23. M.J. Aroney, R.J.W. LeFèvre, R.K. Pierens, and M.G.N. The, *J. Chem. Soc. B*, 666, (1969).
24. T. Schaefer, and T.A. Wildman, *Chem. Phys. Letters*, 80:2,280 (1981).
25. D.G. Lister, P. Palmieri, and C. Zauli, *J. Mol. Struct.* 35,299 (1976).
26. H. Bock. G. Wagner, and J. Kroner, *Tetrahedron Letters* 40,3713 (1971).
27. P.S. Dewar, E. Ernstbrunner, J.R. Gilmore, M. Godfrey, and J.M. Mellor, *Tetrahedron* 30,2455 (1974).
28. F. Bernardi, G. Distefano, A. Mangini, S. Pignatiorion, and G. Spinta, *J. Electron Spectrosc. Relat. Phenom.* 7,457 (1975).
29. A. Schweig, and N. Thon, *Chem. Phys. Letters*, 38:3,482 (1976).
30. E. Honegger, and E. Heilbronner, *Chem. Phys. Letters*, 81:3,15 (1981).
31. A. Modelli, D. Jones, F.P. Colonna, and G. Distefano, *Chem. Phys.* 77,153 (1983).
32. M. Mohraz, W. Jian-qi, E. Heilbronner, and A. Sol-ladié-Cavallo, F. Matloubi-Maghadam, *Helv. Chim. Acta* 64,97 (1981).

33. G.N. Dolenko, A.A. Voityuk, T.N. Dolenko, and L.N. Mazalov, *Zh. Struk. Khimii*, 23:2, 34 (1982).
34. M.J. Aroney, L. Cleaver, R.K. Pierens, R.J.W. and LeFèvre, *J. Chem. Soc. Perkin. Trans. II*, 1854 (1976).
35. A. Alberti, M. Guerra, G. Martelli, F. Bernardi, A. Mangini, and G.F. Pedulli, *J. Am. Chem. Soc.* 101, 4627 (1979).
36. G.W. Buchanan, C. Reyes-Zamora, and D.E. Clarke, *Can. J. Chem.* 52, 3895 (1974).
37. K.S. Dhimi, and J.B. Stothers, *Can. J. Chem.* 44, 2855 (1966).
38. G.A. Kalabin, D.F. Kushnarev, V.M. Bzesovsky, and G.A. Tschmutova, *Org. Mag. Res.* 12:10, 598 (1979).
39. T. Schaefer, R.P. Veregin, and D.M. McKinnon, *Can. J. Chem.* 59, 3204 (1981).
40. T. Schaefer, S.R. Salman, and T.A. Wildman, *Can. J. Chem.* 60, 342 (1982).
41. G. Llabrès, M. Baiwir, L. Christiaens, J. DeNoel, L. Laitem, and J.-L. Piette, *Can. J. Chem.* 56, 2008 (1978).
42. L.B. Krivdin, G.A. Kalabin, and B.A. Trofimov, *Izv. Ak. Nauk SSSR, Ser. Khim.* 3, 565 (1982).
43. P. Diehl, *Helv. Chim. Acta* 44, 829 (1961).
44. J.S. Martin, and J. Dailey, *Chem. Phys.* 39, 1722 (1963).
45. L. Lunazzi, and D. Macciantelli, *J. Chem. Soc. Chem. Commun.*, 333 (1971).
46. T. Schaefer, R. Sebastian, and S.R. Salman, *J. Mag. Res.* 46, 325 (1982).
47. B.C. Musial, and M.E. Peach, *J. Fluor. Chem.* 7, 459 (1976).
48. J. Bardon, *Tetrahedron* 21, 1101 (1965).
49. J.W. Emsley, M. Longeri, C.A. Veracini, D. Catalano, and G.F. Pedulli, *J. Chem. Soc. Perkin Trans. II*, 1289 (1982).

50. T. Matsushita, Y. Osamura, N. Misawa, K. Nishimoto, and Y. Tsuno, *Bull. Chem. Soc. Japan* 59:9,2521 (1976).
51. D.B. Neumann, H. Basch, L. Kornegau, and L.C. Snyder, POLYATOM (Version 2), Program No. 238 Quantum Chemistry Program Exchange, Indiana University, Bloomington, Indiana.
52. W.J. Hehre, W.A. Lathan, R. Ditchfield, M.D. Newton, and J.A. Pople, GAUSSIAN 70, Program No. 216 Quantum Chemistry Program Exchange, Indiana University, Bloomington, Indiana.
53. J.A. Pople, and D.L. Beveridge, Approximate Molecular Orbital Theory, McGraw-Hill, New York, 1970.
54. S. Sanda, and H.M. Seip, *Acta Chim. Scand.* 25,1903 (1971).
55. W.J.E. Parr and T. Schaefer, *Acc. Chem. Res.* 13,400 (1980).
56. R. Wasylishen and T. Schaefer, *Can. J. Chem.* 50,1852 (1972).
57. G.J. Karabatsos and F.M. Vane, *J. Am. Chem. Soc.* 85,3886 (1963).
58. S. Forsén, B. Akermark, and T. Alm, *Acta Chim. Scand.* 18,2313 (1964).
59. T. Schaefer, S.R. Salman, and T.A. Wildman, *Can. J. Chem.* 58,2364 (1980).
60. S. Forsén, and R.A. Hoffman, *J. Mol. Spectrosc.* 20,168 (1966).
61. R. Freeman, *Mol. Phys.* 6,535 (1963).
62. T. Schaefer, R. Sebastian, and T.A. Wildman, *Can. J. Chem.* 57,3005 (1979).
63. T. Schaefer, R. Sebastian, and T.A. Wildman, *Can. J. Chem.* 59,3021 (1981).
64. L.F. Fieser and M. Fieser, Reagents in Organic Synthesis (Wiley and Sons, New York, 1967), p. 682f.
65. J.D. Baleja, *Synth. Commun.* 14,215 (1984).



66. G. Hilgetag and A. Martini (editors), Preparative Organic Chemistry, (John Wiley and Sons, Inc., New York, 1972), p. 269.
67. D.S. Tarbel and D.K. Fukushima, Org. Synth. Coll. III, 809 (1955).
68. E.A. Bartkus, E.B. Hotelling, and M.B. Neuworth, J. Org. Chem. 22,3037 (1974).
69. J.B. Rowbotham and T. Schaefer, Can. J. Chem. 52,3037 (1974).
70. T. Schaefer and K. Marat, Org. Magn. Reson. 15,294 (1981).
71. T. Schaefer, K. Marat, A. Lemire, and A.F. Janzen, Org. Magn. Reson. 18,90 (1980).
72. T.A. Wildman, Ph. D. Thesis, (University of Manitoba, Winnipeg, Canada, 1982), p. 77.
73. G.A. Morris and R.J. Freeman, J. Am. Chem. Soc. 101,760 (1979).
74. S.M.Castellano and A.A. Bothner-By, J. Chem. Phys. 41,3863 (1964).
75. C.W. Haigh and J.W. Williams, J. Mol. Spectrosc. 32,398 (1969).
76. A.R. Quirt and J.S. Martin, J. Mag. Res. 5,318 (1971).
77. D.J. Loomes, R.K. Harris, and P. Ansten, The NMR Program Library (Daresbury: Science Research Council, 1979), 3.98.
78. W.J. Hehre, R.F. Stewart, and J.A. Pople, J. Chem. Phys. 51,2657 (1969).
79. M.R. Petersen and R.A. Poirier, MONSTERGAUSS, Dept. of Chemistry, University of Toronto, Toronto, Canada (1981).
80. J.A. Pople, J.W. McIver Jr., and N.S. Ostlund, J. Chem. Phys. 49,2960,2965 (1968).
81. R. Laatikainen, J. Magn. Reson. 27,169 (1977).
82. O. Manscher, K. Schaumberg, and J.P. Jacobsen, Acta Chem. Scand. A35,13 (1981).

83. A.J. Jones, G.A. Jenkins, and M.L. Heffernan, Aust. J. Chem. 33,1275 (1980).
84. A.W. Douglas and M. Shapiro, Org. Magn. Reson. 14,74 (1973).
85. M. Hansen and H.J. Jakobsen, J. Magn. Reson. 10,74 (1973).
86. J.E. Freund, P.E. Livermore, and I. Miller, Experimental Statistics (Prentice-Hall, Englewood Cliffs, N. J., 1960) p. 123.
87. J.W. Emsley, L. Phillips, and V. Wray, Progress in NMR spectroscopy, 10, (J.W. Emsley, J. Feeney, L.H. Sutcliffe, editors, Pergamon Press, Oxford, 1977) p. 83.
88. P.E. Hansen, A. Berg, H.J. Jakobsen, A.P. Manzara, and J. Michl, Org. Magn. Reson. 11,215 (1978).
89. R.E. Wasylishen, Annual Reports on NMR spectroscopy 7, (G.A. Webb, editor, Academic Press, London, 1977) p. 246.
90. T. Schaefer and J.D. Baleja, J. Magn. Reson., Nov. 1984 (in press).
91. W.J. Orville-Thomas, Ed. Internal Rotation in Molecules (Wiley, New York, 1974).
92. W. Danchura, Ph. D. Thesis (University of Manitoba, Winnipeg, Canada, 1983).
93. M.W. Wierzchorek, Acta Crystallog. 36, Part B,1515 (1980).
94. G.W. Burton, Y. Lepage, E.J. Gabe, and K.U. Ingold, J. Am. Chem. Soc. 102,7792 (1980).
95. G.W. Burton and K.U. Ingold, J. Am.Chem. Soc. 103,6472 (1981).
96. T. Schaefer, R. Laatikainen, T.A. Wildman, J. Peeling, G.H. Penner, J.D. Baleja, and K. Marat, Can. J. Chem. 62,0000 (1984).
97. A.A. Bothner-by and R.K. Harris, J. Am. Chem. Soc. 87,3451 (1965).
98. N.L. Owen and R.F. Hester, Spectrochim. Acta A25,343 (1969).

99. T. Schaefer and R. Laatikainen, *Can. J. Chem.* 61,224 (1983).
100. T. Schaefer, T.A. Wildman, and J. Peeling, *J. Magn. Reson.* 56,144 (1984).
101. A. Pross and L. Radom, "Substituent interactions in substituted benzenes" in Progress in Physical Organic Chemistry (R. W. Taft, ed.) 13,30 (1981).